Institute of Space and Aeronautical Science, University of Tokyo
Report No. 588, December 1980

Binary Mixture Film Condensation of Internal Flows

By

Susumu KOTAKE

Abstract: Film condensation of binary mixture flows in a vertical channel of variable circular cross-section is studied theoretically to predict effects of the channel geometry, vapor flow velocity, system temperature and type of mixture. The condensation is dominated mainly by the liquid-vapor equilibrium characteristics and the mass transfer process in the vapor flow. Nozzle-type flows yield larger values of local condensation rate, although the channel geometry has not a considerable effect on the overall condensation rate. The flow direction has a considerable influence on the condensation rate. Quasi-developed flows show different features from those of developing flows, implying a substantial effect of the flow in the starting region upon the condensation process. By similarity consideration of the governing equations and the boundary conditions, the nondimensional parameters concerning the mass transfer and the phase equilibrium are obtained to characterize the condensation process.

CONTENTS

NOMENCLATURE

C	mass fraction of the volatile species
c_p	specific heat at constant pressure
c'_p	difference of specific heats, $c_{p1}-c_{p2}$
D	binary diffusion coefficient
f	friction coefficient, Eq. (6.9)
G_r	Grashof number, gR_0^3/ν_{r0}^2
g	acceleration of gravity
H_e	Stefan number, $\bar{c}_{pr0}(T_{00}-T_w)/\lambda_{r0}$
h	enthalpy
K_t, K_e, K_e	nondimensional parameters, Eqs. (7.72), (7.73)
k	thermal conductivity
L	length of the cooled wall
N_u	Nusselt number, Eq. (6.2)
M_c	Mach number, $(\rho_{r0}U_{00}^2/P_0)^{1/2}$
M_i	molecular weight of species i
$\dot{m}$	rate of condensation per unit area
P_0	pressure at the vapor-flow inlet
P_r	Prandtl number, $c_{pr0}\mu_{r0}/k_{r0}$
p	pressure
p_{si}	vapor pressure of pure component i
q	heat flux to the wall
q_c^*, q_t^*	mass and heat fluxes, Eqs. (6.2), (6.3)
R	radius of channel
R_c, R_t	radii of concentration and temperature layers
R_e	Reynolds number, $\rho_{r0}U_{00}R_0/\mu_{r0}$
R_δ	radius of the interface, $R-\delta$
$\mathscr{R}$	gas constant
r	radial coordinate
S_c	Schmidt number $\mu_{r0}/(\rho_{r0}D_{r0})$
S_h	Sherwood number, Eq. (6.3)
T	temperature
T_{00}	inlet temperature of vapor flow
T_w	wall temperature

U_{00}	inlet velocity of vapor flow at the channel center
u, v	axial and radial velocity components
X	mole fraction
x	axial coordinate
Y_c, Y_t	ratio of radii, R_c/R_δ, R_t/R_δ
y	radial coordinate from the wall, $R-r$
γ	activity coefficient
δ	condensate film thickness
Δ_w	$=\{C_e(T_w)-C_e(T_{00})\}/\{C_e(T_w)-\bar{C}_e(T_w)\}$
θ	dimensionless temperature, $(T-T_w)/T_{00}-T_w)$
λ	latent heat of vaporization
μ	dynamic viscosity
ν	kinematic viscosity
ρ	density
τ^*	viscous stress, Eq. (6.9)

Subscripts

e	phase equilibrium
i	liquid-vapor interface
m	flow averaged value
0	center of channel
00	vapor-flow inlet
r	ratio of reference values of the vapor to the liquid
$r0$	reference values
w	wall
1, 2	species, 1 = the volatile component

Superscripts

—	condensate
*	$x^*=x/(R_eS_c)\quad \dot{m}^*=R_eS_c\dot{m}\quad v^*=R_eS_cv$

1. Introduction

Film condensation of binary mixtures is one of the most important processes of heat-and-mass transfer engineering. The number of theoretical and experimental studies devoted to this problem, however, is rather limited [*1*~*9*], although from the phenomenological point of view considerable work has been done by Kirschbaum and others [*10*~*12*]. This is caused by the complicated mechanism of physical and chemical processes and the experimental difficulties of the problem.

Theoretical elaboration of the gravity-flow film condensation of a binary mixture on a cooled, isothermal vertical plate was given by Sparrow and Marschall [*2*], on the basis of the conservation laws with an analytical model of boundary layer flows of the condensate and vapors. With the application of such a method of analysis, Denny and Jusionis [*3*] investigated the effect of forced flow on film condensation of binary mixtures on a vertical flat plate. In these theoretical studies, the conservation equa-

tions of boundary layer flow are numerically solved for the vapor layer, whereas for the condensate film the Nusselt assumption of negliginle effects of liquid acceleration and energy convection is employed. The obtained results show that the heat flux toward the wall has a marked dependence on the bulk composition of binary mixture and the overall temperature difference of the system, having a minimum at a certain bulk composition. Experimental studies concerning film condensation of binary mixtures on external bodies have been reported by several investigators, mainly from the standpoint of heat transfer problems [7, 8].

The problem of film condensation of binary mixtures in a tube is often encountered in practice, although relatively little work of it appears to have been done. Van Es and Heertjes [9] studied the channel-flow film condensation of binary mixtures with a simplified model of vapor and liquid flows, in which the convective transports by axial flow were neglected. The agreement between their theoretical and experimental results was only qualitative.

Most of the peculiar phenomena in the condensation of mixtures originate in the fact the equilibrium concentration in the phases will generally differ for each component. Removal of the light component increases or decreases the saturation point owing to the equilibrium characteristics of the mixture. Due to the concentration differences, the liquid phase contains less of the volatile (lower boiling) component than does the vapor. The volatile component of the vapor adjacent to the liquid must be removed away to supply the material of condensation. Thus, a concentration gradient should exist between the liquid-vapor interface and the bulk of the vapor. The volatile component diffuses toward the main stream of the vapor, whereas the material to be condensed is convectively transferred to the interface. The mass transfer process controls directly the rate of condensation. The driving force of the mass transfer is mainly governed by the concentration difference between the interface and the bulk of vapor which is affected by coupling effects between the heat and mass transfer processes. In the case of channel flows, due to a sink of vapor at the interface, the mass composition, velocity and temperature of the main stream of vapor are to be changed appreciably in the flow direction. This is the inherent features of condensation of binary mixtures in channel flows different from that of condensation on external bodies. In the latter, the driving force of the mass transfer is changed only by the interfacial conditions, whereas in the former it is affected by both conditions of the interface and the main flow.

The present study is concerned with film condensation of binary mixture flows in a vertical channel. A binary mixture of vapors, both components of which are condensable, is introduced into a channel of variable cross-section to flow downward (co-current flow) or upward (counter-current flow). The condensate is formed adjacent to the surface of the cooled wall of the channel, being a binary mixture of the liquid phase, and flows downward along the wall under the action of gravity.

The analytical model employed here consists of a thin liquid-layer flow and an inner vapor flow of binary mixtures. Both flows are assumed to be steady and laminar, having an interfacial boundary of infinitesmally thin thickness. At the interface the

mixture is in the state of liquid-vapor equilibrium. The conditions of transport fluxes and saturation state at the interface couple the flow fields of liquid and vapor mixtures. A fully developed vapor flow at a saturation state corresponding to its temperature and pressure comes into the inlet of the channel. Although the vapor mixture may locally attain to a supersaturation state owing to the temperature and pressure variation in the radial and axial directions as it flows in the channel, no dropwise condensation is assumed to take place in the vapor flow because of its longer relaxation time compared with that of film condensation. At larger Reynolds numbers, the interfacial surface may be agitated by large disturbance waves and ripples. In addition, liquid droplets are torn off from the crests of the waves and deposited onto the film. Studies of heat and mass transfer in this highly complex flow have not yet been undertaken. Although the effects connected with the droplet entrainment are manifold, their magnitude are little understood. In the present study, these effects are ignored.

Due to appreciable change of flow variables in the radial direction, the governing equations of boundary-layer flow type are to be solved rigorously by means of finite difference method at a considerable expense of computer time. Especially for counter-current flows, extensive iteration is required to achieve the satisfication of the boundary conditions at both ends of the channel. In a case of binary gravity-flow film condensation on a vertical flat plate, the integral method to solve such governing equations is shown not to introduce serious errors into the results of condensation features [5]. For internal flow condensations, the integral method seems to be more favorable because of its well-defined integral domain. These facts enable one to use the integral method for the solution of the vapor fileld which affords considerable improvement of the computer economy.

The present work deals with film condensation of binary vapor mixture flows in a vertical circular channel of variable cross-section, using the integral method for the vapor flow and the Nusselt assumption for the liquid film flow. The effect of the channel geometry, the vapor flow speed and direction, the temperature difference of the system, and the type of mixture are studied on the behavior of film condensation. In Chapter 2 the physical and chemical model employed is described to obtain the governing equations and their relevant boundary conditions as well as the phase equilibrium characteristics and the physical properties. In Chapter 3, the method of solution for the flow system is mentioned.

Concerning the inlet condition of the vapor flow, two types of vapor condition are considered. First, in Chapters 4 and 5, a saturated binary vapor mixture with a uniform temperature, hence, a uniform mass fraction is introduced into the channel with a cooled wall. As the flow proceeds, the effect of the cooled wall, that is, the condensation on the wall, penetrates gradually into the vapor flow, making the radial gradient of concentration and temperature decrease at the liquid-vapor interface. Layers of boundary-layer type are formed of concentration and temperature in this region, say, the developing region. After the wall effect has penetrated throughout the vapor flow, say, in the developed region, the radial distribution of concentration

and temperature tends to be less changed in the flow direction. The film condensation associated with these flow conditions shows two different features of developing and developed flows.

When the radial transport of species and energy is sufficiently high compared with the axial transport, their radial distributions may tend to be of the developed profile in a short distance from the flow inlet. This is the case for relatively longer channels or smaller radius channels. The tendency is also promoted with some means employed such as a preliminary cooling. In chapter 6, under these conditions, the inlet condition of the binary mixture is assumed to have the quasi-developed profile of mass fraction and temperature, and effects of the various parameters are studied more perspectively.

In chapter 7, based on the results obtained in the preceding chapters, the general features of film condensation of binary mixtures are discussed from the viewpoint of similarity of the phenomena, and the governing nondimensional parameters are obtained to characterize the condensation process.

2. Physical and Chemical Process of Film Condensation

In the physical situation under consideration, a binary vapor mixture is introduced into the inlet of a vertical channel of radius $R(x)$ with a fully developed velocity profile $U(r)$ and at a (uniform) temperature T_{00} (Fig. 1). As a general case, the concerning binary mixture can be specified to be at a saturation state corresponding to its temperature T_{00} and the inlet pressure P_0, having the mass fraction of the volatile component C_{00}. The flow configurations are shown in Fig. 2. Downward distances are measured in terms of the x-coordinate, and radial distances are denoted by r. The corresponding velocity components are denoted by u and v, respectively. Be-

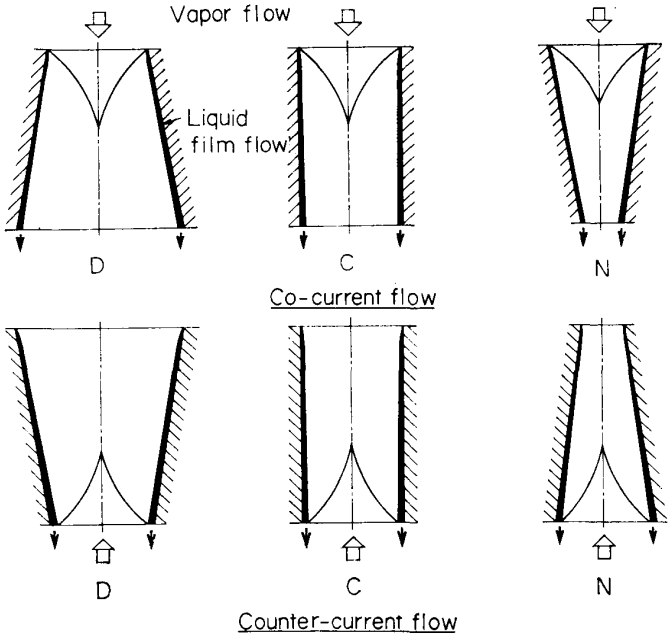

Fig. 1. Flow configurations of film condensation.

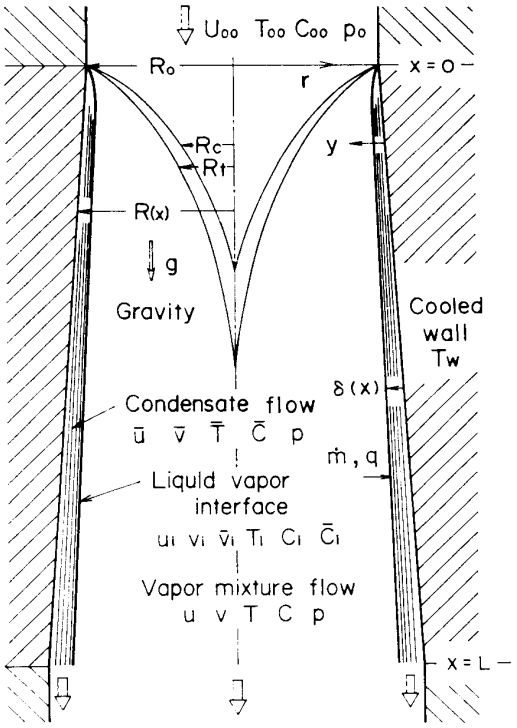

FIG. 2-a. Film condensation of binary mixtures in a vertical channel. (a) Co-current flow.

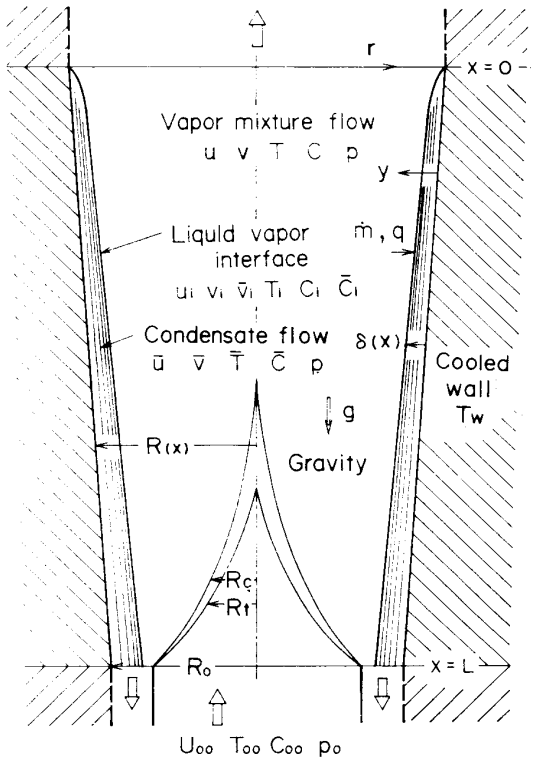

FIG. 2-b. Film condensation of binary mixtures in a vertical channel. (b) Counter-current flow.

tween the inlet and the outlet of the channel, the wall surface is cooled isothermally at a constant temperature T_w.

Flowing through the channel, the vapor condenses outo the surface of the cooled wall. The vapor mixture has the velocity $u(x, r)$, $v(x, r)$, the temperature $T(x, r)$, and the mass fraction of the volatile component $C(x, r)$. The condensate flows downward under the action of gravity force to form a thin liquid layer of thickness $\delta(x)$. The liquid mixture in the film has the velocity $\bar{u}(x, r)$, $\bar{v}(x, r)$, the temperature $\bar{T}(x, r)$, and the mass fraction of the volatile component $\bar{C}(x, r)$, where the superscript ($\bar{}$) refers to the liquid mixture. The condensate film flow is affected additionally by the viscous force of the vapor flow to be accelerated or decelerated owing to the vapor flow direction. Between the condensate and the vapor, there is no relaxation layer assumed from the vapor phase to liquid phase. The interface has thus an infinitesimally thin thickness, and the mixtures are in equilibrium state corresponding to the interfacial temperature T_i and the pressure p. The mass fraction of the volatile component at the interface is denoted by C_i for the vapor phase and $\bar{C}_i$ for the liquid phase.

2.1 *Governing Equations of Mixture Flows*

Because of thin thickness of the liquid film, the variation of flow variables is highly strong across the film compared with that in the axial direction. To account for the transports of species, momentum and energy in the liquid mixture, the governing equation of boundary-layer type can be employed. In the vapor mixture, the diffusive transports in the flow direction are also less effective in comparision with those in the axial direction except for the very short region close to the starting point of condensate flow. Thus, for both flows of the vapor mixture and the condensate, the equations governing conservation of mass, momentum, species and energy are expressed as those of boundary-layer type (Appendix A).

From the fluid-dynamical point of view, it is usefull to express the flow variables in a nondimensional form referred to their appropriate reference values as

$$\frac{\phi}{\phi_{r0}} \rightarrow \phi$$

where ϕ_{r0} is the reference value of the flow variable ϕ. In such a nondimensional form, the governing equations are

$$\frac{\partial}{\partial x}(\rho u)+\frac{1}{r}\frac{\partial}{\partial r}(r\rho v)=0 \tag{2.1}$$

$$\frac{\partial}{\partial x}(\rho uu)+\frac{1}{r}\frac{\partial}{\partial r}(r\rho vu)=-\frac{1}{M_e^2}\frac{dp}{dx}+\frac{Gr}{R_e^2}\rho+\frac{1}{R_e}\frac{1}{r}\frac{\partial}{\partial r}\left(r\mu\frac{\partial u}{\partial r}\right) \tag{2.2}$$

$$\frac{\partial}{\partial x}(\rho uC)+\frac{1}{r}\frac{\partial}{\partial r}(r\rho vC)=\frac{1}{R_eS_c}\frac{1}{r}\frac{\partial}{\partial r}\left(r\rho D\frac{\partial C}{\partial r}\right) \tag{2.3}$$

$$c_p\frac{\partial}{\partial x}(\rho u\theta)+c_p\frac{1}{r}\frac{\partial}{\partial r}(r\rho v\theta)=\frac{1}{R_eP_r}\frac{1}{r}\frac{\partial}{\partial r}\left(rk\frac{\partial\theta}{\partial r}\right)+\frac{1}{R_eS_c}\rho c_p'D\frac{\partial C}{\partial r}\frac{\partial\theta}{\partial r} \tag{2.4}$$

where ρ is the density, p the pressure, C the mass fraction of the volatile conponent, h the enthalpy, g the acceleration of gravity, μ the dynamic coefficient of viscosity, k the thermal conductivity, and D the coefficient of binary diffusion. The second-order effects of thermal diffusion, viscous dissipation and compressible heating are neglected. The pressure is assumed constant across the cross-section due to the assumption of boundary-layer type flow. The nondimensional temperature θ is defined by

$$\theta=\frac{T-T_w}{T_{00}-T_w} \tag{2.5}$$

In Eq. (2.4), c_p is the specific heat at constant pressure defined as

$$c_p=C_1c_{p1}+C_2c_{p2} \qquad c'_p=c_{p1}-c_{p2}$$

where the subscript 1 means the volatile component. The last term on the right hand side of Eq. (2.4) implies energy transport due to the diffusion of species of differing specific heats.

In the above equations, the following properties are chosen as the reference;

$$\begin{array}{lllll} R_0 & U_{00} & T_{00}-T_w & P_0 & \\ \rho_{r0} & \mu_{r0} & k_{r0} & c_{pr0} & D_{r0} \\ \bar{\rho}_{r0} & \bar{\mu}_{r0} & \bar{k}_{r0} & \bar{c}_{pr0} & \bar{D}_{r0} \end{array}$$

where R_0 is the radius of the channel at the flow inlet, U_{00} the center velocity of the vapor mixture at the inlet, T_{00} the vapor temperature at the inlet, T_w the wall temperature. The reference properties for the vapor mixture and the liquid mixture may be evaluated at the state of the inlet flow and the state of the wall temperature, respectively.

The concerning dimensionless parameters relevant to these properties are defined as follows.

$$\begin{array}{llll} R_e=\dfrac{U_{00}R_0}{\nu_{r0}} & P_r=\dfrac{\mu_{r0}c_{pr0}}{k_{r0}} & S_c=\dfrac{\mu_{r0}}{\rho_{r0}D_{r0}} & G_r=\dfrac{gR_0^3}{\nu_{r0}^2} \\ \bar{R}_e=\dfrac{U_{00}R_0}{\bar{\nu}_{r0}} & \bar{P}_r=\dfrac{\bar{\mu}_{r0}\bar{c}_{pr0}}{\bar{k}_{r0}} & \bar{S}_c=\dfrac{\bar{\mu}_{r0}}{\bar{\rho}_{r0}\bar{D}_{r0}} & \bar{G}_r=\dfrac{gR_0^3}{\bar{\nu}_{r0}^2} \\ M_c=\left(\dfrac{\rho_{r0}U_{00}^2}{P_0}\right)^{1/2} & \bar{M}_c=\left(\dfrac{\bar{\rho}_{r0}U_{00}^2}{P_0}\right)^{1/2} & & \\ \rho_r=\dfrac{\rho_{r0}}{\bar{\rho}_{r0}} & \mu_r=\dfrac{\mu_{r0}}{\bar{\mu}_{r0}} & k_r=\dfrac{k_{r0}}{\bar{k}_{r0}} & c_{pr}=\dfrac{c_{pr0}}{\bar{c}_{pr0}} \end{array} \tag{2.6}$$

where ν is the kinematic viscosity ($=\mu/\rho$), R_e the Reynolds number, P_r the Prandtl number, S_c the Schmidt number, G_r the Grashof number, M_c the Mach number.

For turbulent flows, the coefficients of molecular diffusive transports can be replaced formally by those of turbulent transports to obtain the governing equations in the same form (see Chap. 6). However, the turbulent transport coefficients are not well predicted for the flow under consideration. In addition, the assumptions

employed such as no droplet flow and no wavy interface are to be suspicious. By these reasons, most parts of the present study concern laminar flows of vapor mixture as well as liquid mixture.

2.2 *Boundary Conditions of Mixture Flows*

At the flow inlet, $x=0$ for co-current flows, $x=L$ for counter-current flows, the vapor mixture has a fully developed velocity profile with a uniform temperature T_{00} and a saturated mass fraction C_{00}, which can be expressed as

$$\begin{aligned} u&=1-r^2 \\ \theta&=1 \\ C&=C_{00}(T_{00}, P_0) \end{aligned} \tag{2.7}$$

where the velocity is nondimensinalized by the center velocity of the vapor mixture at the inlet U_{00}.

The surface of the channel wall is cooled isothermally at a constant temperature $T_w(<T_{00})$ between $x=0$ and $x=L$. Film condensation starts at $x=0$ with zero film thickness,

$$\delta(0)=0 \tag{2.8}$$

This means that the wall surface preceding the cooled one ($x<0$) should be kept at the same temperature as the vapor. As the transition layer from the vapor phase to the liquid phase, an interface between the liquid and vapor flows with an infinitesmall thickness is assumed at

$$r=R-\delta\equiv R_\delta \tag{2.9}$$

At the interface, the non-slip condition of axial velocity and temperature gives

$$\bar{u}_i=u_i \tag{2.10}$$

$$\bar{\theta}_i=\theta_i \tag{2.11}$$

The transport fluxes of mass, momentum, species and energy from the vapor to the interface must be equal to those passing from the interface to the liquid. The continuity of transport fluxes at the interface can be written as follows (Appendix B).

$$\frac{1}{\rho_r}\left\{\bar{\rho}\left(\bar{v}-\bar{u}\frac{dR_\delta}{dx}\right)\right\}_i=\left\{\rho\left(v-u\frac{dR_\delta}{dx}\right)\right\}_i\equiv\dot{m} \tag{2.12}$$

$$\frac{1}{\mu_r}\left\{\bar{\mu}\frac{\partial\bar{u}}{\partial x}\right\}_i=\left\{\mu\frac{\partial u}{\partial x}\right\}_i \tag{2.13}$$

$$\left\{\dot{m}\bar{C}-\frac{1}{\rho_r\bar{R}_e\bar{S}_c}\left(\bar{\rho}\bar{D}\frac{\partial\bar{C}}{\partial r}\right)\right\}_i=\left\{\dot{m}C-\frac{1}{R_eS_c}\left(\rho D\frac{\partial C}{\partial r}\right)\right\}_i=\dot{m}_c \tag{2.14}$$

$$\left\{-\bar{k}\frac{\partial\bar{\theta}}{\partial r}\right\}_i-k_r\left\{-k\frac{\partial\theta}{\partial r}\right\}_i=\frac{\rho_r\bar{R}_e\bar{P}_r}{H_e}\dot{m}\lambda-\frac{\bar{P}_r}{H_e\bar{S}_c}\left\{(\lambda_1-\lambda_2)\bar{\rho}\bar{D}\frac{\partial\bar{C}}{\partial r}\right\}_i \tag{2.15}$$

where H_e, the Stefan number, is defined as

$$H_e=\frac{\bar{c}_{pr0}(T_{00}-T_w)}{\lambda_{r0}} \tag{2.16}$$

The condensation rate of the vapor mixture per unit area of the interface $\dot{m}$ and the condensation rate of the volatile component per unit area of the interface $\dot{m}_c$ are nondimensionalized by $\rho_{r0}U_{00}$;

$$\frac{\dot{m}}{\rho_{r0}U_{00}}\to\dot{m} \qquad \frac{\dot{m}_c}{\rho_{r0}U_{00}}\to\dot{m}_c$$

The latent heat of vaporization of the mixture based on the liquid state λ is defined as

$$\lambda=\bar{c}_1\lambda_1+\bar{c}_2\lambda_2 \tag{2.17}$$

where λ_i is the latent heat of vaporization of species i,

$$\lambda_i=h_i-\bar{h}_i$$

In addition, the condition of thermodynamic equilibrium at the interface specifies the definite mass fractions of the component vapors and condensed liquids corresponding to the interfacial temperature and pressure,

$$\bar{C}_i=\bar{C}_e(T_i,p) \tag{2.18}$$

$$C_i=C_e(T_i,p) \tag{2.19}$$

The last two equations envolve additional characteristic properties which specify the phase equilibrium (see Eq. 2.24). This fact deteriorates the usefullness of similarity treatment with the dimensionless parameter. Nevertheless, such a dimensionless treatment could be worthwhile to decuce general informations from the systems which are able to be locally similar in the phase equilibrium (see Chapter 7).

The set of these differential equations subject to the boundary conditions at the flow inlet, the wall and the interface provides the solution of film condensation of binary mixture flows in a circular channel. The equations contain thermophysical properties of vapor and liquid mixtures. The evaluation of the relevant thermodynamic and transport properties are to be discussed.

2.4 *Phase Equilibrium of Binary Mixtures*

For a multicomponent, multiphase system in equilibrium, the chemical potential of each component must be the same in each phase in addition to equality of the temperature and pressure. This condition is expressed by equality of fugacities $f_i(=\gamma_i X_i f_{0i})$;

$$\bar{\gamma}_i\bar{X}_i\bar{f}_{0i}=\gamma_i X_i f_{0i}$$

where f_{0i} is the fugacity at the system temperature and pressure, γ_i the activity coefficient and X_i the mole fraction of species i. In terms of the fugacity coefficient $\phi_i=$

$\gamma_i f_{0i}/p$ which is unity for the vapor to behave ideally, these relations can be written as

$$\bar{\gamma}_i \bar{X}_i \bar{f}_{0i} = \phi_i X_i p$$

The fugacity of species i at the system temperature and pressure is obtainable from the value at its own vapor pressure p_{si},

$$\bar{f}_{0si} = \phi_{si} p_{si}$$

with the pressure dependence

$$\frac{\partial}{\partial p}(\ln \bar{f}) = \frac{V}{\mathscr{R}T}$$

where V is the molar volume and $\mathscr{R}$ the universal gas constant. With the assumption that the liquid molar volume is independent of pressure, the fugacity can be obtained as

$$\bar{f}_{0i} = \phi_{si} p_{si} \exp\left\{\frac{V}{\mathscr{R}T}(p - p_{si})\right\}$$

Hence, the equilibrium conditions for binary mixtures are expressed as

$$\phi_i X_i p = \bar{\gamma}_i \bar{X}_i \phi_{si} p_{si} \exp\left\{\frac{V_i}{\mathscr{R}T}(p - p_{si})\right\} \qquad (i = 1, 2)$$

For the binary mixtures under consideration in the present study, these equations can be well approximated by

$$X_i p = \bar{\gamma}_i \bar{X}_i p_{si} \tag{2.20}$$

The activity coefficients for completely miscible binary mixtures are given by the Van Laar equations or the Margules equations. Values of the emprical constants which are involved in these equations are given by Hálá et al. [*13*] for many mixtures at pressures up to 1 atm. They chose values of the constants to give minimum mean errors in prediction of equilibrium concentrations. In the present study, the Van Laar equations are used to obtain the liquid-phase activity coefficients;

$$\log \bar{\gamma}_1 = \frac{A_{12}}{(1 + (A_{12}/A_{21})(\bar{X}_1/\bar{X}_2)^2} \qquad \log \bar{\gamma}_2 = \frac{A_{21}}{(1 + (A_{21}/A_{12})(\bar{X}_2/\bar{X}_1)^2} \tag{2.21}$$

The constants A_{12} and A_{21} are selected from the data by Hálá et al. and shown in Table 1. Their dependency on the pressure, temperature and concentrations are ignored. The vapor pressure of pure component can be given by Antoine equation in the form of

$$\log p_{si} = A_i - \frac{B_i}{T + C_i} \qquad (i = 1, 2) \tag{2.22}$$

The constants A_i, B_i and C_i are also presented in Table 1 [*13*].

TABLE 1. Liquid—vapor equilibrium

(a) Activity coefficients

$$\log \gamma_1 = \frac{A_{12}\bar{X}_2^2}{(\bar{X}_1 A_{12}/A_{21}+\bar{X}_2)^2} \qquad \log \gamma_2 = \frac{A_{21}\bar{X}_1^2}{(\bar{X}_2 A_{21}/A_{12}+\bar{X}_1)^2}$$

Species 1—2	A_{12}	A_{21}
Ethanol—water	0.7236	0.3818
Methanol—water	0.3625	0.2418
Methanol—ethanol	−0.0201	1.2664
Hexane—benzene	0.2704	0.1290
Acetone—water	0.9050	0.6161

(b) Pure—component vapor pressure

$$\log p_{si} = A_i - \frac{B_i}{T+C_i} \quad (p\text{: mmHg, } T\text{: K})$$

Species	A_i	B_i	C_i	T_b (1 atm)
Water	7.96681	1668.210	−45.16	100.0°C
Ethanol	8.16290	1623.220	−44.18	78.3
Methanol	8.07246	1574.990	−34.29	64.7
Hexane	6.87776	1171.530	−48.78	68.7
Benzene	6.90565	1211.033	−52.36	80.1
Acetone	7.23967	1279.870	−35.65	56.2

Combining Eq. (2.20) with Eqs. (2.21) and (2.22) and with the relation

$$X_1+X_2=1 \qquad \bar{X}_1+\bar{X}_2=1 \tag{2.23}$$

gives the equilibrium concentrations of the component vapors and liquids corresponding to the specified pressure and temperature;

$$\bar{X}_1 = \frac{p-\gamma_2 p_{s2}}{\bar{\gamma}_1 p_{s1}-\bar{\gamma}_2 p_{s2}} \qquad X_1 = \frac{1}{1+(\bar{\gamma}_2/\bar{\gamma}_1)(p_{s2}/p_{s1})(\bar{X}_2/\bar{X}_1)} \tag{2.24}$$

The conversion from mole fraction to mass fraction is

$$\bar{C}_1 = \frac{M_1\bar{X}_1}{M_1\bar{X}_1+M_2\bar{X}_2} \qquad C_1 = \frac{M_1 X_1}{M_1 X_1+M_2 X_2} \tag{2.25}$$

where M_1 is the molecular weight of species i.

In order to deal with binary mixtures of different liquid-vapor equilibrium diagrams, the following systems of species combination are considered,

ethanol-water
methanol-water
acetone-water
methanol-ethanol
hexane-benzene

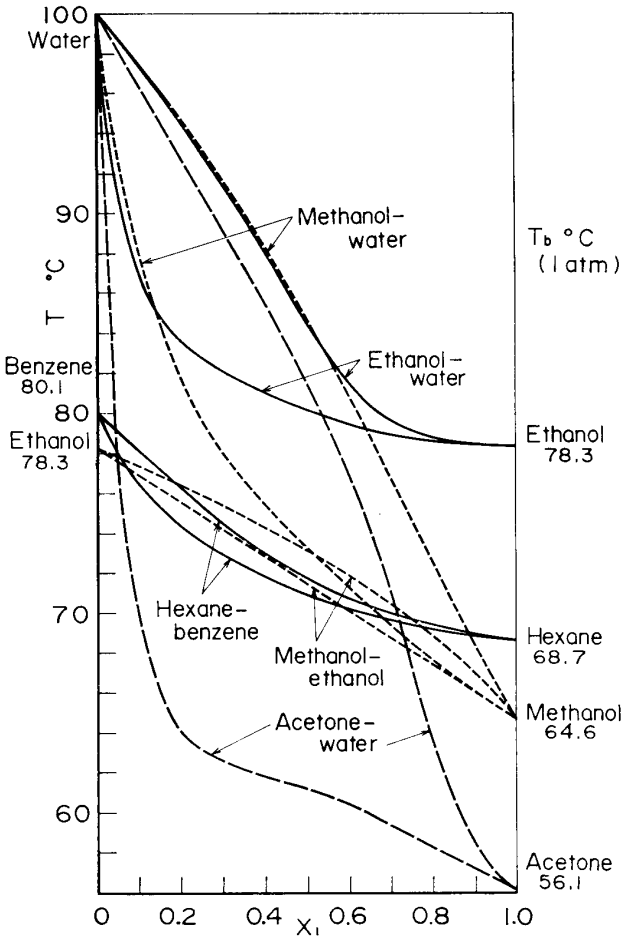

FIG. 3. Liquid-vapor equilibrium diagrams for binary mixtures at one atmosphere; ethanol-water (E-W), methanol-water (M-W), acetone-water (A-W), methanol-ethanol)M-E) and hexane-benzene (H-B).

where the first species is the more volatile component and the mass fraction denoted by C is refered to this component. Equilibrium diagrams calculated by Eq. (2.24) are shown in Fig. 3 for these combinations of species.

2. PHYSICAL PROPERTIES OF BINARY MIXTURES

Viscosity, thermal conductivity and binary diffusion coefficient of binary mixtures can be predicted by the way recommended by Bretsznajder [*14*]. Density, specific heat and latent heat of vaporization also are expressed in terms of the value of pure component. Values of transport and physical properties for pure component are taken from sources in Ref. 15 and fitted algebraically within the temperature range between the boiling temperatures of mixture components at 1 atm. as shown in Tables 2 and 3.

Viscosity For the vapor, the mixture viscosity is evaluated by Wilke's rule,

$$\mu=\frac{\mu_1}{1+(x_1/x_2)\phi_{12}}+\frac{\mu_2}{1+(x_2/x_1)\phi_{21}} \tag{2.26}$$

TABLE 2. Transport properties

Properties			Water	Ethanol	Methanol	Hexane	Benzene	Acetone
Viscosity cp (10^{-2} g/cm s)	Vapor	μ_{i0} (0°C)	8.61×10^{-5}	7.52×10^{-5}	8.65×10^{-5}	5.86×10^{-5}	6.77×10^{-5}	6.60×10^{-5}
	Liquid	α_i	$23.611\times10^{4(1)}$	$-1.145\times10^{4(1)}$	$3.421\times10^{4(1)}$	$3.337\times10^{-4(2)}$	$6.181\times10^{-4(2)}$	$3.115\times10^{-4(2)}$
		β_i	-6.892×10^{2}	7.807×10^{2}	2.750×10^{2}	1.122×10^{-2}	1.861×10^{-2}	1.064×10^{-2}
		γ_i	-0.3908	-2.459	-1.567	3.965×10^{-3}	9.055×10^{-3}	3.945×10^{-3}
Thermal conductivity cal/cm s°C	Vapor	k_{i0} (100°C)	0.60×10^{-4}	0.50×10^{-4}	0.52×10^{-4}	0.47×10^{-4}	0.41×10^{-4}	0.40×10^{-4}
	Liquid	k_{i0} (20°C)	14.30×10^{-4}	4.30×10^{-4}	5.00×10^{-4}	3.30×10^{-4}	3.53×10^{-4}	3.86×10^{-4}
Diffusion coefficient cm^2/s	Vapor	$V_{bi}(T_b)$ cm^3	18.9	63.0	42.5	128.9	91.5	77.5
		C_{si} K	650	407	487	436	448	541
		M_i	18.2	46.07	32.04	26.17	78.11	58.08

NB (1) $\log\bar{\mu}=\alpha/\bar{T}^2+\beta/\bar{T}+\gamma$ (T,K)

(2) $\bar{\mu}=\gamma/(\alpha\bar{t}^2+\beta\bar{t}+1)$ $(t,°C)$

Table 3. Physical properties

Properties			Water	Ethanol	Methanol	Hexane	Benzene	Acetone
Density g/cm³	Liquid	$\bar{a}_{\rho i}$	-3.995×10^{-6}	-0.800×10^{-6}	0	0	0	0
		$\bar{b}_{\rho i}$	2.144×10^{-3}	-3.830×10^{-4}	-1.02×10^{-3}	-1.02×10^{-3}	-1.08×10^{-3}	-1.17×10^{-3}
		$\bar{c}_{\pi i}$	0.7126	0.9703	1.0946	0.9606	1.1960	1.1341
Specific heat cal/g°C	Vapor	a_{ci}	5.971×10^{-6}	0	0	0	0	0
		b_{ci}	-3.561×10^{-3}	7.325×10^{-4}	5.987×10^{-4}	1.0254×10^{-3}	9.204×10^{-4}	7.452×10^{-4}
		c_{ci}	0.9830	0.1626	0.1576	0.1013	−0.0243	0.0938
	Liquid	$\bar{a}_{ci}$	1.725×10^{-6}	0	0	0	0	0
		$\bar{b}_{ci}$	-1.042×10^{-3}	3.119×10^{-3}	1.760×10^{-3}	7.404×10^{-4}	7.022×10^{-4}	7.643×10^{-4}
		$\bar{c}_{ci}$	1.1552	−0.3390	0.0415	0.3149	0.2080	0.2909
Latent heat of vaporization cal/g		$\mathcal{H}B_i$	416.56	154.45	212.10	58.813	68.279	99.340
		C_i	−45.16	−44.18	−34.29	−48.78	−52.36	−35.65

where

$$\phi_{12}=\frac{\{1+(\mu_1/\mu_2)^{1.5}(M_2/M_1)^{0.25}\}^2}{2\sqrt{2}(1+M_1/M_2)^{0.5}} \qquad \phi_{21}=\frac{\{1+(\mu_2/\mu_1)^{0.5}(M_1/M_2)^{0.25}\}^2}{2\sqrt{2}(1+M_1/M_2)^{0.5}}$$

The pure component viscosity μ_i is calculated by the Sutherland equation,

$$\mu_i=\mu_{i0}\frac{T_{i0}+C_{si}}{T+C_{si}}\left(\frac{T}{T_{i0}}\right)^{3/2} \tag{2.27}$$

where μ_{i0} is the viscosity at temperature T_{i0} and C_{si} the Sutherland constants.

For the liquid, the mixture viscosity is estimated by Arrhenius-Kendall equation

$$\log\bar{\mu}=\bar{X}_1\log\bar{\mu}_1+\bar{X}_2\log\bar{\mu}_2 \tag{2.28}$$

where the pure component viscosity of liquid is given by Girifalco equation

$$\log\bar{\mu}_i=\frac{\alpha_i}{\bar{T}^2}+\frac{\beta_i}{\bar{T}}+\gamma_i \tag{2.29}$$

or by the Thorpe-Rodger's equation

$$\bar{\mu}_i=\frac{\gamma_i}{\alpha_i\bar{T}^2+\beta_i\bar{T}+1} \tag{2.29}$$

Thermal conducticity For the vapor mixture, the thermal conductivity is estimated by the principle of additivity

$$k=X_1k_1+X_2k_2 \tag{2.30}$$

where the thermal conductivity of pure component is given by the Sutherland's equation

$$k_i=k_{i0}\frac{T_{i0}+C_{si}}{T+C_{si}}\left(\frac{T}{T_{i0}}\right)^{3/2} \tag{2.31}$$

where k_{i0} is the thermal conductivity at $T=T_{i0}$.

For the liquid mixture, the thermal conductivity is predicted by Filippov and Novoselova's emprical equation

$$\bar{k}=\bar{C}_1\bar{k}_1+\bar{C}_2\bar{k}_2-0.72\bar{C}_1\bar{C}_2(\bar{k}_2-\bar{k}_1) \qquad (k_2>k_1) \tag{2.32}$$

The pure component thermal conductivity $\bar{k}_i$ is given by the Weber equation

$$\bar{k}_i=\bar{k}_{i0}\left(\frac{\bar{\rho}_i}{\bar{\rho}_{i0}}\right)^{4/3} \tag{2.33}$$

where $\bar{k}_{i0}$ and $\bar{\rho}_{i0}$ are the thermal conductivity and the density at $\bar{T}=\bar{T}_{i0}$, respectively.

Binary diffusion coefficient For the vapor, the binary diffusion coefficient is obtained by Arnold's equation which is a modified Suthrland's equation

$$D=\frac{0.00837T^{5/2}}{p(V_{b1}^{1/3}+V_{b2}^{1/3})(T+F\sqrt{C_{s1}C_{s2}})}\left(\frac{M_1+M_2}{M_1M_2}\right)^{1/2} \tag{2.34}$$

where V_{bi} is the molar volume at the normal boiling point and F is a function of V_{b2}/V_{b1}, taken values of $1.0\sim0.9$ for $V_{b2}/V_{b1}=1\sim5$. In the present study with the Nusselt assumption of the liquid film flow, there is no need of the binary diffusion coefficient for the liquid mixture as mentioned later.

Density For the vapor mixture, the density is given by the Gibbs-Dalton law which assumes ideal gas behavior,

$$p=\rho\left(\frac{C_1}{M_1}+\frac{C_2}{M_2}\right)\mathscr{R}T \tag{2.35}$$

The density of liquid mixture is given by

$$\bar{\rho}=\left(\frac{\bar{C}_1}{\bar{\rho}_1}+\frac{\bar{C}_2}{\bar{\rho}_2}\right)^{-1} \tag{2.36}$$

where the pure component density is estimated by the algebraic equation of temperature

$$\bar{\rho}_i=\bar{a}_\rho\bar{T}^2+\bar{b}_\rho\bar{T}+\bar{c}_\rho \tag{2.37}$$

Specific heat For both phases of vapor and liquid, the specific heat of mixture at constant pressure is predicted by the additive rule

$$c_p=C_1c_{p1}+C_2c_{p2} \tag{2.38}$$

$$\bar{c}_p=\bar{C}_1\bar{c}_{p1}+\bar{C}_2\bar{c}_{p2} \tag{2.39}$$

The specific heats of pure component are expressed by

$$c_{pi}=a_{ci}T^2+b_{ci}T+c_{ci} \tag{2.40}$$

$$\bar{c}_{pi}=\bar{a}_{ci}\bar{T}^2+\bar{b}_{ci}\bar{T}+\bar{c}_{ci} \tag{2.41}$$

Latent heat of vaporization The latent heat of vaporization for binary mixture can be expressed as

$$\lambda=\bar{C}_1\lambda_1+\bar{C}_2\lambda_2+h_s-\bar{h}_s \tag{2.42}$$

where λ_i is the latent heat of vaporization of pure component and h_s the heat of solution. By virture of the Clasius-Clapayron relation of the pure-component vapor pressure, the latent heat of the pure component is given by Eq. (2.22) as

$$\lambda_i=\mathscr{R}T^2\frac{d}{dT}(\ln p_{si})=\frac{\mathscr{R}B_i}{(1+C_i/T)^2} \tag{2.43}$$

The heat of solution for binary mixtures is obtained by

$$h_s=x_1h_{s1}+x_2h_{s2} \tag{2.44}$$

where h_{si} is given by using the activity coefficient as

$$h_{si}=-\mathscr{R}T^2\left\{\frac{\partial}{\partial T}(\ln\gamma_i)\right\}_{p,\,x_i} \tag{2.45}$$

The contribution of the heat of solution to the specific heat of mixture is then

$$c_s=x_1\frac{\partial h_{s1}}{\partial T}+x_2\frac{\partial h_{s2}}{\partial T} \tag{2.46}$$

which is negligibly small for the present case. The difference between heats of solution for the vapor and liquid mixtures is given approximately by

$$h_s-\bar{h}_s=-\mathscr{R}T(\bar{X}_1\ln\bar{\gamma}_1+\bar{X}_2\ln\bar{\gamma}_2) \tag{2.47}$$

of which value is of the order less than 5% of the overall latent heat for the present case.

Reference temperature and concentration In the following chapters, the physical properties involved in the governing equations are evaluated at an appropriate reference state to be regarded as constant across the channel. As for such a reference state, although a definitive recommandation is not available, the arithmetic mean state of the center and the interface is chosen for the vapor flow; that is, the properties are evaluated at

$$T=\frac{1}{2}(T_0+T_i)\qquad C=\frac{1}{2}(C_0+C_i) \tag{2.48}$$

For the liquid properties, on the basis of Ref. 2, the reference state is taken as

$$\bar{T}=T_w+\frac{1}{3}(\bar{T}_i-T_w)\qquad \bar{C}=\bar{C}_w+\frac{1}{3}\bar{C}_i-\bar{C}_w) \tag{2.49}$$

3. Method of Solution

The set of governing equations described in the preceding chapter may be solved by means of finite difference methods. However, a significant difficulty remains in the inevitable requirement of extensive computation for such numerical solutions. Fortunately for practical values of liquid flow parameters, it has been found that the convection terms in the conservation equations play a negligible role. Hence, the so-called Nusselt solution can be used for the liquid film flow. From the practical point of view, not detailed informations about the distribution of vapor flow variables but their integrated values at the boundaries are much interested. For this purpose, solutions of the system equations can be examined with the integral method by assuming appropriate distribution profiles for the vapor flow variables.

3.1 *Liquid Film Flow*

As noted later, the Reynolds number of the liquid film flow based on the liquid

volocity at the film surface and the film thickness, $u_i\delta/\bar{\nu}$, takes values less than 10^{-1} for practical flow properties. This means that the convection term has little effect on the conservation equations to be ignored. Because little change in fluid properties is expected across the thin film, they are evaluated at a reference state of temperature and concentration and regarded as constant within the film. By neglecting the convection terms and introducing constant properties and a new coordinate

$$y=R-r \tag{3.1}$$

Eqs. (2.1) to (2.4) are reduced to

$$\frac{\partial \bar{u}}{\partial x}-\frac{\partial \bar{v}}{\partial y}=0 \tag{3.2}$$

$$-\frac{\bar{R}_e}{\bar{M}_c^2}\frac{dp}{dx}+\frac{\bar{G}_r}{\bar{R}_e}\bar{\rho}+\bar{\mu}\frac{\partial^2 \bar{u}}{\partial y^2}=0 \tag{3.3}$$

$$\frac{\partial^2 \bar{C}}{\partial y^2}=0 \tag{3.4}$$

$$\bar{k}\frac{\partial^2 \bar{\theta}}{\partial y^2}+\frac{\bar{P}_s}{\bar{S}_c}\bar{\rho}\bar{c}_p'\bar{D}\frac{\partial \bar{C}}{\partial y}\frac{\partial \bar{\theta}}{\partial y}=0 \tag{3.5}$$

These equations are subject to the boundary conditions at the wall, $y=0$

$$\bar{u}=\bar{v}=0 \qquad \bar{\theta}=0 \qquad \frac{\partial \bar{C}}{\partial y}=0 \tag{3.6}$$

and at the interface, $y=\delta$

$$\bar{u}=\bar{u}_i \qquad \bar{\theta}=\bar{\theta}_i \qquad \bar{C}=\bar{C}_i \tag{3.7}$$

The wall surface is assumed to be impermeable to both components of the mixture. Equations (3.2) to (3.7) yield the following analytical solutions for the velocity, mass fraction and temperature of the condensate flow.

$$\bar{u}=\frac{\delta^2}{2\bar{\mu}}\left(\frac{\bar{R}_e}{\bar{M}_c^2}\frac{dp}{dx}-\frac{\bar{G}_r}{\bar{R}_e}\bar{\rho}\right)\left\{\left(\frac{y}{\delta}\right)^2-\frac{y}{\delta}\right\}+\bar{u}_i\frac{y}{\delta} \tag{3.8}$$

$$\bar{v}=\int_0^y \frac{\partial \bar{u}}{\partial x}dy \tag{3.9}$$

$$\bar{C}=\bar{C}_i \tag{3.10}$$

$$\bar{\theta}=\bar{\theta}_i\frac{y}{\delta} \tag{3.11}$$

where δ is the thickness of the condensate film. It is seen from Eq. (3.10) that the mass fraction is uniformly distributed across the film.

3.2 *Integral Method for the Vapor Flow*

Integration of Eqs. (2.1) to (2.4) with respect to r from the center of the channel ($r=0$) to the interface ($r=R_\delta$) provides the following conservation equations in the integral form.

$$\frac{d}{dx^*}\int_0^{R_\delta}\rho u r dr+\dot{m}^* R_\delta=0 \tag{3.12}$$

$$\frac{d}{dx^*}\int_0^{R_\delta}\rho u u r dr+\dot{m}^* u_i R_\delta=\int_0^{R_\delta}\left(-\frac{1}{M_c^2}\frac{dp}{dx^*}+\frac{G_r S_c}{R_e}\rho\right)r dr+S_c R_\delta\left(\mu\frac{\partial u}{\partial r}\right)_i \tag{3.13}$$

$$\frac{d}{dx^*}\int_0^{R_\delta}\rho u C r dr+\dot{m}^* C_i R_\delta=R_\delta\left(\rho D\frac{\partial C}{\partial r}\right)_i \tag{3.14}$$

$$\frac{d}{dx^*}\int_0^{R_\delta}\rho u c_p\theta r dr+\dot{m}^* c_p\theta_i R_\delta=\frac{S_c}{P_r}R_\delta\left(k\frac{\partial\theta}{\partial r}\right)_i+\int_0^{R_\delta}\rho c_p' D\frac{\partial C}{\partial r}\frac{\partial\theta}{\partial r}r dr \tag{3.15}$$

where

$$x^*=\frac{x}{R_e S_c}\qquad \dot{m}^*=R_e S_c\dot{m}\qquad v^*=R_e S_c v \tag{3.16}$$

These quantities are obtained by inspecting into the governing equations and their boundary conditions, being x, $\dot{m}$ and v nodimensionalized by $U_{00}R_0^2/D_0$, $\rho_0 D_0/R_0$ and D_0/R_0, respectively.

The boundary conditions, Eqs. (2.12) to (2.15), with the solution for the liquid film flow, Eqs. (3.8) to (3.11), are reduced to

$$\frac{1}{\rho_r}\left\{\bar{\rho}\left(\bar{v}^*-\bar{u}\frac{dR_\delta}{dx^*}\right)\right\}_i=\left\{\rho\left(v^*-u\frac{dR_\delta}{dx^*}\right)\right\}_i=\dot{m}^* \tag{3.17}$$

$$\frac{\delta}{2}\left(\frac{\bar{R}_e}{\bar{M}_c^2 R_e S_c}\frac{dp}{dx^*}-\frac{\bar{G}_r}{\bar{R}_e}\bar{\rho}\right)+\bar{\mu}\frac{u_i}{\delta}=-\mu_r\left(\mu\frac{\partial u}{\partial r}\right)_i \tag{3.18}$$

$$\dot{m}^*\bar{C}_i=\dot{m}^* C_i-\left(\rho D\frac{\partial C}{\partial r}\right)_i \tag{3.19}$$

$$\bar{k}\frac{\theta_i}{\delta}+k_r\left(k\frac{\partial\theta}{\partial r}\right)_i=\frac{\rho_r\bar{R}_e\bar{P}_r}{H_e R_e S_c}\dot{m}^*\lambda \tag{3.20}$$

The vapor mixture has a uniform distribution of temperature and concentration in the radial direction at the flow inlet. As the mixture proceeds along the cooled wall, the effect of condensation penetrates gradually into the center of the flow, forming a boundary-layer of concentration and temperature. In this layer the radial distribution of mass fraction and temperature may be assumed to be of a parabolic profile for the purpose of the integral method;

$$C=\begin{cases} C_0 & 0\leqslant r\leqslant R_c \\ C_0+(C_i-C_0)\left(\dfrac{r-R_c}{R_\delta-R_c}\right)^2 & R_c\leqslant r\leqslant R_\delta \end{cases}$$
$$\theta=\begin{cases} \theta_0 & 0\leqslant r\leqslant R_t \\ \theta_0+(\theta_i-\theta_0)\left(\dfrac{r-R_t}{R_\delta-R_t}\right)^2 & R_t\leqslant r\leqslant R_\delta \end{cases} \tag{3.21}$$

R_c and R_t may be called as the radius of the concentration and temperature layer, respectively; $R_\delta-R_c$ and $R_\delta-R_t$ are the thickness of the layers. The mass fraction and temperature at the center, C_0 and θ_0, are kept unchanged until the layer reaches the center, say, in the developing region ($R_c>0$, $R_t>0$). Beyond the distance at which the layer extends throughout the cross-section of the flow passage, say, in the developed region ($R_c=0$, $R_t=0$), they are forced to change in the flow direction. In the developing region

$$\begin{aligned} R_c&=R_c(x)>0 \qquad & C_0&=C_{00} \\ R_t&=R_t(x)>0 \qquad & \theta_0&=\theta_{00} \end{aligned} \tag{3.22}$$

and in the developed region

$$\begin{aligned} R_c&=0 \qquad & C_0&=C_0(x) \\ R_t&=0 \qquad & \theta_0&=\theta_i(x) \end{aligned} \tag{3.23}$$

Corresponding to Eq. (3.21), the radial distribution of velocity may be assumed as

$$u=u_0+(u_i-u_0)\left(\frac{r}{R_\delta}\right)^2 \tag{3.24}$$

where at the flow inlet

$$u_0=1 \qquad u_i=0 \tag{3.25}$$

With this radial distribution of velocity, mass fraction and temperature, the integrals in Eqs. (3.12) to (3.15) are expressed in terms of their values at the center and the interface, if the involved physical properties are evaluated at an approximate reference state as constant across the vapor flow. Then, Eqs. (3.12) to (3.15) are reduced to ordinary differential equations with respect to x. The resulted ordinary equations provide the axial change of characteristic flow variables; R_c, R_t, u_0 and p in the developing region, and C_0, θ_0, u_0 and p in the developed region.

The integral equation of concentration, Eq. (3.14), with the mass fraction profile, Eq. (3.21), determines the radius of the concentration layer R_c for the developing flow and the mass fraction at the center C_0 for the developed flow.

R_c: By using the continuity equation Eq. (3.11) and the relation

$$\int_0^{R_\delta} uCrdr=\int_0^{R_\delta} uC_0rdr+\int_{R_c}^{R_\delta}(C_i-C_0)\left(\frac{r-R_c}{R_\delta-R_c}\right)^2 urdr$$

Eq. (3.14) can be reduced to

$$\frac{d}{dx^*}\int_{R_c}^{R_\delta}\rho(C_i-C_0)\left(\frac{r-R_c}{R_\delta-R_c}\right)^2 urdr+\dot{m}^*(C_i-C_0)R_\delta=R_\delta\left(\rho D\frac{\partial C}{\partial r}\right)_i \tag{3.26}$$

The integral on the left hand side is written as

$$\int_{R_c}^{R_\delta}\left(\frac{r-R_c}{R_\delta-R_c}\right)^2 urdr=R_\delta^2\left\{\frac{u_0-u_i}{60}(Y_c-1)^2(Y_c^2+4Y_c+5)-\frac{u_i}{12}(Y_c^2+2Y_c-3)\right\}$$

where

$$Y_c=\frac{R_c}{R_\delta} \tag{3.27}$$

Hence, Eq. (3.26) becomes

$$\frac{d}{dx^*}\left[\rho(C_i-C_0)R_\delta^2\left\{\frac{u_0-u_i}{60}(Y_c-1)^2(Y_c^2+4Y_c+5)-\frac{u_i}{12}(Y_c^2+2Y_c-3)\right\}\right]$$
$$=(C_i-C_0)\left(\frac{2\rho D}{1-Y_c}-\dot{m}^*R_\delta\right) \tag{3.28}$$

from which R_c is obtainable.

C_0: Eqs. (3.14) and (3.21) with $R_c=0$ give

$$\frac{d}{dx^*}\left[\frac{\rho}{12}R_\delta^2\{(2u_0+u_i)C_0+(u_0+2u_i)C_i\}\right]=-\dot{m}^*\bar{C}_iR_\delta \tag{3.29}$$

which determines the axial change in C_0.

Similarly, the integral equation of energy, Eq. (3.15), with the temperature profile, Eq. (3.21), gives the radius of the temperature layer R_t for the developing flow and the temperature at the center θ_0 for the developed flow.

R_t: With the continuity equation Eq. (3.12) and the relation

$$\int_0^{R_\delta}u\theta rdr=\int_0^{R_\delta}u\theta_0 rdr+\int_{R_t}^{R_\delta}(\theta_i-\theta_0)\left(\frac{r-R_t}{R_\delta-R_t}\right)^2 urdr$$

Eq. (3.15) becomes

$$\frac{d}{dx^*}\int_{R_t}^{R_\delta}\rho c_p(\theta_i-\theta_0)\left(\frac{r-R_t}{R_\delta-R_t}\right)^2 urdr+\dot{m}^*c_p(\theta_i-\theta_0)R_\delta$$
$$=\frac{S_c}{P_r}R_\delta\left(k\frac{\partial\theta}{\partial r}\right)_i+\int_{R_c}^{R_\delta}\rho c_p' D\frac{\partial C}{\partial r}\frac{\partial\theta}{\partial r}rdr \tag{3.30}$$

The integrals involved are expressed as

$$\int_{R_t}^{R_\delta}\left(\frac{r-R_t}{R_\delta-R_t}\right)^2 urdr=R_\delta^2\left\{\frac{u_0-u_i}{60}(Y_t-1)^2(Y_t^2+4Y_t+5)-\frac{u_i}{12}(Y_t^2+2Y_t-3)\right.$$

$$\int_{R_c}^{R_\delta}\frac{\partial C}{\partial r}\frac{\partial\theta}{\partial r}rdr=4(C_i-C_0)(\theta_i-\theta_0)\left(\frac{1-Y_t}{1-Y_c}\right)^2 \cdot\left[\frac{Y_t-Y_c}{1-Y_c}\left\{\frac{Y_t}{1-Y_t}\frac{1-\sigma^2}{2}+\frac{1-\sigma^3}{3}\right\}+\left\{\frac{Y_t}{1-Y_t}\frac{1-\sigma^3}{3}+\frac{1-\sigma^4}{4}\right\}\right] \equiv(C_i-C_0)(\theta_i-\theta_0)S_{tc}$$

where

$$Y_t=\frac{R_t}{R_\delta} \tag{3.31}$$

$$\sigma=\begin{cases}0 & R_c\leqslant R_t\\ \dfrac{Y_c-Y_t}{1-Y_t} & R_c\geqslant R_t\end{cases}$$

Then, Eq. (3.30) is rewritten as

$$\frac{d}{dx^*}\left[\rho c_p(\theta_i-\theta_0)R_\delta^2\left\{\frac{u_0-u_i}{60}(Y_t-1)^2(Y_t^2+4Y_t+5)-\frac{u_i}{12}(Y_t^2+2Y_t-3)\right\}\right] =(\theta_i-\theta_0)R_\delta\left\{\frac{S_c}{P_r}\frac{2k}{R_\delta-R_t}-\dot m^*c_p\right\}+\rho c_p'D(C_i-C_0)(\theta_i-\theta_c)S_{tc} \tag{3.32}$$

which gives the axial change of R_t,

θ_0: Eqs. (3.15) and (3.21) with $R_t=0$ lead to

$$\frac{d}{dx^*}\left[\frac{\rho c_p}{12}R_\delta^2\{(2u_0+u_i)\theta_0+(u_0+2u_i)\theta_i\}\right] =R_\delta\left\{\frac{2kS_c}{P_r}\frac{\theta_i-\theta_0}{R_\delta}-\dot m^*c_p\theta_i\right\}+\rho c_p'D(C_i-C_0)(\theta_i-\theta_0) \tag{3.33}$$

which determines the temperature at the center θ_0.

u_0: The integral equation of continuity Eq. (3.12) with the velocity profile Eq. (3.24) gives the axial velocity at the center u_0,

$$\frac{d}{dx^*}\left[R_\delta^2\left\{\frac{\rho_r}{4}\rho(u_0+u_i)+\frac{1}{3}\bar\rho\frac{\delta}{R_\delta}\left(2u_i-\mu_r\frac{\mu}{\bar\mu}\frac{u_0-u_i}{R_\delta}\delta\right)\right\}\right]=0 \tag{3.34}$$

which is subject to the boundary condition that $u_0=1$ at $x^*=0$ for co-current flows or at $x^*=L/(R_eS_c)$ for counter-current flows.

p: The axial change of the pressure can be calculated by the integral equation of motion Eq. (3.13) with the velocity profile Eq. (3.24),

$$\left(1+\frac{\delta}{R_\delta}\right)\frac{R_\delta^2}{2M_e^2}\frac{dp}{dx^*}=\frac{\bar G_r R_eS_c}{2\bar R_e^2}R_\delta^2\left(\rho+\frac{\bar\rho}{\rho_r}\frac{\delta}{R_\delta}\right) -\frac{d}{dx^*}\left\{\frac{\rho}{6}R_\delta^2(u_0^2+u_0u_i+u_i^2)\right\}-u_i\left(\dot m^*R_\delta+S_c\frac{\bar\mu}{\mu_r}\frac{R_\delta}{\delta}\right) \tag{3.35}$$

of which boundary condition is $p=1$ at $x^*=0$ for co-current flows or at $x^*=L/(R_eS_c)$ for counter-current flows.

u_i: The continuity condition of shearing stress at the interface Eq. (3.18) with Eq. (3.24) gives the interfacial velocity,

$$u_i\left(1+2\mu_r\frac{\mu}{\bar{\mu}}\frac{\delta}{R_\delta}\right)=\frac{\delta^2}{2\bar{\mu}}\left(\frac{\bar{G}_r}{\bar{R}_e}\bar{\rho}-\frac{\bar{R}_e}{\bar{M}_c^2R_eS_c}\frac{dp}{dx^*}\right)+2\mu_r\frac{\mu}{\bar{\mu}}\frac{\delta}{R_\delta}u_0 \tag{3.36}$$

θ_i: The interfacial temperature is given by the continuity of energy flux at the interface Eq. (3.20)

$$\theta_i\left(1+2k_r\frac{k}{\bar{k}}\frac{\delta}{R_\delta-R_t}\right)=2k_r\frac{k}{\bar{k}}\frac{\delta}{R_\delta-R_t}\theta_0+\frac{\rho_r\bar{R}_e\bar{P}_r}{H_eR_eS_c}\frac{\lambda\delta}{k}\dot{m}^* \tag{3.37}$$

C_i, $\bar{C}_i$: The mass fractions at the interface are obtained by the phase equilibrium Eqs. (2.20) to (2.24) corresponding to the interfacial temperature.

$\dot{m}^*$: The mass flux of the condensate or the condensation rate per unit area of the interface $\dot{m}^*$ is expressed by the continuity condition of mass, species and energy, Eqs. (3.17), (3.19) and (3.20), respectively;

$$\dot{m}^*=\frac{1}{\rho_rR_\delta}\frac{d}{dx^*}\left[\rho\delta R\left\{\frac{\delta^2}{3\bar{\mu}}\left(\frac{\bar{G}_r}{\bar{R}_e}\bar{\rho}-\frac{\bar{R}_e}{\bar{M}_c^2R_eS_c}\frac{dp}{dx^*}\right)+\mu_r\frac{\mu}{\bar{\mu}}\frac{\delta}{R_\delta}u_0\right\}\right] \tag{3.38}$$

$$\dot{m}^*=\frac{2\rho D}{R_\delta-R_c}\frac{C_i-C_0}{C_i-\bar{C}_i} \tag{3.39}$$

$$\dot{m}^*=\frac{H_eR_eS_c}{\rho_r\bar{R}_e\bar{P}_r}\frac{1}{\lambda}\left\{\frac{\bar{k}}{\delta}\theta_i+2k_r\frac{k}{R_\delta-R_t}(\theta_i-\theta_0)\right\} \tag{3.40}$$

These expressions relate the condensation rate to the velocities, mass fractions and temperatures at the center and the interface, respectively.

δ: The film thickness can be obtained by solving Eq. (3.38) with Eq. (3.40),

$$\begin{aligned}\delta\frac{d}{dx^*}&\left[R\left\{\frac{\bar{\rho}}{3\bar{\mu}}\left(\bar{G}_r\bar{\rho}-\frac{\bar{R}_e^2}{\bar{M}_c^2R_eS_c}\frac{dp}{dx^*}\right)\delta^3+\mu_r\bar{R}_e\bar{\rho}\frac{\mu}{\bar{\mu}}\frac{u_0}{R_\delta}\delta^2\right\}\right]\\&=\frac{H_eR_eS_c}{\bar{P}_r}\frac{R_\delta}{\lambda}\left\{\bar{k}\theta_i+2k_rk(\theta_i-\theta_0)\frac{\delta}{R_\delta-R_t}\right\}\end{aligned} \tag{3.41}$$

which is subject to the boundary condition $\delta=0$ at $x^*=0$. It should be noted that, when $u_0=0$, $dp/dx=0$ and $\theta_i=\theta_0$, Eqs. (3.41) leads to the classical Nusselt solution,

$$\frac{\delta}{x}=\left(\frac{4H_e}{\bar{G}_r\bar{P}_rx^3}\right)^{1/4} \tag{3.42}$$

$\dot{m}_c^*$, q: The condensation rate of the volatile component $\dot{m}_c{}^*$ and the heat flux q per unit area of the interface are given by

$$\dot{m}_c^*=\dot{m}^*C_i \tag{3.43}$$

$$q=\bar{k}\frac{\theta_i}{\delta} \tag{3.44}$$

where $\dot{m}_c^*$ and q are nondimensionalized by $\rho_0 U_{00}/(R_e S_c)=\rho_0 D_0/R_0$ and $k_0(T_{00}-T_w)/R_0$, respectively.

The set of this ordinary differential equations coupled with the flow variables at the interface provides the solution of the film condensation of binary mixtures in a circular channel. The equations require the starting conditions at $x=0$ for co-current flows or at $x=L$ for counter-current flows where they tend to have some singular solutions. Because of the assumption of boundary layer type flow, the validity of the equations deteriorates very close to the starting point of condensation. To solve the equations, such singularities must be appropriately manipulated, although they have not a considerable influence on the behavior of condensation far from the starting point.

4. Co-current Flow Film Condensation

The vapor mixture of binary components is introduced downward into a vertical circular channel, having a uniform temperature T_{00} and an uniform mass fraction of the volatile component C_{00} (Fig. 2-a). Ahead of the cooled wall, the channel has a wall kept at temperature T_{00}, and from the point $x=0$ the wall is cooled isothermally at a constant temperature T_w. Film condensation starts at $x=0$, and the condensate flows downward along the wall, forming a thin liquid layer. At the interface between the liquid and the vapor, the fluids are in equilibrium state corresponding to the local temperature and pressure. The vapor-flow forms a boundary-layer type flow along the interface. At the point $x=0$, the governing equations have a singularity due to $\delta=0$ which makes it difficult to proceed in a direct numerical computation of the equations. To deal with such a singularity, the behavior of solutions close to the starting point must be examined. Using the result as the starting condition, the numerical computation can start into run.

4.1 *Behavior of Solutions Close to the Flow Inlet*

From Eqs. (3.39) and (3.40), it is seen that the condensation rate and the heat fluxes from the vapor to the interface and from the interface to the liquid go to infinity at the point $x=0$ where $(R_\delta-R_c)$, $(R_\delta-R_t)$ and δ tend to zero. However, if these singularities are of the same order, definite solutions can be expected close to $x=0$.

Conservation equations of species and energy, Eqs. (3.28) and (3.32) are rewritten as, respectively,

$$\frac{1}{60}\frac{1}{C_i-C_0}\frac{d}{dx^*}[\rho R_\delta^2(C_i-C_0)\{u_0(1-Y_c)^2(Y_c^2+4Y_c+5)$$
$$+u_i(1-Y_c)(Y_c^3+3Y_c^2+6Y_c+10)\}]=\frac{2\rho D}{1-Y_c}-\dot{m}^* R_\delta \tag{4.1}$$

$$\frac{1}{60}\frac{1}{\theta_i-\theta_0}\frac{d}{dx^*}[\rho c_p R_\delta^2(\theta_i-\theta_0)\{u_0(1-Y_t)^2(Y_t^2+4Y_t+5)$$
$$+u_i(1-Y_t)(Y_t^3+3Y_t^2+6Y_t+10)\}]=\frac{S_c}{P_r}\frac{2k}{1-Y_t}-\dot{m}^* c_p R_\delta+\frac{\rho c_p' D}{\theta_i-\theta_0}S_{tc} \quad (4.2)$$

Close to $x=0$, the radii of concentration and temperature layers can be assumed to take the following form,

$$Y_c=\frac{R_c}{R_\delta}=1-a_c x^{*n} \qquad Y_t=\frac{R_t}{R_\delta}=1-a_t x^{*m} \quad (4.3)$$

With Eq. (4.3), Eqs. (4.1) and (4.2) yield

$$na_c x^{*n-1}(a_c x^{*n}u_0+u_i)$$
$$=\frac{3}{\rho R_\delta^2}\left(\frac{2\rho D}{a_c x^{*n}}-\frac{2\rho D}{a_c x^{*n}}\frac{C_i-C_0}{C_i-\bar{C}_i}\right)-a_c x^{*n}\frac{du_i}{dx^*}$$
$$-\left\{\frac{1}{2}(a_c x^{*n})^2 u_0+a_c x^{*n}u_i\right\}\frac{d}{dx^*}\ln\{\rho R_\delta^2(C_i-C_0)\} \quad (4.4)$$

$$ma_t x^{*m-1}(a_t x^{*m}u_0+u_i)$$
$$=\frac{3}{\rho c_p R_\delta^2}\left(\frac{S_c}{P_r}\frac{2k}{a_t x^{*m}}-\frac{2\rho D}{a_c x^{*n}}\frac{C_i-C_0}{C_i-\bar{C}_i}\right)-a_t x^{*m}\frac{du_i}{dx^*}$$
$$-\left\{\frac{1}{2}(a_c x^{*m})^2 u_0+a_c x^{*m}u_i\right\}\frac{d}{dx^*}\ln\{\rho c_p R_\delta^2(\theta_i-\theta_0)\}+S_{tc}' \quad (4.5)$$

where S_{tc}' means the contribution from the term of S_{tc}. As $x^*\to 0$, predominant terms in these equations lead to

$$na_c^3 x^{*3n-1}u_0=\frac{6\rho D}{\rho R_\delta^2}\left(1-\frac{C_i-C_0}{C_i-\bar{C}_i}\right) \quad (4.6)$$

$$ma_t^3 x^{*3m-1}u_0=\frac{6k}{\rho c_p R_\delta^2}\left(\frac{S_c}{P_r}-\frac{\rho D}{k}\frac{C_i-C_0}{C_i-\bar{C}_i}\frac{a_t}{a_c}x^{*m-n}\right) \quad (4.7)$$

From the inspection into the above equations, one obtains

$$m=n=\frac{1}{3} \quad (4.8)$$

$$a_c^3=\frac{18\rho D}{\rho R_\delta^2 u_0}\frac{C_0-\bar{C}_i}{C_i-\bar{C}_i}\simeq 18\frac{C_0-\bar{C}_i}{C_i-\bar{C}_i} \quad (4.9)$$

$$a_t^3=\frac{18k}{\rho c_p R_\delta^2 u_0}\left(\frac{S_c}{P_r}-\frac{\rho D}{k}\frac{C_i-C_0}{C_i-\bar{C}_i}\frac{a_t}{a_c}\right)\simeq 18\left(\frac{S_c}{P_r}-\frac{C_i-C_0}{C_i-\bar{C}_i}\frac{a_t}{a_c}\right) \quad (4.10)$$

By assuming the liquid film thickness as

$$\delta=a_\delta x^{*l} \quad (4.11)$$

Eq. (3.41) is reduced to

$$a_\delta^4 x^{*4l}\left(\frac{d}{dx^*}+\frac{3l}{x^*}\right)\left\{\frac{\bar{\rho}R}{3\bar{\mu}}\left(\bar{G}_r\bar{\rho}-\frac{\bar{R}_e^2}{\bar{M}_c^2 R_e S_c}\frac{dp}{dx^*}\right)\right\}$$
$$+a_\delta^3 x^{*3l}\left(\frac{d}{dx^*}+\frac{2l}{x^*}\right)\left(\mu_r\frac{\mu}{\bar{\mu}}\frac{\bar{R}_e}{R_\delta}\bar{\rho}Ru_0\right)$$
$$=\frac{H_e R_e S_c}{\bar{P}_r}\frac{R_\delta}{\lambda}\left\{\bar{k}\theta_i+2k_r\frac{k}{R_\delta}(\theta_i-\theta_0)\frac{a_\delta}{a_t}x^{*l-m}\right\} \tag{4.12}$$

For $x^*\to 0$, the above equation gives

$$l=\frac{1}{3} \tag{4.13}$$

$$\frac{2}{3}a_\delta^3\left(\mu_r\frac{\mu}{\bar{\mu}}\frac{\bar{R}_e}{R_\delta}\bar{\rho}\bar{R}u_0\right)=\frac{H_e R_e S_c}{\bar{P}_r}\frac{R_\delta}{\lambda}\left\{\bar{k}\theta_i+2k_r\frac{k}{R_\delta}(\theta_i-\theta_0)\frac{a_\delta}{a_t}\right\} \tag{4.14}$$

The growth rate of film thickness is then given by

$$a_\delta^3=\frac{3}{2}\frac{H_e R_e S_c}{\mu_r \bar{R}_e \bar{P}_r}\theta_i \tag{4.15}$$

The interfacial temperature can be obtained by Eq. (3.37),

$$\theta_i=\frac{2\mu_r\bar{P}_r}{H_e S_c}\frac{a_\delta}{a_c}\frac{C_i-C_0}{C_i-\bar{C}_i} \tag{4.16}$$

The interfacial velocity is given by Eq. (3.36),

$$u_i=2\mu_r a_\delta x^{*1/3} \tag{4.17}$$

The condensation rate is given by Eq. (3.39)

$$\dot{m}^*=\left(\frac{4}{9x^*}\right)^{1/3}\frac{C_i-C_0}{C_i-\bar{C}_i}\left(\frac{C_i-\bar{C}_i}{C_0-\bar{C}_i}\right)^{1/3} \tag{4.18}$$

From Eqs. (4.9), (4.15) to (4.17), one obtains the following solution close to the flow inlet;

$$\theta_i=\sqrt{\frac{2}{3}\rho_r\mu_r}\frac{\bar{P}_r}{H_e S_c}\frac{C_i-C_0}{C_i-\bar{C}_i}\left(\frac{C_i-C_0}{C_0-\bar{C}_i}\right)^{1/2} \tag{4.19}$$

$$u_i=2\sqrt{\rho_r\mu_r}\left\{\sqrt{\frac{3}{2}}\frac{C_i-C_0}{C_i-\bar{C}_i}\left(\frac{C_i-C_0}{C_0-\bar{C}_i}\right)^{1/2}x^*\right\}^{1/3} \tag{4.20}$$

$$\delta=\sqrt{\frac{\rho_r}{\mu_r}}\left\{\sqrt{\frac{1}{2}}\frac{C_i-C_0}{C_i-\bar{C}_i}\left(\frac{C_i-C_0}{C_i-\bar{C}_i}\right)^{1/2}x^*\right)^{1/3} \tag{4.21}$$

$$R_c=1-\left(18\frac{C_0-\bar{C}_i}{C_i-\bar{C}_i}x^*\right)^{1/3} \tag{4.22}$$

$$R_t=1-\left[\frac{18S_c}{P_r}\left\{1-\frac{C_i-C_0}{C_i-\bar{C}_i}\left(\frac{P_r}{S_c}\right)^{2/3}\right\}x^*\right]^{1/3} \tag{4.23}$$

4.2 *Numerical Procedures*

The system condition is specified by

U_{00}: the inlet flow velocity at the center,
T_{00}: the inlet flow temperature,
P_0: the inlet flow pressure,
T_w: the colled-wall temperature,
$R(x)$: the channel geometry, and
the type of binary mixture.

The composition of the incoming mixture flow is determined by the equilibrium condition corresponding to the inlet flow temperature. With these specified values, the relevant dimensionless parameters are evaluated. For this purpose, it is practical to use physical properties evaluated at T_{00} for the vapor and at T_w for the liquid.

The results obtained in the preceding section give the starting condition at a certain point close to $x=0$. Then, the ordinary differential equations coupled with the boundary conditions at the interface are solved by means of finite difference method with respect to the flow direction. Because of nonlinear coupling of flow variables, an iterative procedure is required at each axial marching step. From the view-point of numerical technique, the iteration at each axial step is not always necessary. However, when the iteration is not employed, excessively small marching steps are required to obtain sufficient accurate solutions. Once a sufficient convergence of iteration is established, the numerical solution is advanced axially step by step.

For the computational purpose, it is convenient to express the radius of the concentration layer by Eq. (3.28) as

$$Y_c=1-\left[\frac{60}{(u_0-u_i)(Y_c^2+4Y_c+5)}\left\{\frac{\int_0^{x^*}A_c dx^*}{\rho(C_i-C_0)R_\delta^2}-\frac{u_i}{12}(1-Y_c)^2(Y_c+3)\right\}\right]^{1/3} \tag{4.24}$$

$$A_c\equiv(C_i-C_0)\left\{2\rho D-\dot{m}^*R_\delta(1-Y_c)+B_c\frac{dY_c}{dx^*}\right\}$$

$$B_c\equiv\rho R_\delta^2\left\{\frac{u_0-u_i}{60}(Y_c-1)^2(Y_c^2+4Y_c+5)+\frac{u_i}{12}(1-Y_c)(Y_c+3)\right\}$$

and the radius of the temperature layer by Eq. (3.32) as

$$Y_t=1-\left[\frac{60}{(u_0-u_i)(Y_t^2+4Y_t+5)}\left\{\frac{\int_0^{x^*}A_t dx^*}{\rho c_p(\theta_i-\theta_0)R_\delta^2}-\frac{u_i}{12}(1-Y_t)^2(Y_t+3)\right\}\right]^{1/3} \tag{4.25}$$

$$A_t\equiv(\theta_i-\theta_0)\left\{2k\frac{S_c}{P_r}+\rho c_p' DS_{tc}(1-Y_t)-\dot{m}^*c_pR_\delta(1-Y_t)+B_t\frac{dY_t}{dx^*}\right\}$$

$$B_t \equiv \rho c_p R_\delta^2 \left\{ \frac{u_0 - u_i}{60}(Y_t - 1)^2(Y_t^2 + 4Y_t + 5) + \frac{u_i}{12}(1 - Y_t)(Y_t + 3) \right\}$$

When these radii go to zero, the mass fraction and temperature at the center of the channel are forced to change in the axial direction. The mass fraction C_0 is given by Eq. (3.29),

$$\frac{\rho}{12} R_\delta^2 \{(2u_0 + u_i)C_0 + (u_0 + 2u_i)C_i\}$$
$$= \left[\frac{\rho}{12} R_\delta^2 \{(2u_0 + u_i)C_0 + (u_0 + 2u_i)C_i\} \right]_{x_{c0}^*} - \int_{x_{c0}^*}^{x^*} \dot{m}^* \bar{C}_i R_\delta dx^* \qquad (4.26)$$

where x_{c0}^* is the axial distance at which $R_c = 0$. The temperature θ_0 is obtained by Eq. (3.33).

$$\frac{\rho c_p}{12} R_\delta^2 \{(2u_0 + u_i)\theta_0 + (u_0 + 2u_i)\theta_i\}$$
$$= \left[\frac{\rho c_p}{12} R_\delta^2 \{(2u_0 + u_i)\theta_0 + (u_0 + 2u_i)\theta_i\} \right]_{x_{t0}^*}$$
$$+ \int_{x_{t0}^*}^{x^*} \left\{ \frac{2kS_c}{P_r}(\theta_i - \theta_0) - \dot{m}^* c_p \theta_i R_\delta - \rho c_p' D R_\delta^2 (C_i - C_0)(\theta_i - \theta_0) \right\} dx^* \qquad (4.27)$$

where x_{t0}^* is the axial distance at which $R_t = 0$.

The center velocity u_0 is calculated by Eq. (3.34),

$$R_\delta^2 \left[\frac{\rho_r}{4} \rho (u_0 + u_i) + \frac{\bar{\rho}\delta}{3R_\delta} \left\{ 2u_i - \mu_r \frac{\mu\delta}{\bar{\mu} R_\delta}(u_0 - u_i) \right\} \right] = \frac{\rho_r}{4} \qquad (4.28)$$

and the film thickness δ is given by Eq. (3.41),

$$\left\{ \frac{\bar{\rho}}{3\bar{\mu}} R \left(\bar{G}_r \bar{\rho} - \frac{\bar{R}_e^2}{\bar{M}_c^2 R_e S_c} \frac{dp}{dx^*} \right) \right\} \delta^4 + \left(\mu_r \bar{R}_e \bar{\rho} \frac{\mu}{\bar{\mu}} \frac{R}{R_\delta} u_0 \delta \right) \delta^2$$
$$= \int_0^{x^*} \left\{ \frac{H_e R_e S_c}{\bar{P}_r} \frac{R_\delta}{\lambda} \left(\bar{k}\theta_i + 2k_r k \delta \frac{\theta_i - \theta_0}{R_\delta - R_t} \right) + B_\delta \frac{d\delta}{dx^*} \right\} dx^* \qquad (4.29)$$

where

$$B_\delta = \left\{ \frac{\bar{\rho}}{3\bar{\mu}} R \left(\bar{G}_r \bar{\rho} - \frac{\bar{R}_e^2}{\bar{M}_c^2 R_e S_c} \frac{dp}{dx^*} \right) \right\} \delta^3 + \left(\mu_t \bar{R}_e \bar{\rho} \frac{\mu}{\bar{\mu}} \frac{R}{R_\delta} u_0 \delta \right) \delta$$

The velocity and temperature at the interface are given by Eqs. (3.36) and (3.37), respectively,

$$u_i \left(1 + 2\mu_r \frac{\mu}{\bar{\mu}} \frac{\delta}{R_\delta} \right) = \frac{\delta^2}{2\bar{\mu}} \left(\frac{\bar{G}_r}{\bar{R}_e} \bar{\rho} - \frac{\bar{R}_e}{\bar{M}_c R_e S_c} \frac{dp}{dx^*} \right) + 2\mu_r \frac{\mu}{\bar{\mu}} \frac{\delta}{R_\delta} u_0 \qquad (4.30)$$

$$\theta_i \left(1 + 2k_r \frac{k}{\bar{k}} \frac{\delta}{R_\delta - R_t} \right) = 2k_r \frac{k}{\bar{k}} \frac{\delta}{R_\delta - R_t} \theta_0 + \frac{\rho_r \bar{R}_e \bar{P}_r}{H_e R_e S_c} \frac{\lambda\delta}{\bar{k}} \dot{m}^* \qquad (4.31)$$

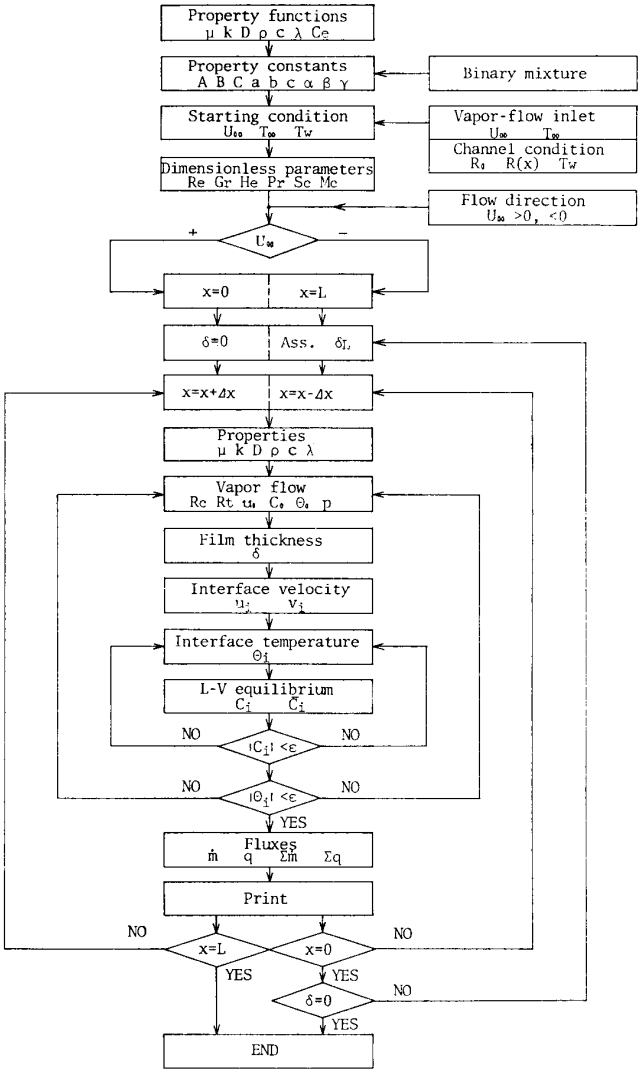

FIG. 4. Flow chart of numerical procedure.

The axial change in the pressure is calculated by Eq. (3.35), and the mass fractions at the interface are given by Eqs. (2.20) to (2.25). Finally, the condensation rate and the heat flux are obtainable by Eqs. (3.39) and (3.44), respectively.

$$\dot{m}^* = \frac{2\rho D}{R_\delta - R_c} \frac{C_i - C_0}{C_i - \bar{C}_i} \tag{4.32}$$

$$q = \bar{k} \frac{\theta_i}{\delta} \tag{4.33}$$

A detailed description of the overall numerical procedure is given in Appendix C and graphically shown in Fig. 4.

4.3 *Results and Discussions*

By employing the forgoing physical model and analytical method, the behavior of film condensation of binary mixture flows in a vertical channel having an isothermally

cooled wall is studied for vapor mixtures of ethanol-water, methanol-water, acetone-water, methanol-ethanol, and hexane-benzene. Effects of the channel geometry, the vapor flow speed and direction, the temperature of the vapor and the cooled wall, and the type of binary mixtures are investigated on the features of film condensation. Three different types of circular channel are employed as for having divergent, constant and convergent cross-sections with respect to the vapor flow direction;

$$\begin{aligned} R(x)&=1+0.1x && \text{Diffuser: } D \\ R(x)&=1 && \text{Cylinder: } C \\ R(x)&=1-0.05x && \text{Nozzle: } N \end{aligned} \tag{4.34}$$

A typical example of numerical results is shown in Fig. 5 for the case of ethanol-

Table 4. Nondimensional parameters

	T_{00} °C	T_w °C	C_{00}	Re	$\bar{R}e$	Pr	$\bar{P}r$	Sc	He	$\bar{G}r$	Mc^2	$RePr$	$ReSc$	Δw
				$\times 10^2$	$\times 10^2$	$\times 10^{-1}$			$\times 10^{-2}$	$\times 10^7$	$\times 10^{-7}$			
E—W	90	85	0.570	1.010	15.11	9.26	5.03	0.636	0.988	2.238	1.165	93.48	64.27	0.3369
E—W	90	87.5	0.570	1.010	15.11	9.26	5.03	0.636	0.461	2.238	1.165	93.48	64.27	0.1662
E—W	90	82.5	0.570	1.010	15.11	9.26	5.03	0.636	1.482	2.238	1.165	93.48	64.27	0.6808
E—W	95	90	0.363	0.791	15.87	9.56	4.60	0.790	0.953	2.466	0.953	75.55	62.47	0.4737
E—W	85	80	0.708	1.186	13.96	9.05	5.94	0.558	1.073	1.909	1.315	107.3	66.15	0.2764
M—W	90	85	0.793	1.950	15.32	9.27	4.83	0.803	0.956	2.300	0.854	64.41	55.78	0.3400
A—W	90	85	0.101	1.310	15.90	8.49	4.57	0.585	0.942	2.478	1.441	111.2	76.68	0.1771
M—E	75	74	0.252	1.326	10.53	9.65	12.98	0.760	0.346	1.087	1.520	128.0	100.8	0.7959
H—B	75	74	0.286	2.804	25.45	8.68	4.58	0.863	0.518	6.348	2.872	243.5	241.9	0.5425

NB. $U_{00}=10$ cm/s $R_0=1$ cm

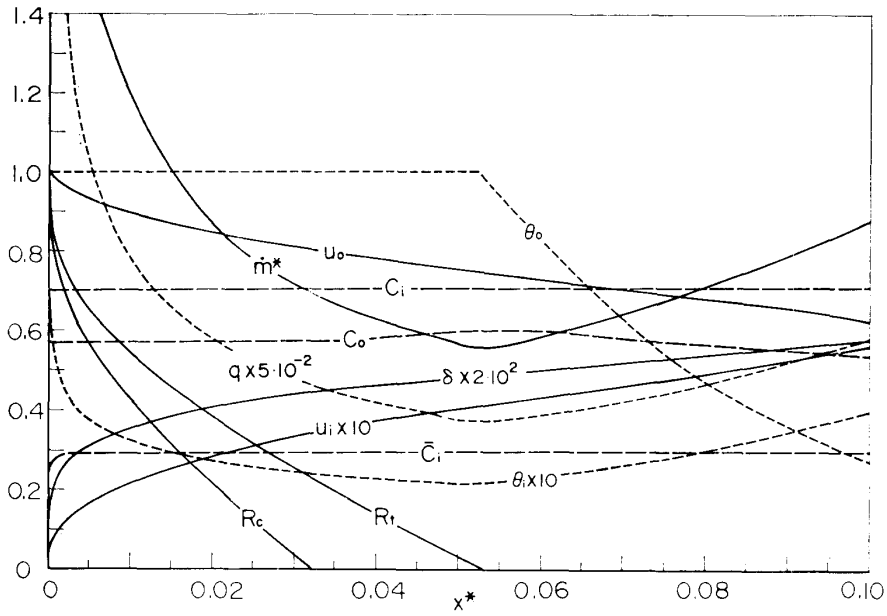

FIG. 5. Co-current flow film condensation; ethanol-water, C, $T_{00}=90°$C, $T_w=85°$C, $U_{00}=10$ cm/s.

water mixture. The system condition is $T_{00}=90°C$ ($C_{00}=0.507$), $T_w=85°C$, and $U_{00}=10$ cm/s ($R_0=1$ cm). Values of nondimensional parameters are listed in Table 4, where the length scale is chosen as $R_0=1$ cm. The condensation rate per unit interfacial area first decreases axially and reaches a minimum at a point near the end of the thermal developing region. After taking the minimum value, the condensation rate keeps nearly constant values or increases again owing to the flow condition (cf. Figs. 7-1, 8-a and 9-a). The first decrease of the rate is attributed to the growth of concentration layer which reduces the diffusion flux of the volatile component from the interface to the bulk flow. The increase of the rate after the minimum may be attributed mainly from the axial decrease of the mass fraction of the volatile component in the main stream. As for the concentration field of the vapor mixture, the volatile species is always transferred from the interface to the center by binary diffusion and from the bulk to the interface by convection. After the end of the developing region of concentration, the maass fraction of the volatile species in the main flow increases due to the higher diffusion flux from the interface to the bulk than the overall convective flux from the bulk to the interface. Further condensation, however, leads to the superiority of the convection flux to the diffusion flux. Under this condistion, the condensation rate is increased due to increasing the driving force (C_i-C_0). This increase in the condensation rate sometimes accelerates the tendency of decreasing the mass fraction of the volatile species in the main stream to result in very rapid increase in the condensation rate (see Figs. 8-a and 9-d). The heat flux to the wall shows the same behavior as the condensation rate since it is approximately proportional to the latter.

Because of small difference between the interface and wall temperatures, the mass fractions at the interface hardly change axially except for in the vicinity of the starting point of condensation. The thickness of concentration and temperature layer, $(R_\delta-R_c)$ and $(R_\delta-R_t)$, respectively, vary as being approximately proportional to $x^{0.4}$. Since $\dot{m}\propto(R_\delta-R_c)^{-1}$, the condensation rate in the developing region changes as $m\propto x^{-0.4}$. It can be seen from Eq. (3.38) that $d\delta^3/dx\propto\dot{m}$, hence, the film thickness changes axially as $\delta\propto x^{1/5}$. This relation holds approximately up to $x^*\simeq 0.1$. For one-component gravity-flow film condensation on a vertical flat plate, the film thickness follows the $x^{1/4}$ rule of the Nusselt solution, Eq. (3.42).

The interfacial temperature given by the heat balance at the interface is mainly dominated by the film thickness and the condensation rate, being approximately proportional to them. The interfacial velocity behaves like the film thickness, being approximately proportional to the square of the latter. It should be noted that rapid reduction in the main stream temperature after the thermal entry-length may result in a supersaturation of the vapor mixture, hence, a possibility of dropwise condensation which is not accounted for in the present study. The pressure gradient keeps almost constant.

In Fig. 6, the effect of channel geometry for co-current flows is presented. The condensation rate is highly reduced for the case of diffuser-type channel, whereas onto the wall of the nozzle-type channel the vapor mixture condenses at considerably

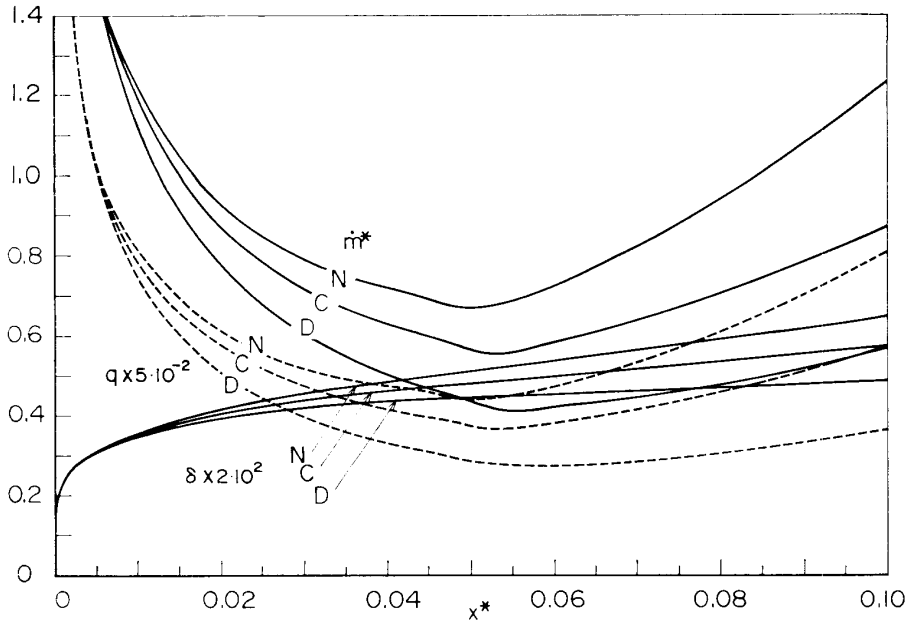

FIG. 6-a. Effect of channel geometry on the co-current flow film condensation; ethanol-water, $T_{00}=90°C$, $T_w=85°C$, $U_{00}=10$ cm/s. (a) m^*, q and δ.

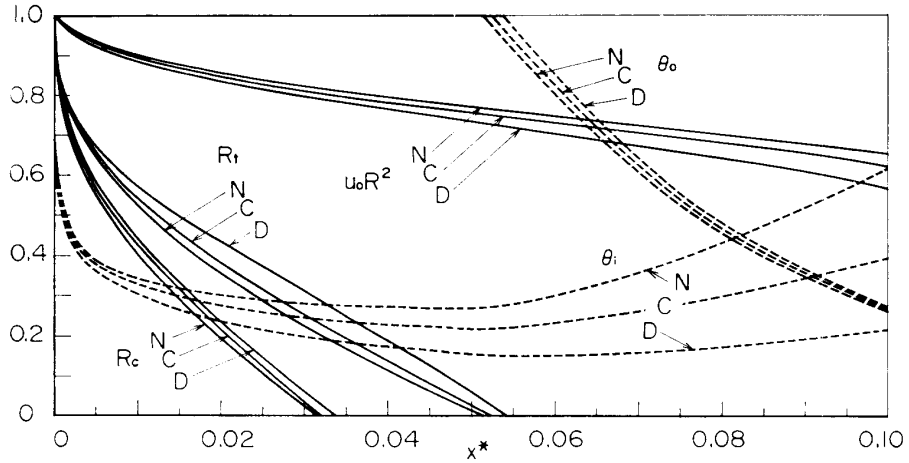

FIG. 6-b. Effect of channel geometry on the co-current flow film condensation; ethanol-water, $T_{00}=90°C$, $T_w=85°C$, $U_{00}=10$ cm/s.
(b) R_c, R_t, θ_i, θ_0 and u_0.

higher rates as shown in Fig. 6-a. However, as for the overall condensate mass flux or the condensate mass flux per unit axial length, $\dot{m}R$, the diffuser flow takes larger values than the nozzle flow. The overall condensation of total mass, the overall condensation of the volatile species and the oberall heat flux are 1.3%, 1.9% and 1.0% higher for the diffuser flow, and 1.2%, 1.7% and 1.0% lower for the nozzle flow than those for the constant cross-section flow, respectively. Due to this fact, the vapor mass flux, u_0R^2, changes more rapidly in the diffuser channel than in the nozzle. The diffuser flow requires longer developing lengths. The liquid film on the wall of the nozzle flow is thicker than that of the diffuser flow. The exponent of axial variation of the film thickness ($\delta \propto x^n$) is $n=0.2\sim0.23$ for the nozzle flow and $n=0.17\sim0.2$ for

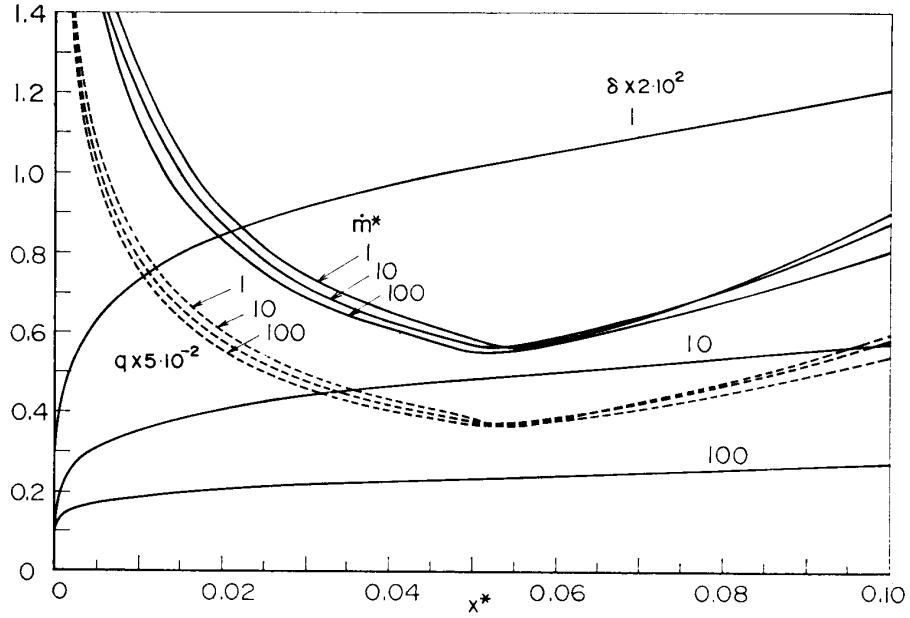

FIG. 7-a. Effect of vapor-flow velocity (U_{00} cm/s) on the co-current flow film condensation; ethanol-water, C, $T_{00}=90°C$, $T_w=85°C$. (a) m^*, q and δ.

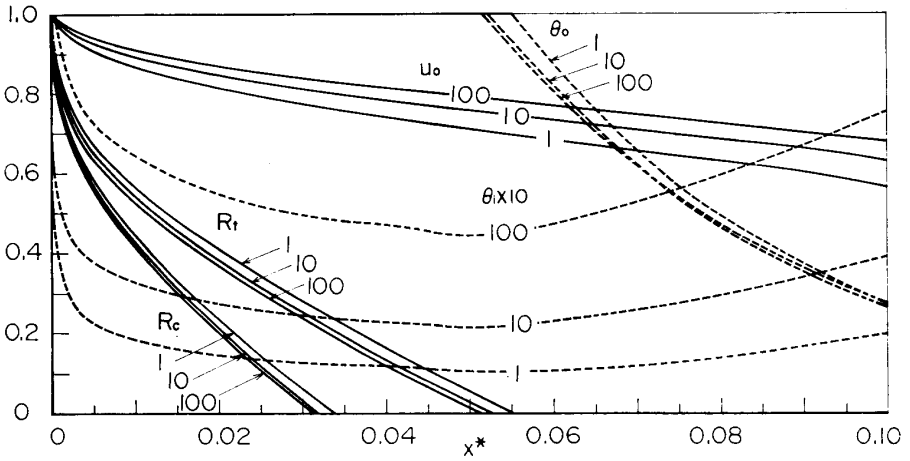

FIG. 7-b. Effect of vapor-flow velocity (U_{00} cm/s) on the co-current flow film condensation; ethanol-water, C, $T_{00}=90°C$, $T_w=85°C$.
(b) R_c, R_t, θ_i, θ_0 and u_0.

the diffuser. Owing to the increased film thickness and condensation rate, the nozzle flow has larger values of the interfacial temperature and velocity than the diffuser flow.

The effect of the vapor flow velocity (Reynolds number) is demonstrated in Fig. 7. It should be called to mind that the abscisa of the figures means x/R_eS_c. In the coordinates of $R_eS_c\dot{m}$ vs. x/R_eS_c, higher flow velocities yield lower condensation rates and shorter developing lengths of concentration and temperature. The film thickness takes larger values for higher velocity flows, being approximately proportional to $R_e^{1/3}$ (see Eq. (3.38) with Eq. (3.39)). The interfacial velocity and temperature are approximately proportional to $R_e^{-1/3}$ and $R_e^{1/3}$, respectively.

The vapor temperature at the flow inlet and the wall temperature have a considerable effect on the behavior of film condensation. As shown in Fig. 8, larger difference between two temperatures, $T_{00}-T_w$, results in higher condensation rates which are roughly proportional to Δ_w defined by

$$\Delta_w = \frac{C_e(T_w)-C_e(T_{00})}{C_e(T_w)-\bar{C}_e(T_w)} \tag{4.35}$$

It is seen from the result that, when the inlet temperature and the wall temperature are varied simultaneously with keeping a constant temperature difference between

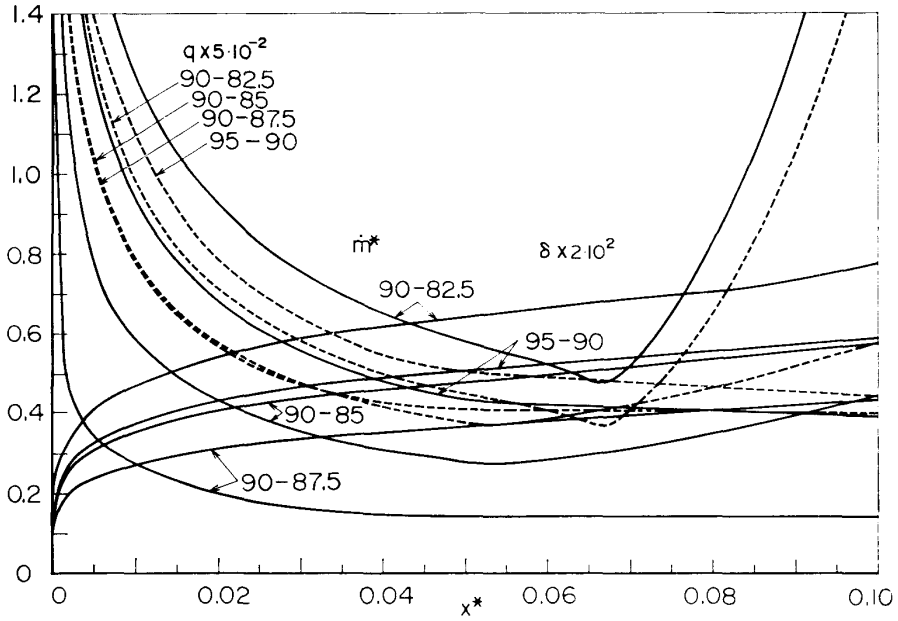

FIG. 8-a. Effect of inlet-vapor and wall temperatures ($T_{00}-T_w$, °C) on the co-current flow film condensation; ethanol-water, C, $U_{00}=10$ cm/s. (a) m^*, q and δ.

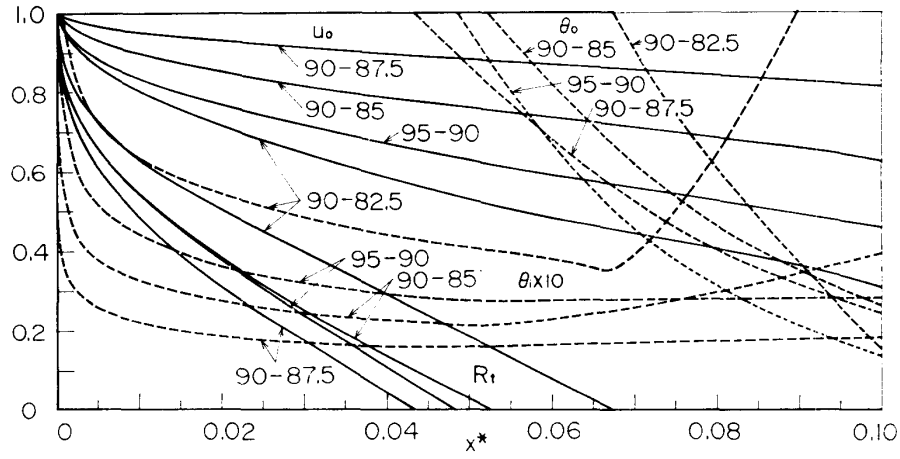

FIG. 8-b. Effect of inlet-vapor and wall temperatures ($T_{00}-T_w$, °C) on the co-current flow film condensation; ethanol-water, C, $U_{00}=10$ cm/s. (b) R_t, θ_i, θ_0 and u_0.

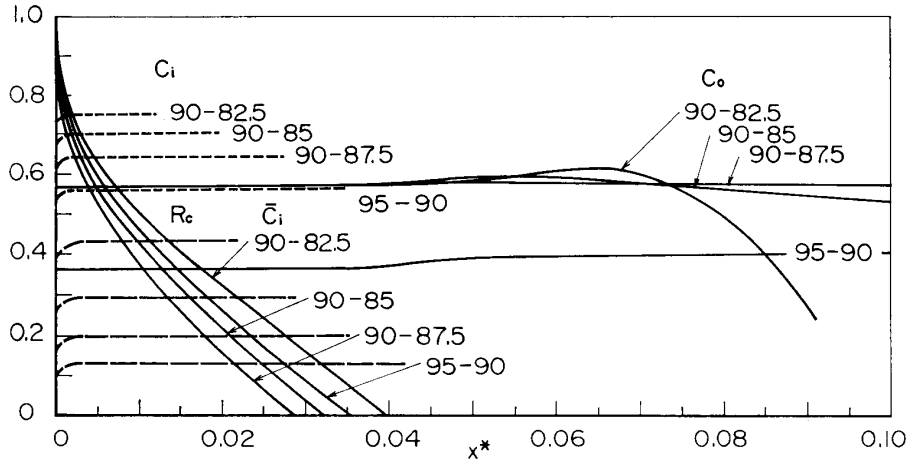

FIG. 8-c. Effect of inlet-vapor and wall temperatures ($T_{00}-T_w$, °C) on the co-current flow film condensation; ethanol-water, C, $U_{00}=10$ cm/s.
(c) R_c, C_i, $\bar{C}_i$ and C_0.

them (approximately $C_e(T_{00})-C_e(T_w)=\text{const}$), the condensation rate takes a minimum value at the temperatures close to which the difference of equilibrium mass fractions, $C_e(T)-\bar{C}_e(T)$, is maximum. Larger values of the condensation rate are always associated with higher interfacial temperatures and longer developing lengths of concentration and temperature. Longer developing lengths result in relatively slower change of the condensation rate in the axial direction. Since $d\delta^3/dx \propto \dot{m}$, the exponent of the axial variation of film thickness is larger for the case of larger values of Δ_w. The exponent ($\delta \propto x^n$) is $n \simeq 0.22$ for $T_{00}=90°C$ and $T_w=82.5°C$ and $n \simeq 0.19$ for $T_{00}=90°C$ and $T_w=87.5°C$. The film thickness is approximately proportional to $\Delta_w^{1/3}$ (see Eq. (7.66)).

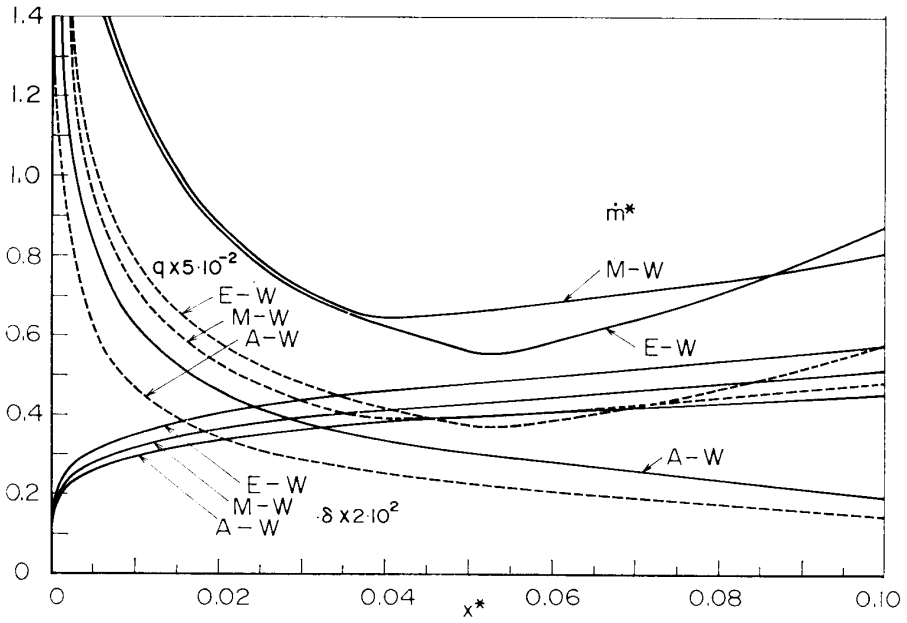

FIG. 9-a. Effect of type of binary mixtures (E-W, M-W, A-W) on the co-current film flow condensation; C, $T_{00}=90°C$, $T_w=85°C$, $U_{00}=10$ cm/s.
(a) m^*, q and δ.

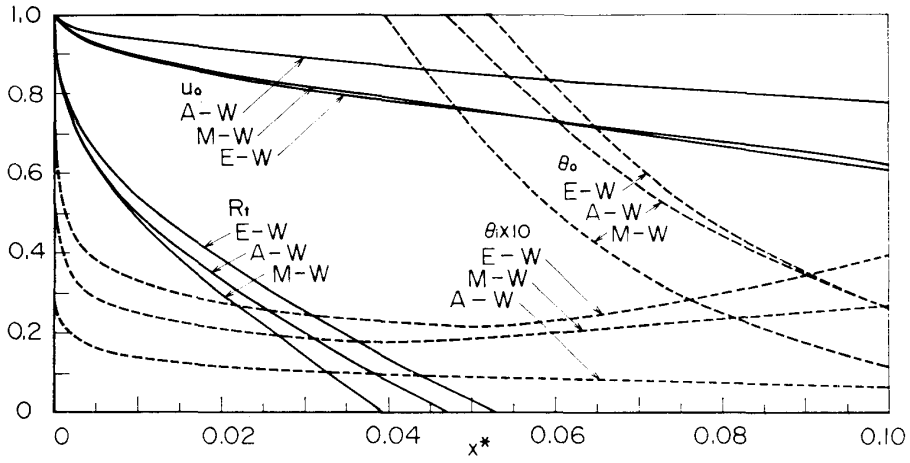

FIG. 9-b. Effect of type of binary mixtures (E-W, M-W, A-W) on the co-current film flow condensation; C, T_{00}=90°C, T_w=85°C, U_{00}=10 cm/s. (b) R_t, θ_i, θ_0 and u_0.

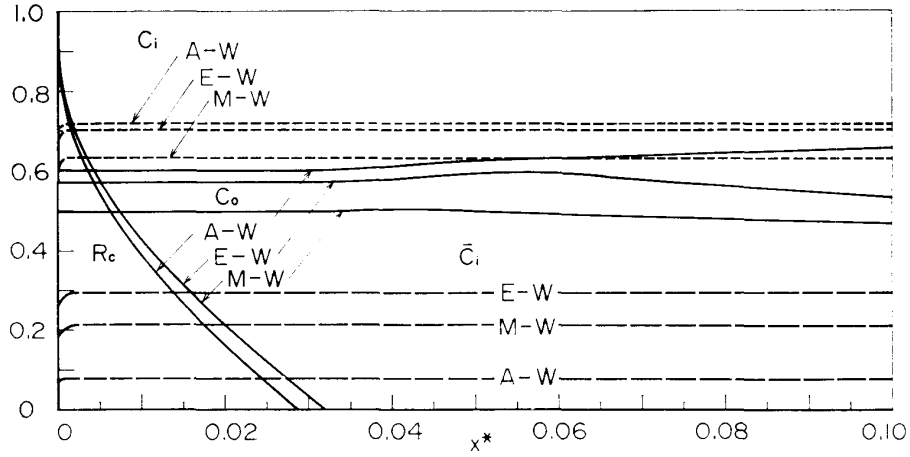

FIG. 9-c. Effect of type of binary mixtures (E-W, M-W, A-W) on the co-current film flow condensation; C, T_{00}=90°C, T_w=85°C, U_{00}=10 cm/s. (c) R_c, C_i, $\bar{C}_i$ and C_0.

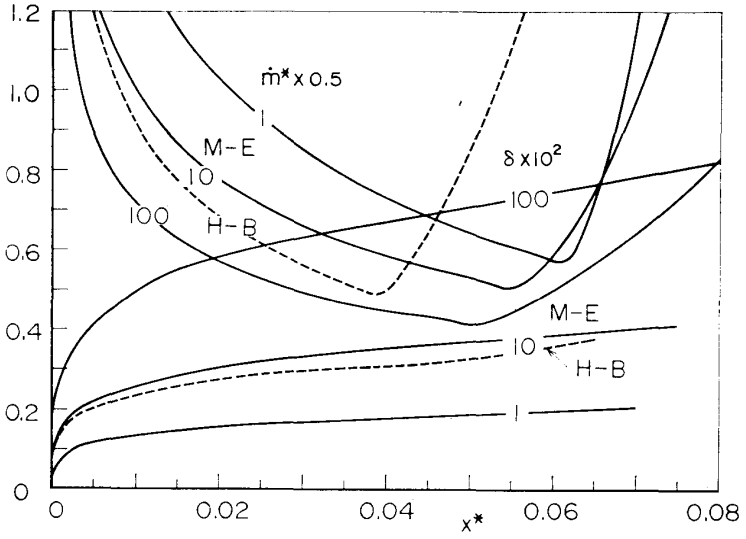

FIG. 9-d. Effect of type of binary mixtures (M-E, H-B) on the co-current film flow condensation; C, T_{00}=75°C, T_w=74°C, U_{00}=10 cm/s.

The type of binary mixture also has an appreciable effect on the film condensation through its equilibrium characteristics and physical properties as shown in Fig. 9. In the figure, the results for ethanol-water, methanol-water and aceton-water are compared. Figure 9-d shows the case of methanol-ethanol and hexane-benzene, which have very narrow equilibrium curves (Fig. 3), that is, larger values of Δ_w. The condensation rate is highly characterized by the factor. Larger values of Δ_w result in higher condensation rates and larger values of the exponent of the axial change in the film thickness. The latter takes $n=0.33\sim0.25$ for the case of methanol-ethanol and hexane-benzene. The film thickness is approximately proportional to $(\Delta_w\bar{R}_e/\bar{G}_r)^{1/3}$ and the interfacial velocity to $(\Delta_w^2\bar{G}_r/\bar{R}_e)^{1/3}$. The pressure gradient is roughly proportional to $\bar{M}_c^2R_eS_c\bar{G}_r/\bar{R}_e^2$ in the x^* scale and to $\bar{M}_c^2\bar{G}_r/\bar{R}_c^2$ in the x scale. It should be noted that the effect of the diffusion process of the volatile component can be expressed by the factor Δ_w, since it includes the mass transfer potential at the interface.

5. Counter-current Flow Film Condensation

In the case of counter-current flows, the vapor mixture is introduced upward into a vertical channel at the end of the cooled wall (Fig. 2-b). The vapor mixture is in equilibrium at the inlet temperature and pressure, T_{00} and P_0, having the mass fraction of the volatile species, C_{00}. The wall is cooled isothermally at a constant temperature T_w between $x=0$ and $x=L$. Condensation starts at $x=0$, and the condensate flows downward along the wall in the opposite direction to the vapor flow.

Under this condition, it is likely that the governing equations might have two singularities at the starting point of condensation ($x=0$) and at the vapor flow inlet ($x=L$). At $x=0$, the thickness of the condensate film should be extinguished and the heat flux through the film might go to infinity due to Eq. (3.44). From further inspection into Eq. (3.37), however, it is seen that the interfacial temperature θ_i can also vanish at $x=0$ so as to yield a finite value of the heat flux. Thus, there is no singularity at the starting point of condensation.

At the vapor flow inlet, it is necessary to consider more detailed configurations of the vapor and liquid flows. Close to the liquid vapor interface, the axial velocity of the vapor mixture approaches the one of the liquid flow. Hence, there must be a zero-velocity point somewhere in the vicinity of the interface. In order to force the vapor mixture flow into the channel, an inner tube should be located at the zero-velocity point so that the vapor and liquid mixtures in the annular section between the inner tube and the outer channel are to be sucked in together in the same direction (Fig. 2-b). Within the cross-section of the inner tube, the vapor mixture can be assumed to have a uniform temperature and concentration with a fully developed velocity profile. In the space between the zero-velocity point and the liquid-vapor interface, the concentration and temperature of the vapor mixture are to be diffused. Taking such a configuration of flow, it is also possible to avoid the singularity at the vapor-flow inlet.

5.1 *Boundary Conditions at the Flow Inlet*

The vapor layer between the liquid-vapor interface and the zero-velocity point has a thickness of δ_v. Since the velocity profile is assumed as

$$u=u_0+(u_i-u_0)\left(\frac{r}{R_\delta}\right) \tag{5.1}$$

the thickness δ_v is given by

$$\delta_v=R_\delta\left(1-\sqrt{\frac{-u_0}{u_i-u_0}}\right) \tag{5.2}$$

Within the cross-section of the inner tube, the mass fraction and temperature are uniform,

$$\begin{aligned} &C=C_{00}(T_{00}) \\ &\theta=1 \end{aligned} \qquad (R_\delta-\delta_v\geqslant r\geqslant 0) \tag{5.3}$$

Of the vapor layer between the liquid-vapor interface and the zero-velocity point, they are assumed to be of a parabolic profile,

$$C=C_{00}+(C_i-C_{00})\left(\frac{r-R_\delta-\delta_v}{\delta_v}\right)^2 \tag{5.4}$$

$$(R_\delta\geqslant r\geqslant R_\delta-\delta_v)$$

$$\theta=1+(\theta_i-1)\left(\frac{r-R_\delta-\delta_v}{\delta_v}\right)^2 \tag{5.5}$$

This means that at the flow inlet the radius of the concentration and temperature is $R_\delta-\delta_v$;

$$R_c=R_\delta-\delta_v \tag{5.6}$$

$$(x=L)$$

$$R_t=R_\delta-\delta_v \tag{5.7}$$

Because of the finiteness of δ_v, the quantities at the interface such as u_i, θ_i, C_i and $\bar{C}_i$ are directly given by Eqs. (3.36), (3.37) and (2.20) to (2.25) with an assumed value of the film thickness.

$$u_i\left(1+2\mu_r\frac{\mu}{\bar{\mu}}\frac{\delta}{R_\delta}\right)=\frac{\delta^2}{2\bar{\mu}}\frac{\bar{G}_r}{\bar{R}_e}\bar{\rho}+2\mu_r\frac{\mu}{\bar{\mu}}\frac{\delta}{R_\delta} \tag{5.8}$$

$$\theta_i\left(1+2k_r\frac{k}{\bar{k}}\frac{\delta}{\delta_v}\right)=2k_r\frac{k}{\bar{k}}\frac{\delta}{\delta_v}\theta_0+\frac{\rho_r\bar{R}_e\bar{P}_r}{H_eR_eS_c}\frac{\lambda\delta}{\bar{k}}\dot{m}^* \tag{5.9}$$

where the condensation rate is given by

$$\dot{m}^*=\frac{2\rho D}{\delta_v}\frac{C_i-C_{00}}{C_i-\bar{C}_i}$$

To obtain the solution of the governing equations with these starting conditions, the film thickness at the flow inlet must be adjusted iteratively so as to satisfy the condition of $\delta=0$ at $x=0$.

5.2 *Numerical Procedures*

The system is specified by

U_{00}: the inlet flow velocity at the center,
T_{00}: the inlet flow temperature,
P_0: the inlet flow pressure,
T_w: the cooled-wall temperature,
$R(x)$: the channel geometry, and
the type of binary mixture.

To start the stepwise calculation, a film thickness at the flow inlet is assumed. With this film thickness, the quantities at the interface, u_i, θ_i, C_i, $\bar{C}_i$ and $\dot{m}^*$, are estimated by Eqs. (5.8) and (5.9). The thicknesses of the concentration and temperature layer, R_c and R_t, are given by Eqs. (5.6) and (5.7). Using these values as the starting conditions, the set of governing differential equations of the first order with respect to x can be solved by means of finite difference method toward the negative direction of the x-axis. The governing equations to be solved are same as those for co-current flows;

R_c: Eq. (4.24),
R_t: Eq. (4.25),
u_0: Eq. (4.28)
δ: Eq. (4.29)
u_i: Eq. (4.30)
θ_i: Eq. (4.31)
$C_i, \bar{C}_i$: Eqs. (2.20) to (2.25)
p: Eq. (3.35)
$\dot{m}^*$: Eq. (4.32)
$\dot{m}_c^*$: Eq. (3.43)
q: Eq. (4.33)
c_0: Eq. (4.26)
θ_0: Eq. (4.27)

The numerical solution advanced axially step by step gives finally the value of the liquid film thickness at $x=0$. If this value is not within a specified small value, say, $10^{-3}\,\delta_v$, the thickness of the liquid film at the flow inlet is reassumed and the same procedure is repeated until the condition of $\delta=0$ at $x=0$ is satisfied with an appropriate accuracy.

5.3 *Results and Discussions*

A typical example of numerical results is shown in Fig. 10 for ethanol-water mixture with $T_{00}=90°C$, $T_w=85°C$, $U_{00}=-10$ cm/s, and $L/R_0=10$ ($R_0=1$ cm). The concentration and temperature layers are developed from the outlet of the liquid film flow toward its starting point. From comparing Fig. 10 with Fig. 5, it is seen that the behavior of the developing layers along the flow passage are almost similar in both

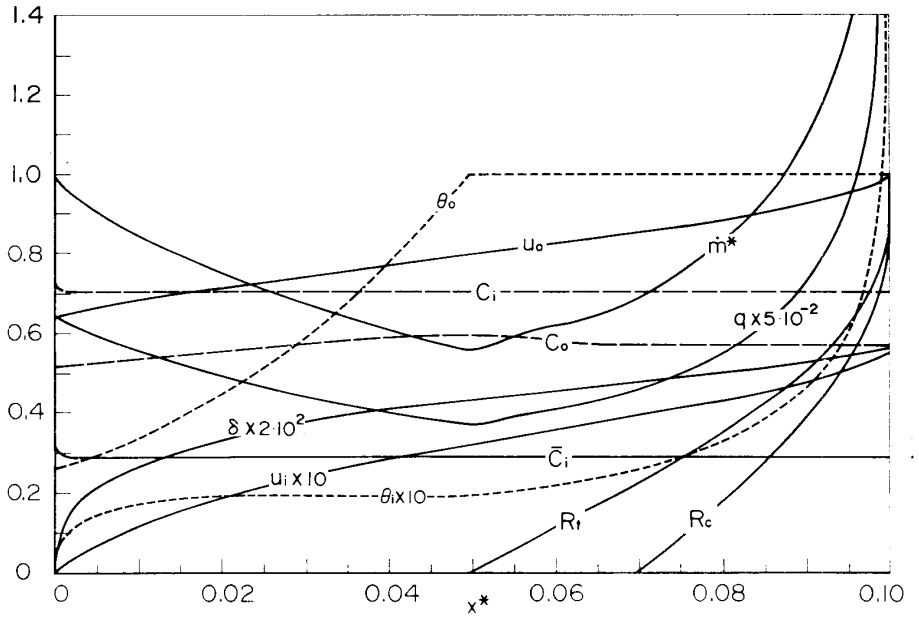

FIG. 10. Counter-current flow film condensation; ethanol-water, C, $T_{00}=90°C$, $T_w=85°C$, $U_{00}=-10$ cm/s.

cases. The condensation rate and the heat flux are at first rapidly decreased due to the growth of the layer. After taking a minimum value, they again increase. Because of relatively smaller variation of the condensation rate at the beginning of the liquid film flow (in the developed region), the film thickness varies more rapidly in the x-direction than that of the co-current flow. The exponent of variation ($\delta \sim x^n$) is $n=0.25\sim0.30$. Further in the developing region of concentration and temperature, it changes more sharply ($n>0.30$). Due to this fact, the interfacial velocity also changes more rapidly than that of the co-current flow. The interfacial temperature, hence, the interfacial concentration, shows somewhat different behavior at the beginning of the film flow, approaching the wall temperature. The length of the developing region is not found to be appreciably affected by the flow direction.

The effect of channel geometry is shown in Fig. 11. It is seen from this figure compared with Fig. 6 that the channel geometry has qualititavely the same effect upon the features of film condensations as in the co-current flow. The nozzle flow results in larger values of the condensation rate, heat flux, film thickness, interfacial velocity and temperature. Concerning the overall condensation rate, the diffuser flow provides larger amount of the condensate than the nozzle flow does. For the present case, the overall condensation rate of total mass, that of the volatile component and the overall heat flux are 1.4%, 2.0% and 1.3% higher for the diffuser flow, and 0.6%, 1.0% and 0.4% lower for the nozzle flow, respectively, than those for the constant cross-section flow. The channel geometry (nozzle and diffuser) is termed with respect to the vapor flow. From the standpoint of the liquid film flow, the "diffuser" in counter-current flows corresponds to the "nozzle" in co-current flows. Considering the result mentioned above from this point of view leads to the fact that the behavior of the vapor flow might not be drastically affected by the flow

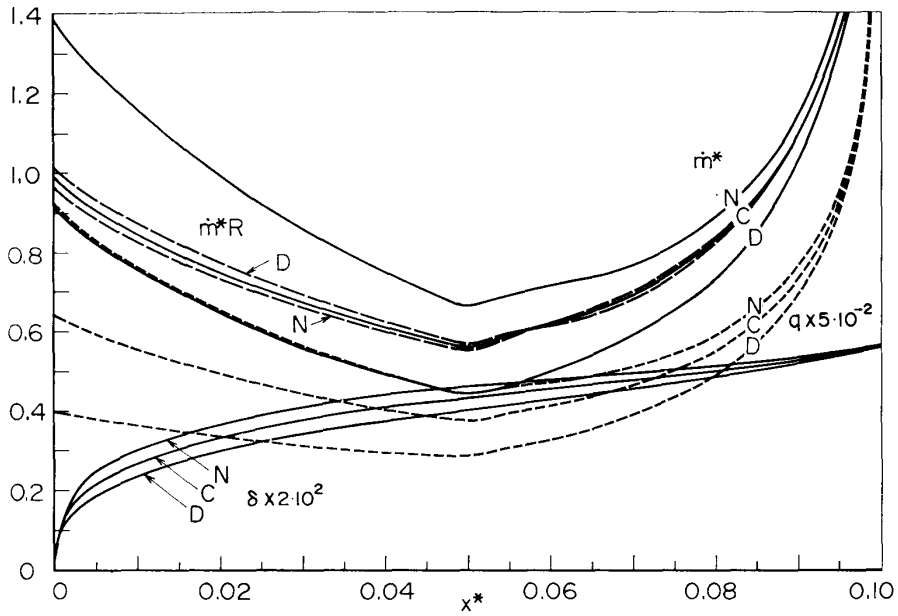

FIG. 11-a. Effect of channel geometry on the counter-current flow film condensation; ethanol-water, $T_{00}=90°C$, $T_w=85°C$, $U_{00}=-10$ cm/s.
(a) m^*, q and δ.

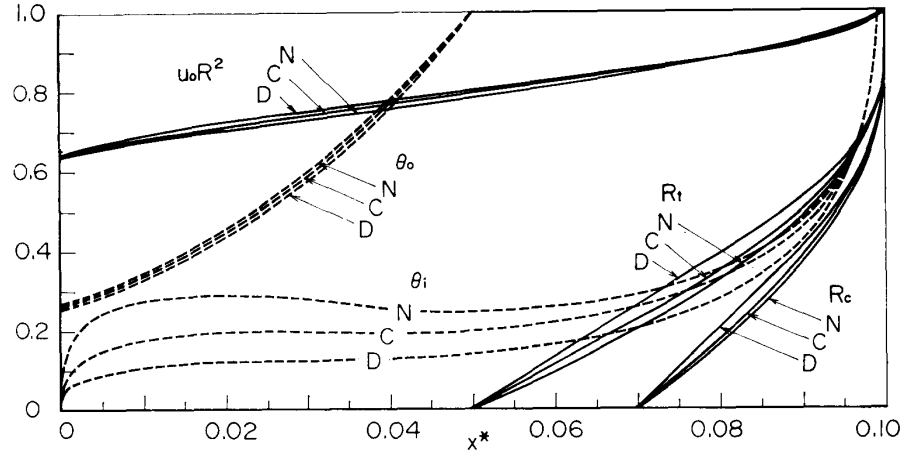

FIG. 11-b. Effect of channel geometry on the counter-current flow film condensation; ethanol-water, $T_{00}=90°C$, $T_w=85°C$, $U_{00}=-10$ cm/s.
(b) R_c, R_t, θ_i, θ_0 and u_0.

direction and that the film condensation could be considerably dominated by the diffusion and convection processes of the vapor mixture.

These features are demostrated evidently in Fig. 12, in which the condensation rate for the counter-current flow is plotted against the distance from the flow inlet, $(1-x^*)$. Roughly speaking, the condensation rate has a similar feature for both flows except for the region close to the flow outlet. In the developing region, the counter-current flow yields smaller values of the condensation rate, whereas in the developed region it takes larger values than the co-current flow. At the outlet of the counter-current flow, the interfacial temperature approaches the wall temperature, whereas

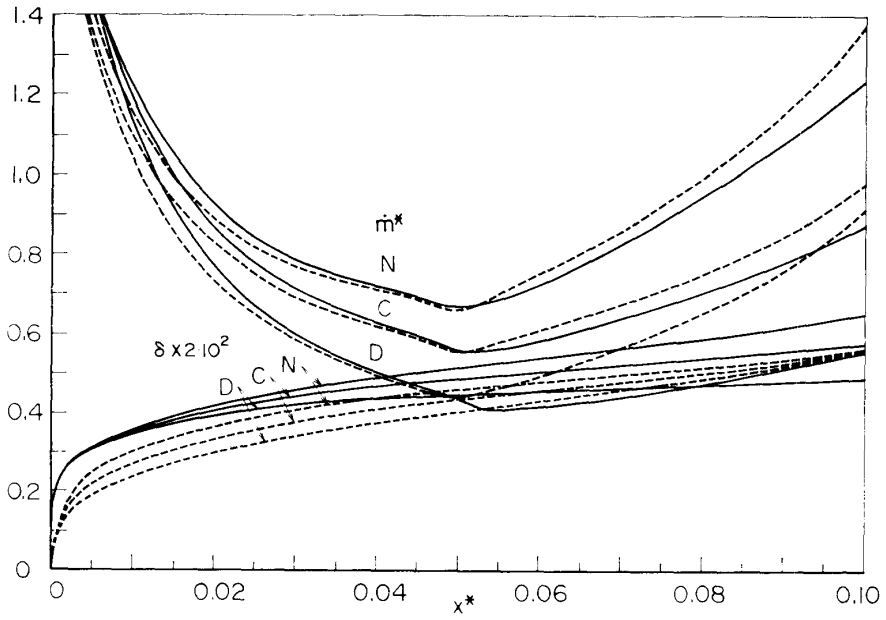

FIG. 12. Comparison of co-current and counter-current flow film condensations; ethanol-water, $T_{00}=90°\,C$, $T_w=85°\,C$, $|U_{00}|=10\,cm/s$; —, co-current flow; ---, counter-current flow.

at the outlet of the co-current flow it goes off from the latter (cf. Figs. 6-b and 11-b) This opposite tendency yields different interfacial mass fractions and results in appreciable difference of condensation rate between the co-current and counter-current flows at the flow-outlet. The film thickness takes larger values for the co-current flow due to the higher condensation rates in the developing region.

6. Quasi-developed Flow Film Condensation

When the radial transports of species and energy are sufficiently higher compared with the axial convection of them as in the case of small Reynolds numbers, the radial distributions of concentration and temperature tend to be of the developed profile in a short distance from the start of condensation. This is the case for relatively long tubes of small radius. The tendency is also promoted by employing some means such as preliminary cooling or condensation before the inlet. In these cases, the radii of concentration and temperature layers, R_c and R_t, go to zero within a short distance from $x=0$, and the radial distribution of velocity, concentration and temperature may be approximated by a simple function of r/R_δ such as

$$\begin{aligned} u &= u\left\{(u_i-u_0)\left(\frac{r}{R_\delta}\right)^n\right\} \\ \theta &= \theta\left\{(\theta_i-\theta_0)\left(\frac{r}{R_\delta}\right)^m\right\} \\ C &= C\left\{(C_i-C_0)\left(\frac{r}{R_\delta}\right)^l\right\} \end{aligned} \tag{6.1}$$

Under these conditions, the flow field of vapor mixture will be much perspective for the effects of each parameter on the behavior of film condensation of binary mixtures in a channel flow.

For the purpose to deal with such quasi-developed flows, it is convenient to introduce transfer coefficients for the radial fluxes of species, energy and momentum. The nondimensional heat and mass transfer coefficients, the Nusselt number N_u and the Sherwood number S_h, can be defined in the relation with heat and mass fluxes, respectively, as

$$\left(k\frac{\partial\theta}{\partial r}\right)_i = N_u k\frac{\theta_i-\theta_m}{2R_\delta} \equiv q_t^* \tag{6.2}$$

$$\left(\rho D\frac{\partial C}{\partial r}\right)_i = S_h\rho D\frac{C_i-C_m}{2R_\delta} \equiv q_c^* \tag{6.3}$$

where θ_m and C_m are the flow-averaged temperature and mass fraction;

$$\theta_m = \frac{\int_0^{R_\delta} u\theta r dr}{\int_0^{R_\delta} ur dr} \qquad C_m = \frac{\int_0^{R_\delta} uCr dr}{\int_0^{R_\delta} ur dr} \tag{6.4}$$

In this expression, equations of concentration and temperature, Eqs. (3.14) and (3.15), are written as

$$\frac{d}{dx^*}\int_0^{R_\delta} \rho uCr dr + \dot{m}^* C_i R_\delta = q_c^* R_\delta \tag{6.5}$$

$$\frac{d}{dx^*}\int_0^{R_\delta} \rho uc_p\theta r dr + \dot{m}^* c_p\theta_i R_\delta = \frac{S_c}{P_r} q_t^* R_\delta + \int_0^{R_\delta} \rho c_p' D\frac{\partial C}{\partial r}\frac{\partial\theta}{\partial r} r dr \tag{6.6}$$

The continuity conditions of species and energy fluxes, Eqs. (3.19) and (3.20), are

$$\dot{m}^*\bar{C}_i = \dot{m}^* C_i - \frac{S_h}{2}\frac{\rho D}{R_\delta}(C_i - C_m) \tag{6.7}$$

$$k_r\frac{N_u}{2}\frac{k}{R_\delta}(\theta_i-\theta_m) + \bar{k}\frac{\theta_i}{\delta} = \frac{\rho_r H_e \bar{P}_r \bar{R}_e}{R_e S_c}\lambda\dot{m}^* \tag{6.8}$$

The viscous stress nondimensionalized by $\rho_r u_r u_r$ can be expressed with the friction coefficient f as

$$\left(\mu\frac{\partial u}{\partial r}\right)_i = -\frac{f}{8}\rho u_m^2 R_e = \tau^* \tag{6.9}$$

where u_m is the mean velocity defined by

$$u_m = \frac{\int_0^{R_\delta} ur dr}{\int_0^{R_\delta} r dr} \tag{6.10}$$

This expression reduces equation of motion, Eq. (3.13), to

$$\frac{d}{dx^*}\int_0^{R_\delta}\rho uurdr+\dot{m}^*u_iR_\delta=\int_0^{R_\delta}\left(-\frac{1}{M_c^2}\frac{dp}{dx^*}+\frac{G_rS_c}{R_e}\rho\right)rdr+S_c\tau^*R_\delta \tag{6.11}$$

and its boundary condition at the interface, Eq. (3.18), to

$$\frac{\delta}{2}\left(\frac{\bar{R}_e}{\bar{M}_c^2R_eS_c}\frac{dp}{dx^*}-\frac{\bar{G}_r}{\bar{R}_e}\bar{\rho}\right)+\bar{\mu}\frac{u_i}{\delta}=-\mu_r\tau^* \tag{6.12}$$

The equation of continuity and its boundary condition at the interface are given by, respectively

$$\frac{d}{dx^*}\int_0^{R_\delta}\rho urdr+\dot{m}^*R_\delta=0 \tag{6.13}$$

$$\frac{1}{\rho_r}\left\{\bar{\rho}\left(\bar{v}^*-\bar{u}\frac{dR_\delta}{dx^*}\right)\right\}_i=\left\{\rho\left(v^*-u\frac{dR_\delta}{dx^*}\right)\right\}_i=\dot{m}^* \tag{6.14}$$

The interfacial temperature and axial velocity are obtained by Eqs. (6.8) and (6.12), respectively

$$\theta_i\left(\bar{k}+k_r\frac{N_u}{2}\frac{k}{R_\delta}\delta\right)=\frac{\rho_rH_e\bar{P}_r\bar{R}_e}{R_eS_c}\lambda\dot{m}^*\delta+k_r\frac{N_u}{2}\frac{k}{R_\delta}\delta\theta_m \tag{6.15}$$

$$u_i=\frac{\delta^2}{2\bar{\mu}}\left(\frac{\bar{G}_r}{\bar{R}_e}\bar{\rho}-\frac{\bar{R}_e}{\bar{M}_c^2R_eS_c}\frac{dp}{dx^*}\right)-\frac{\mu_r}{\bar{\mu}}\delta\tau^* \tag{6.16}$$

The mass fractions at the interface, C_i and $\bar{C}_i$, are determined by the equilibrium conditions, Eqs. (2.20) to (2.25).

The rate of condensation, $\dot{m}^*$, can be expressed by Eqs. (3.38) to (3.40), respectively, as

$$\dot{m}^*=\frac{1}{\rho_r}\frac{1}{R_\delta}\frac{d}{dx^*}\left[R\delta\bar{\rho}\left\{\frac{u_i}{2}+\frac{1}{6}\frac{\delta^2}{2\mu}\left(\frac{\bar{G}_r}{\bar{R}_e}\bar{\rho}-\frac{\bar{R}_e}{\bar{M}_c^2R_eS_c}\frac{dp}{dx^*}\right)\right\}\right] \tag{6.17}$$

$$\dot{m}^*=\frac{S_h}{2}\frac{\rho D}{R_\delta}\frac{C_i-C_m}{C_i-\bar{C}_i} \tag{6.18}$$

$$\dot{m}^*=\frac{R_eS_c}{\rho_rH_e\bar{P}_r\bar{R}_e}\frac{1}{\lambda}\left\{\frac{\bar{k}}{\delta}\theta_i+k_r\frac{N_u}{2}\frac{k}{R_\delta}(\theta_i-\theta_m)\right\} \tag{6.19}$$

Combining Eq. (6.17) with Eqs. (6.16) and (6.19) gives the film thickness as a solution of the equation

$$\delta\frac{d}{dx^*}\left[R\left\{\frac{\bar{\rho}}{3\bar{\mu}}\left(\bar{G}_r\bar{\rho}-\frac{\bar{R}_e^2}{\bar{M}_c^2R_eS_c}\frac{dp}{dx^*}\right)\delta^3-\frac{\bar{R}_e}{2}\frac{\mu_r}{\bar{\mu}}\tau^*\delta^2\right\}\right]$$
$$=\frac{R_eS_cR_\delta}{H_e\bar{P}_r}\frac{1}{\lambda}\left\{\bar{k}\theta_i+k_r\frac{N_u}{2}\frac{k}{R_\delta}\delta(\theta_i-\theta_m)\right\} \tag{6.20}$$

which is subject to the starting condition at $x=0$

$$\delta(0)=0 \tag{6.21}$$

At the starting point of condensation, $x=0$, Eqs. (6.15) and (6.16) yield $\theta_i=0$ and $u_i=0$. For the case of co-current flows, thus, the radial distributions of velocity, temperature and concentration may be expressed as

$$\begin{aligned} u&=u(r^n)\\ \theta&=\theta(r^m)\\ C&=C\{(C_{i0}-C_{00})r^l\} \end{aligned} \tag{6.22}$$

where C_{i0} is evaluated at $\theta_i=0$. For the case of counter-current flows, the film thickness at the flow inlet, $x=L$, should be determined so as to be $\delta=0$ at the starting point of condensation, $x=0$, by an iterative method. Corresponding to the film thickness at $x=L$, the interfacial temperature (hence, mass fractions) and velocity are obtained by Eqs. (6.15) and (6.16), respectively.

The most leading contribution to the axial change in $\dot{m}^*$ and θ_i comes from the axial variation of C_0 which is controlled by Eq. (6.5). For quasi-developed flows, the axial change of C_0 is not substantial due to small values of radial mass transfer. The condensation rate, $\dot{m}^*$, and the states of the mixture at the interface, θ_i, C_i and $\bar{C}_i$, are weakly changed in the flow-direction. These features make it much easy to examine the effect of each parameter.

6.1 *Laminar Flows*

With the assumption of a parabolic profile for the radial distribution of velocity, concentration and temperature, Eq. (6.1) gives

$$\begin{aligned} u&=u_0+(u_i-u_0)\left(\frac{r}{R_\delta}\right)^2\\ C&=C_0+(C_i-C_0)\left(\frac{r}{R_\delta}\right)^2\\ \theta&=\theta_0+(\theta_i-\theta_0)\left(\frac{r}{R_\delta}\right)^2 \end{aligned} \tag{6.23}$$

Equations (6.5) and (6.6) are rewirtten as

$$\frac{d}{dx^*}\left[\frac{\rho}{12}R_\delta^2\{2u_0+u_i)C_0+(u_0+2u_i)C_i\}\right]=-\dot{m}^*C_iR_\delta+q_c^*R_\delta \tag{6.24}$$

$$\begin{aligned} \frac{d}{dx^*}\left[\frac{\rho c_p}{12}R_\delta^2\{(2u_0+u_i)\theta_0+(u_0+2u_i)\theta_i\}\right]&=-\dot{m}^*c_p\theta_iR_\delta\\ &+\frac{S_c}{P_r}q_i^*R_\delta+\rho c_p'DR_\delta^2(C_i-C_0)(\theta_i-\theta_0) \end{aligned} \tag{6.25}$$

which give the axial change of C_0 and θ_0, respectively.

Equations of continuity and motion, Eqs. (6.13) and (6.12), are

$$\frac{d}{dx^*}\left[R_\delta^2\left\{\frac{\rho_r}{4}\rho(u_0+u_i)+\bar{\rho}\frac{\delta}{R_\delta}\left(\frac{2}{3}u_i+\frac{1}{6}\frac{\mu_r}{\bar{\mu}}\delta\tau^*\right)\right\}\right]=0 \tag{6.26}$$

$$\left(1+\frac{\delta}{R_\delta}\right)\frac{R_\delta^2}{2M_c^2}\frac{dp}{dx^*}=\frac{\bar{G}_r R_e S_c}{2\bar{R}_e^2}R_\delta^2\left(\rho+\frac{\bar{\rho}}{\rho_r}\frac{\delta}{R_\delta}\right)-u_i\left(\dot{m}^* R_\delta+S_c\frac{\bar{\mu}}{\mu_r}\frac{R_\delta}{\delta}\right)$$
$$-\frac{d}{dx^*}\left\{\frac{\rho}{6}R_\delta^2(u_0^2+u_0u_i+u_i^2)\right\} \tag{6.27}$$

from which the axial variation of u_0 and p can be obtained.

Concerning the transfer coefficients, S_h, N_u and f, for laminar flows, it may be consistent to evaluate them from the assumed profiles. The profiles yield

$$S_{hp}=4\frac{C_i-C_0}{C_i-C_m} \qquad N_{up}=4\frac{\theta_i-\theta_0}{\theta_i-\theta_m} \qquad f_p=32\frac{u_0-u_i}{u_m}\left(R_e\frac{2u_mR_\delta}{\nu}\right)^{-1} \tag{6.28}$$

Since the assumed profiles are of approximation through the cross section of the channel, it is likely that they are insufficient close to the interface. In such cases, the coefficients should be given a priori by some empirical estimations. When the fields of velocity, concentration and temperature are weakly coupled, they may be approximated by an empirical correlation of heat transfer in a tube flows [16] such as

$$S_{he}=3.66 \qquad N_{ue}=3.66 \qquad f_e=64\left(R_e\frac{2u_mR_\delta}{\nu}\right)^{-1} \tag{6.29}$$

The flow averaged values of mass fraction, temperature and velocity are

$$C_m=\frac{1}{3}\{(2u_0+u_i)C_0+(u_0+2u_i)C_i\}\frac{1}{u_0+u_i}$$
$$\theta_m=\frac{1}{3}\{(2u_0+u_i)\theta_0+(u_0+2u_i)\theta_i\}\frac{1}{u_0+u_i} \tag{6.30}$$
$$u_m=\frac{1}{2}(u_0+u_i)$$

In Fig. 13, a typical example of numerical results is shown for the case of ethanol-water mixture at $T_{00}=90°C$, $T_w=85°C$ and $U_{00}=100$ cm/s in a circular tube ($R_0=1$ cm). The flow variables change more slowly in the flow direction than they do in the developing flows. In the latter case, the high rate of condensation close to the flow inlet results in the reduction of the bulk mass fraction of the volatile component of vapor mixture after the end of the developing region, which leads to an increase in the condensation rate again. In the quasi-developed case, the condensation rate as well as the heat flux to the wall decreases monotonously in the flow direction. Comparison between the developing and quasi-developed flows is shown in Fig. 14. The difference is quite remarkable. In addition to the behavior mentioned above, the condensation rate takes much lower values than those of the developing flow.

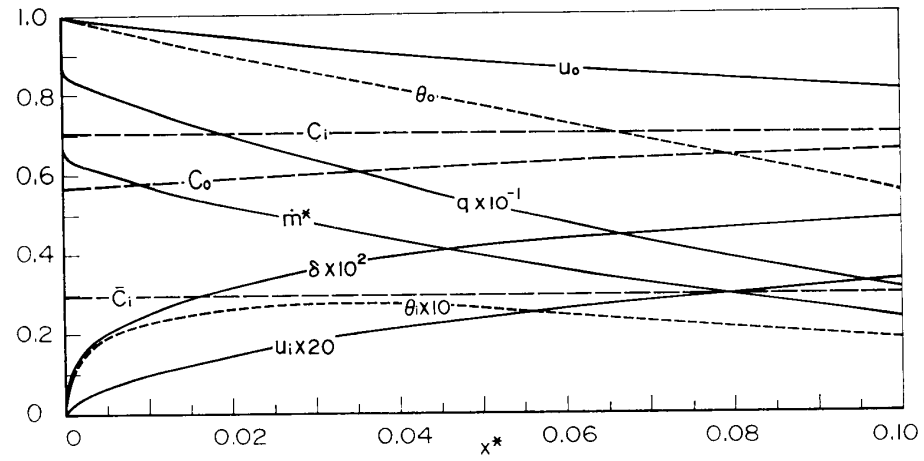

FIG. 13. Laminar co-current developed flow; ethanol-water, C, $T_{00}=90°C$, $T_w=85°C$, $U_{00}=100$ cm/s.

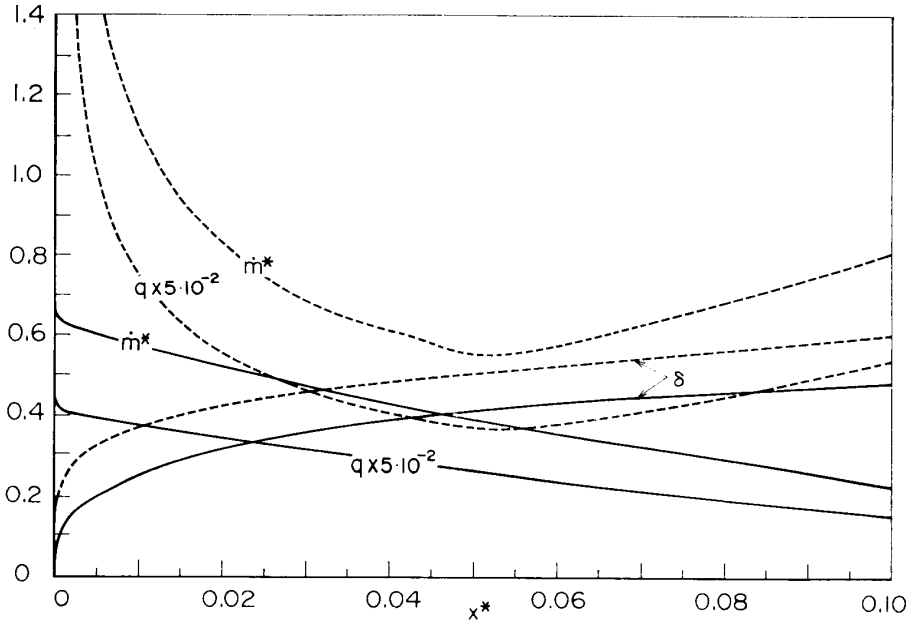

FIG. 14. Comparison between developed (—) and developing (---) flows; lamiuar co-current, ethanol-water, C, $T_{00}=90°C$, $T_w=85°C$, $U_{00}=100$ cm/s.

The heat flux to the wall, the film thickness and the interfacial temperature and velocity are also considerably small. Further, the interfacial temperature behaves quite differently, increasing from the wall temperature ($\theta_i=0$) at $x=0$ and decreasing gradually after taking a maximum. These imply that the flow behavior in the starting region of condensation has a very important role on the film condensation of binary mixtures in a vertical channel.

The effects of transfer coefficients, S_h, N_u and f, are shown in Fig. 15. Dashed lines mean the result with the coefficients of parabolic profile, Eq. (6.28). For full lines, the coefficients are varied by a factor ($1\sim2$) of the values of Eq. (6.29). The friction factor and the heat transfer coefficient have little effect on the condensation

features, whereas the mass transfer coefficient has an appreciable effect (dotted lines). It is noted that, although large values of mass transfer coefficient yield high rates of condensation at the beginning, the rate decreases in the flow-direction so rapidly to become smaller than that of smaller mass transfer coefficients.

Figures 16-a to 16-c show the effects of the channel geometry, the vapor flow velocity at the inlet, the temperatures at the inlet and the wall, and the type of binary mixture, respectively. They have qualitatively the same effect as they have in the case of developing flows. Nozzle flows result in higher local rates of condensation, although they give smaller values of overall condensation mass flux than diffuser

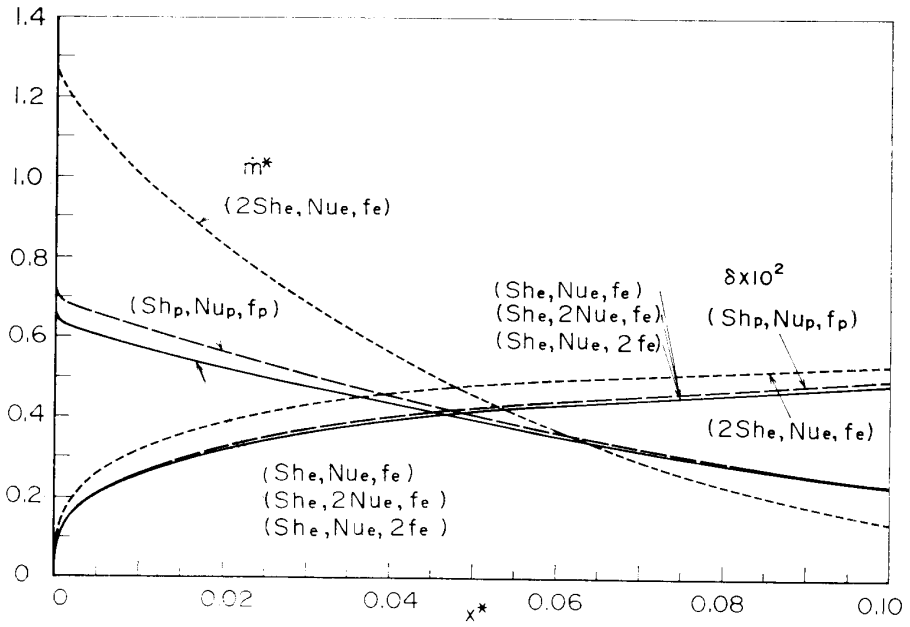

FIG. 15. Effect of transfer coefficients (*Sh*, *Nu*, *f*) on the film condensation of laminar-developed flow; ethanol-water, C, T_{00}=90°C, T_w=85°C, U_{00}= 100 cm/s.

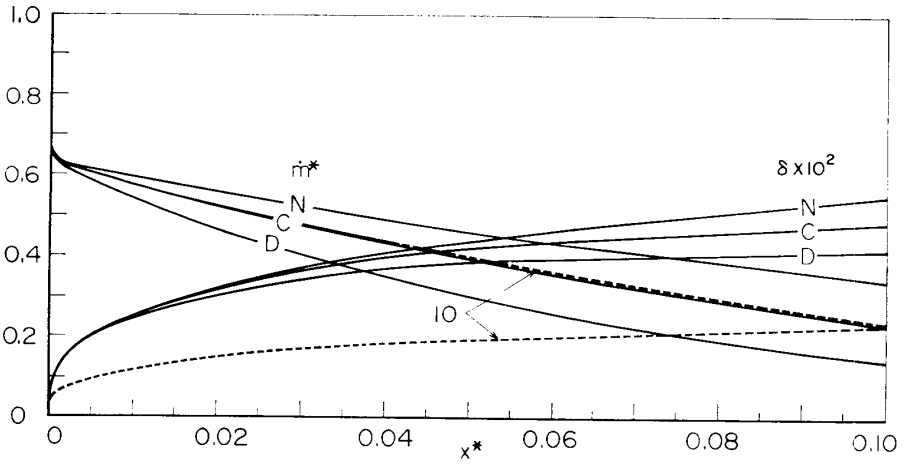

FIG. 16-a. Effects of channel geometry and vapor-flow velocity on the film condensation of laminar developed flow; ethanol-water, T_{00}=90°C, T_w=85°C, U_{00}=100 cm/s (—), 10 cm/s (---)

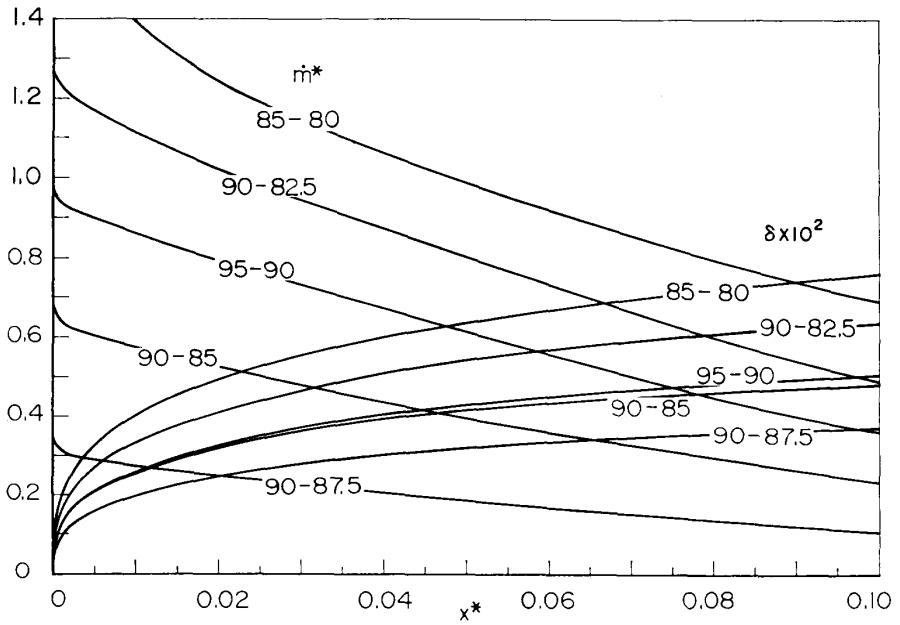

FIG. 16-b. Effect of inlet-vapor and wall temperatures ($T_{00}-T_w$, °C) on the film condensation of laminar developed flow; ethanol-water, C,U_{00}=100 cm/s.

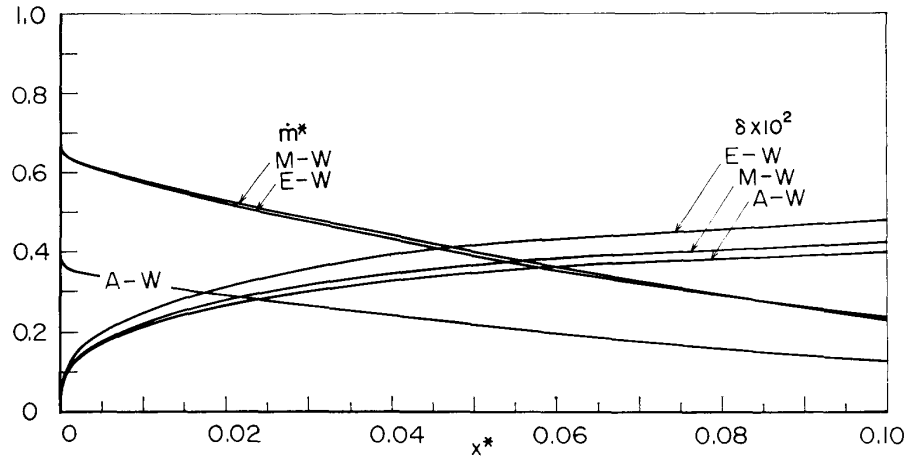

FIG. 16-c. Effect of type of binary mixtures (E-W, M-W, A-W) on the film condensation of laminar developed flow; C, T_{00}=90°C, T_w=85°C, U_{00}=100 cm/s.

flows; in Fig. 16-a, $\int_0^{0.1} \dot{m}^* dx^* = 0.0824$(D), 0.0814(C), 0.0805(N). Lower vapor velocities yield slightly higher condensation rates in the $\dot{m}^* - x^*$ coordinates (Fig. 16-a). Larger values of the factor Δ_w lead to higher condensationrates (Fig. 16-b, c).

Figure 17 represents the condensation behavior of counter-current flow of ethanol-water mixture under the same condition as in Fig. 13. The interfacial temperature increases from the wall temperature at $x=0$ monotonously in the liquid flow direction. The film thickness is smaller than that of co-current flows. However, values of the local condensation rate and the local heat flux to the wall hardly differ from

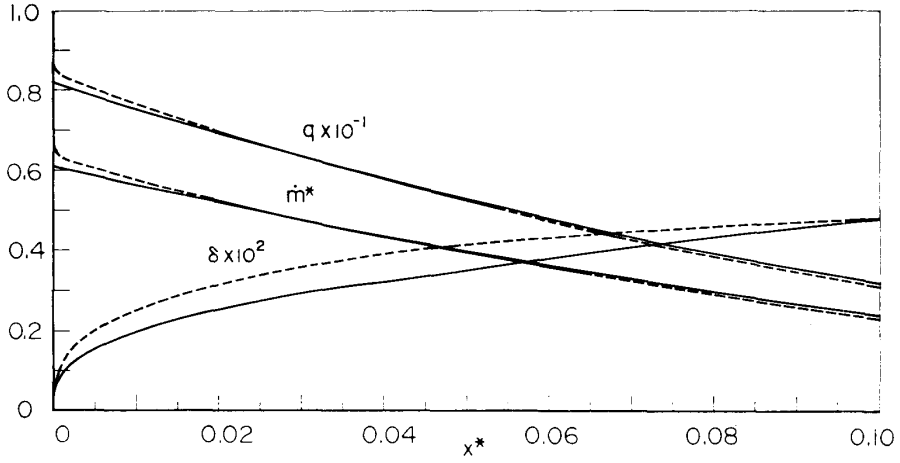

FIG. 17. Laminar counter-current developed flow; ethanol-water, C, $T_{00}=90°C$, $T_w=85°C$, $U_{00}=-100$ cm/s, (---, co-current flow).

those of co-current flows. It implies that the direction of the vapor flow has little influence upon the condensation behavior of quasi-developed flows.

6.2 *Turbulent Flows*

In the case of smooth-tube flows which are not strongly coupled with heat and mass transfer processes, experiments have shown that many of the relations with regard to flat-plate flows may be applied to developed tube-flows. It may be assumed that the radial distributions of velocity, temperature and mass fraction of the vapor mixture are approximated by a power-low profile

$$\begin{aligned}\frac{u-u_i}{u_0-u_i}&=\left\{1-\left(\frac{r}{R_\delta}\right)^n\right\}\\ \frac{\theta-\theta_i}{\theta_0-\theta_i}&=\left\{1-\left(\frac{r}{R_\delta}\right)^m\right\}\\ \frac{C-C_i}{C_0-C_i}&=\left\{1-\left(\frac{r}{R_\delta}\right)^\ell\right\}\end{aligned}\tag{6.31}$$

With these profiles, the integrals involved in Eqs. (6.13), (6.11), (6.6) and (6.5) can be evaluated as

$$\frac{1}{R_\delta^2}\int_0^{R_\delta} urdr=\frac{1}{(n+1)(n+2)}(u_0-u_i)+\frac{1}{2}u_i$$

$$\begin{aligned}\frac{1}{R_\delta^2}\int_0^{R_\delta} uurdr&=\frac{1}{(2n+1)(2n+2)}u_0u_0+\left\{\frac{1}{(n+1)(n+2)}-\frac{1}{(2n+1)(2n+2)}\right\}2u_0u_i\\&\quad+\left\{\frac{1}{2}-\frac{2}{(n+1)(n+2)}-\frac{1}{(2n+1)(2n+2)}\right\}u_iu_i\\&\equiv a_{u00}u_0u_0+a_{u0i}u_0u_i+a_{uii}u_iu_i\end{aligned}$$

$$\frac{1}{R_\delta^2}\int_0^{R_\delta} u\theta rdr=\left[\frac{1}{(n+m+1)(n+m+2)}u_0\right.$$

$$+\left\{\frac{1}{(m+1)(m+2)}-\frac{1}{(n+m+1)(n+m+2)}\right\}u_i\Big]\theta_0$$
$$+\Big[\left\{\frac{1}{(n+1)(n+2)}-\frac{1}{(n+m+1)(n+m+2)}\right\}u_0$$
$$+\left\{\frac{1}{2}-\frac{1}{(n+1)(n+2)}-\frac{1}{(m+1)(m+2)}+\frac{1}{(n+m+1)(n+m+2)}\right\}u_i\Big]\theta_i$$
$$\equiv(a_{t00}u_0+a_{t0i}u_i)\theta_0+(a_{ti0}u_0+a_{tii}u_i)\theta_i$$

$$\frac{1}{R_\delta^2}\int_0^{R_\delta}uCrdr=\Big[\frac{1}{(n+l+1)(n+l+2)}u_0$$
$$+\left\{\frac{1}{(l+1)(l+2)}-\frac{1}{(n+l+1)(n+l+2)}\right\}u_i\Big]C_0$$
$$+\Big[\left\{\frac{1}{(n+1)(n+2)}-\frac{1}{(n+l+1)(n+l+2)}\right\}u_0$$
$$+\left\{\frac{1}{2}-\frac{1}{(n+1)(n+2)}-\frac{1}{(l+1)(l+2)}+\frac{1}{(n+l+1)(n+l+2)}\right\}u_i\Big]C_i$$
$$\equiv(a_{c00}u_0+a_{c0i}u_i)C_0+(a_{ci0}u_0+a_{cii}u_i)C_i$$

where the constants a_{u00}, a_{t00}, a_{c00} etc. denote the coefficients concerned with u_0u_0, $u_0\theta_0$, u_0c_0 etc. respectively. The integral of $(\partial c/\partial r)(\partial\theta/\partial r)$ involved in the equation of energy, Eq. (6.6), is not always integrated due to the term $(r/R_\delta)^{m+l-2}$ in which $m+l<1$. The contribution of laminar diffusion to the mass transfer process in the turbulent flow may be negligible compared with the turbulent convection. Hence, in the turbulent case, the omission of the integral can be assumed.

With the integrals, the governing equation of vapor flow, Eqs. (6.5), (6.6), (6.11) and (6.13), are written as follows.

$$\frac{d}{dx^*}[\rho R_\delta^2\{(a_{c00}u_0+a_{c0i}u_i)C_0+(a_{ci0}u_0+a_{cii}u_i)C_i\}]=-\dot{m}^*C_iR_\delta+q_c^*R_\delta \quad (6.32)$$

$$\frac{d}{dx^*}[\rho c_pR_\delta^2\{(a_{t00}u_0+a_{t0i}u_i)\theta_0+(a_{ti0}u_0+a_{tii}u_i)\theta_i\}]=-\dot{m}^*c_p\theta_iR_\delta+q_t^*R_\delta \quad (6.33)$$

$$\frac{d}{dx^*}\left[\rho_r\rho R_\delta^2\left\{\frac{u_0-u_i}{(n+1)(n+2)}+\frac{u_i}{2}\right\}+\bar{\rho}R_\delta\delta\left(\frac{2}{3}u_i+\frac{1}{6}\frac{\mu_r}{\bar{\mu}}\delta\tau^*\right)\right]=0 \quad (6.34)$$

$$\left(1+\frac{\delta}{R_\delta}\right)\frac{R_\delta^2}{2M_c^2}\frac{dp}{dx^*}=\frac{\bar{G}_rR_eS_c}{2\bar{R}_e^2}R_\delta^2\left(\rho+\frac{\bar{\rho}}{\rho_r}\frac{\delta}{R_\delta}\right)-u_i\left(\dot{m}^*R_\delta+S_c\frac{\bar{\mu}}{\mu_r}\frac{R_\delta}{\delta}\right)$$
$$-\frac{d}{dx^*}\{\rho R_\delta^2(a_{u00}u_0u_0+a_{u0i}u_0u_i+a_{uii}u_iu_i) \quad (6.35)$$

from which C_0, θ_0, u_0 and p can be obtained.

It should be noted that the profile given by Eq. (6.31) are only approximate and cannot describe accurately the flow behavior close to the interface even in the sence of approximation. It does serve to give an adequate representation of the gross

behavior of the flow. Thus, for estimation of the flux rates close to the interface, additional informations are required. There is no knowledge of such a flow behavior available for binary mixture condensation in turbulent-tube flows. When the flow field is weakly coupled with heat and mass transfer processes, empirical correlations may be employed from textbooks of heat transfer. In Ref. 16, the transfer coefficients are recommended as

$$\begin{aligned} S_h &= 0.023 R_{ed}^{0.8} S_c^{0.3} \\ N_u &= 0.023 R_{ed}^{0.8} P_r^{0.3} \\ f &= 0.316 R_{ed}^{-0.25} \end{aligned} \tag{6.36}$$

where

$$R_{ed} = R_e \frac{2u_m R_\delta}{\nu} \tag{6.37}$$

and the average velocity is

$$u_m = \frac{1}{R_\delta^2} \int_0^{R_\delta} 2urdr = 2\left\{ \frac{u_0 - u_i}{(n+1)(n+2)} + \frac{u_i}{2} \right\} \tag{6.38}$$

The fluxes, q_c^*, q_t^* and τ^*, are expressed as

$$\begin{aligned} q_c^* &= \frac{0.023}{2} R_{ed}^{0.8} S_c^{0.3} \frac{C_i - C_m}{R_\delta} \\ q_t^* &= \frac{0.023}{2} R_{ed}^{0.8} P_r^{0.3} \frac{\theta_i - \theta_m}{R_\delta} \\ \tau^* &= -\frac{0.316}{16} R_{ed}^{0.75} \frac{u_m}{R_\delta} \end{aligned} \tag{6.39}$$

where the flow-average mass-fraction and temperature are given by

$$\begin{aligned} C_m &= \frac{2}{u_m} \{ (a_{c00} u_0 + a_{c0i} u_i) C_0 + (a_{ci0} u_0 + a_{cii} u_i) C_i \} \\ \theta_m &= \frac{2}{u_m} \{ (a_{t00} u_0 + a_{t0i} u_i) \theta_0 + (a_{ti0} u_0 + a_{tii} u_i) \theta_i \} \end{aligned} \tag{6.40}$$

With these coefficients, the interfacial varaibles, θ_i, u_i, $\dot{m}^*$ and δ, are calculated by Eqs. (6.15) to (6.20).

In Fig. 18, a numerical result of turbulent flow condensation is shown for the same flow conditions as in Fig. 13; ethanol-water, $T_{00} = 90°C$, $T_w = 85°C$, $U_{00} = 100$ cm/s, constant cross section. Owing to Ref. 17, power indexes of the profile are used of $n = m = 1 = 1/5$. As shown in Fig. 20, these power indexes have little effect. The condensation rate take larger values for $n = m = 1 = 1/7$ than those for $n = m = 1 = 1/5$. This is resulted from the fact that smaller values of power index lead to larger mean

flow velocities, hence, larger values of mass transfer coefficient; $u_m=0.595$ ($n=1/5$), 0.680 ($n=1/7$).

In Fig. 19, the result is compared with that of laminar flow. Large values of transfer coefficients yield higher rates of condensation and heat flux to the wall. The general features are almost same for both cases. The mass transfer coefficient has

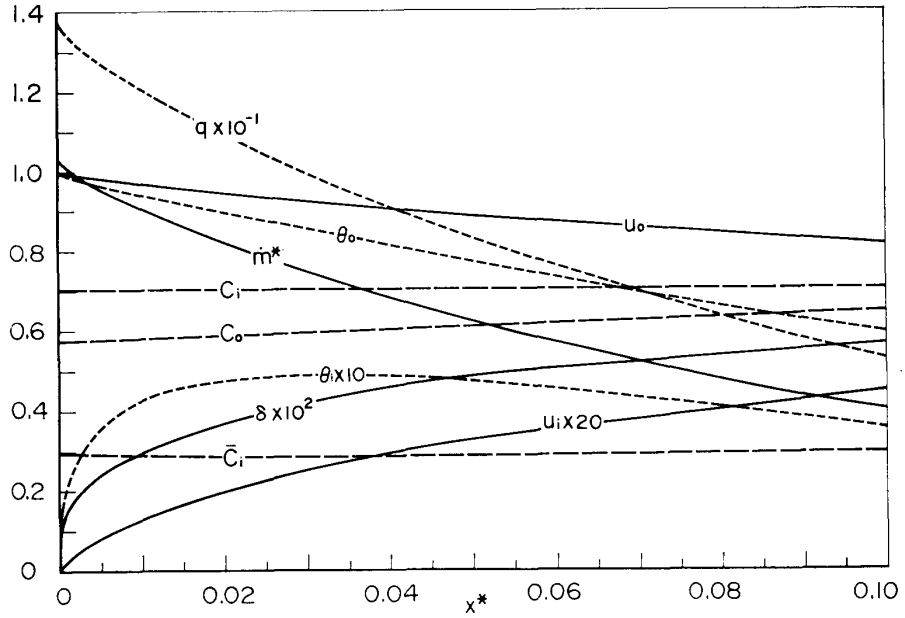

FIG. 18. Turbulent co-current developed flow; ethanol-water, C, $T_{00}=90°C$, $T_w=85°C$, $U_{00}=100$ cm/s.

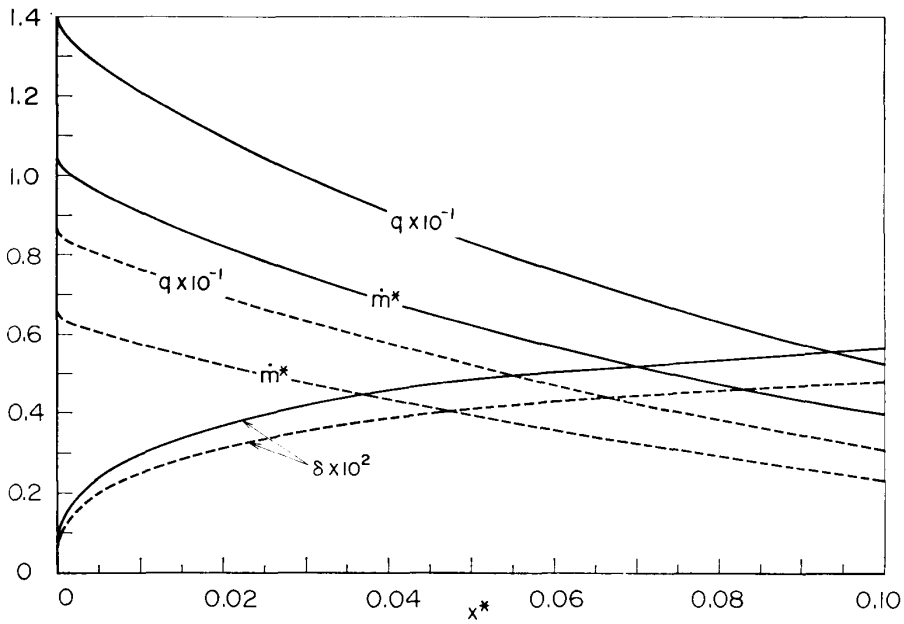

FIG. 19. Comparison between turbulent (—) and laminar (---) developed flows; ethanol-water, C, $T_{00}=90°C$, $T_w=85°C$, $U_{00}=100$ cm/s.

an appreciable effect whereas the friction coefficient and the heat transfer coefficient have little influence (Fig. 20). Nozzle flows lead to higher condensation rates than diffuser flows (Fig. 21-a). In the case of Fig. 21-a, the overall condensation rate is larger for the nozzle flow; $\int_0^{0.1} \dot{m}^* dx^* = 0.116$ (D), 0.129 (C), 0.137 (N). Vapor flow

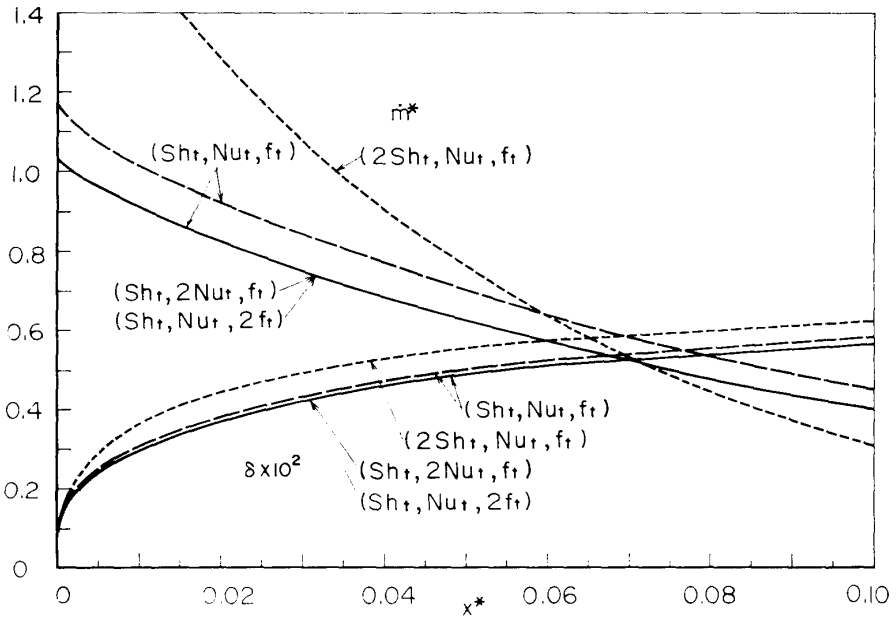

FIG. 20. Effect of transfer coefficients (S_{ht}, N_{ut}, f_t) on the film condensation of turbulent developed flow; ethanol-water, C, $T_{00}=90°C$, $T_w=85°C$, $U_{00}=100$ cm/s; —, $n=m=1=1/5$; ——, $n=m=1=1/7$.

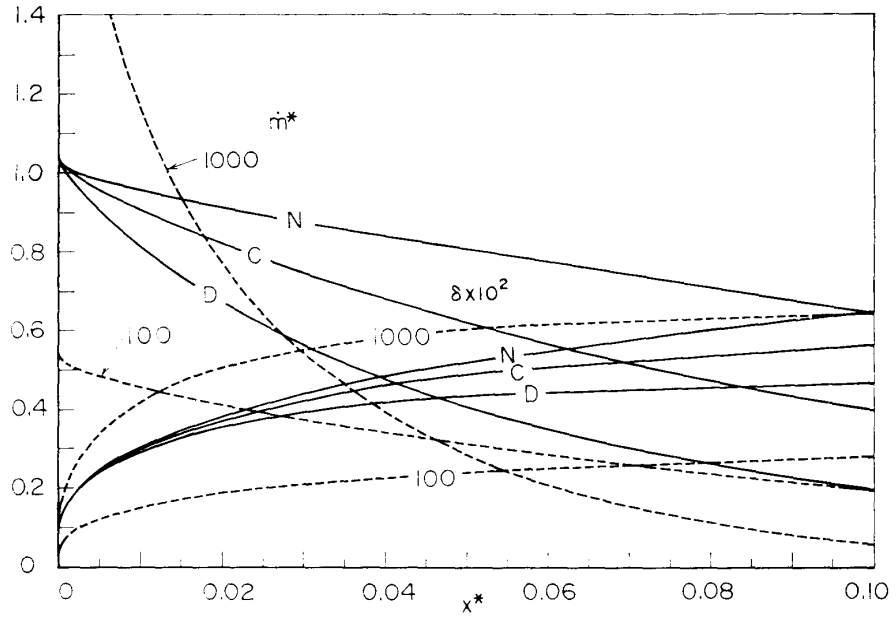

FIG. 21-a. Effects of channel geometry and vapor-flow velocity on the film condensation of turbulent developed flow; ethanol-water, $T_{00}=90°C$, $T_w=85°C$: N, C, D, $U_{00}=100$ cm/s (m^*, $\delta\times10^2$); C, $U_{00}=100$, 1000 cm/s ($m^*/2$, $\delta\times10^2/2$).

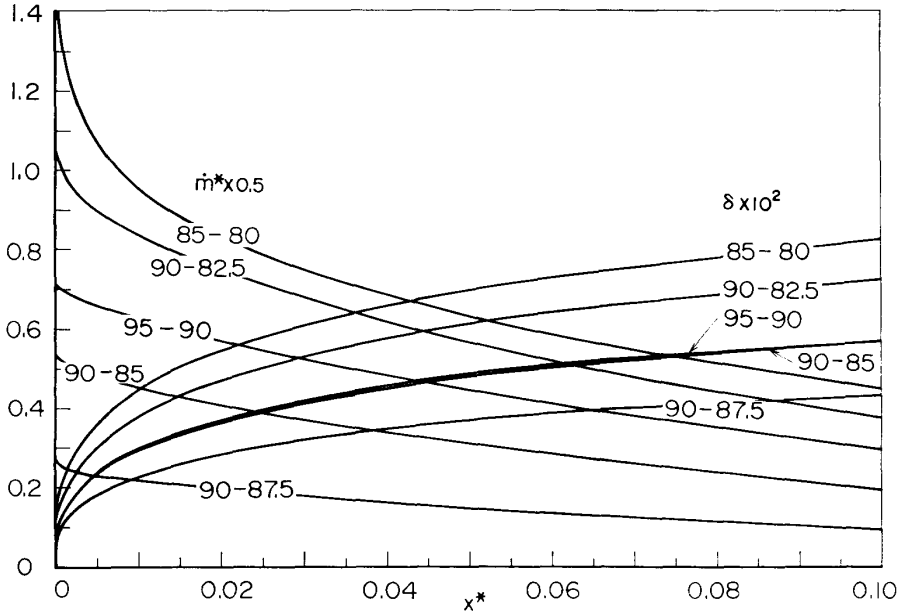

FIG. 21-b. Effect of inlet-vapor and wall temperatures ($T_{00}-T_w$, °C) on the film condensation of turbulent developed flow; ethanol-water, C, $U_{00}=100$ cm/s.

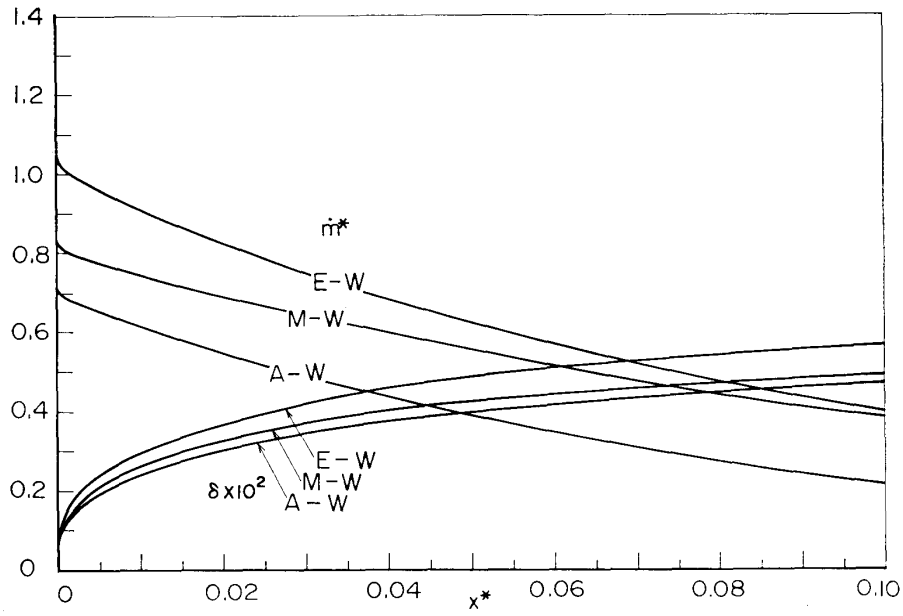

FIG. 21-c. Effect of type of binary mixtures (E-W, M-W, A-W) on the film condensation of turbulent developed flow; C, $T_{00}=90°C$, $T_w=85°C$, $U_{00}=100$ cm/s.

velocities give a considerable effecton condensation rates through the mass transfer coefficient (Fig. 21-a). For different conditions of the inlet-vapor and wall temperature and different types of binary mixture, the condensation behavior is largely characterized by the factor Δ_w (Figs. 21-b and 21-c). As shown in Fig. 22, the effect of the vapor flow direction is also not appreciable.

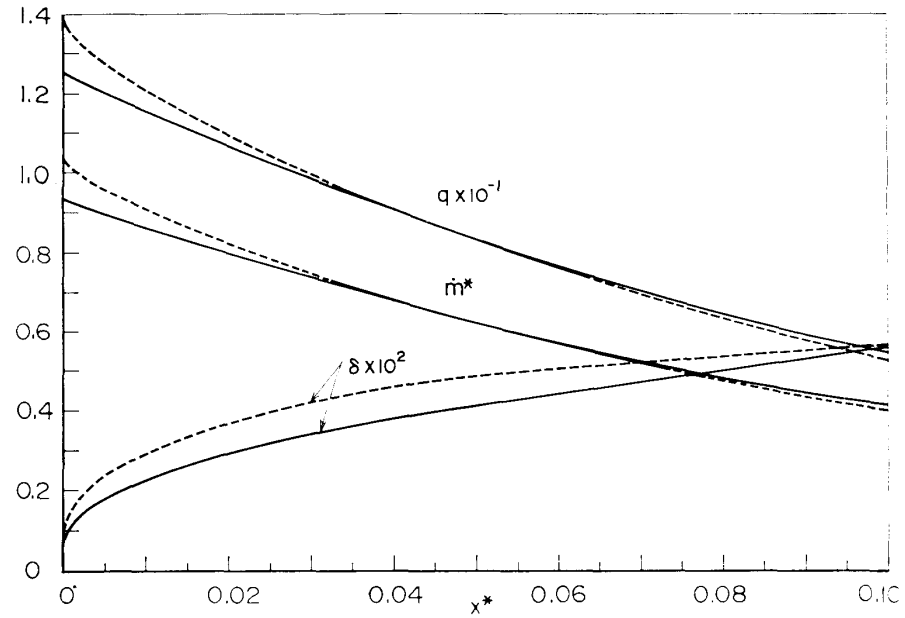

FIG. 22. Turbulent counter-current developed flow; ethanol-water, C, $T_{00}=90°\mathrm{C}$, $T_w=85°\mathrm{C}$, $U_{00}=-100$ cm/s, (---, co-current flow).

7. Similarity Characteristics of Film Condensation

As shown in the preceding chapters, film condensation of binary mixtures is controlled largely by the phase equilibrium characteristics which are inherent to the mixture. The physical features of systems tend to be less similar, as the factors proper to each system play a more important role. From the standpoint of application of the results as well as understanding them, however, it is substantial to examine the phenomena on the basis of the similarity concept. Although it has also been considered with a similarity concept in the preceding chapters, more general similarity will be studied in the present chapter.

Taking the characteristic lengths and velocities in the x and r directions, respectively as

$$X,\ Y;\ U,\ V$$

and denoting the characteristic properties by suffix $r0$, the conservation equations are written as

$$\frac{\partial}{\partial x}(\rho u)+\frac{XV}{YU}\frac{1}{r}\frac{\partial}{\partial r}(r\rho v)=0 \tag{7.1}$$

$$\frac{\partial}{\partial x}(\rho uu)+\frac{XV}{YU}\frac{1}{r}\frac{\partial}{\partial r}(r\rho vu)=-\frac{p_{r0}}{\rho_{r0}U^2}\frac{\partial p}{\partial x}+\frac{gX}{U^2}\rho$$
$$+\frac{XV}{YU}\frac{\nu_{r0}}{VY}\left\{\left(\frac{Y}{X}\right)^2\frac{\partial}{\partial x}\left(\mu\frac{\partial u}{\partial x}\right)+\frac{1}{r}\frac{\partial}{\partial r}\left(r\mu\frac{\partial u}{\partial x}\right)\right\} \tag{7.2}$$

$$\frac{\partial}{\partial x}(\rho uv)+\frac{XV}{YU}\frac{1}{r}\frac{\partial}{\partial r}(r\rho vv)=-\frac{p_{r0}}{\rho_{r0}V^2}\frac{XV}{YU}\frac{\partial p}{\partial r}$$
$$+\frac{XV}{YU}\frac{\nu_{r0}}{VY}\left\{\left(\frac{Y}{X}\right)^2\frac{\partial}{\partial x}\left(\mu\frac{\partial v}{\partial x}\right)+\frac{1}{r}\frac{\partial}{\partial r}\left(r\mu\frac{\partial v}{\partial r}\right)\right\} \tag{7.3}$$

$$\frac{\partial}{\partial x}(\rho uC)+\frac{XV}{YU}\frac{1}{r}\frac{\partial}{\partial r}(r\rho vC)$$
$$=\frac{XV}{YU}\frac{\nu_{r0}}{VY}\frac{1}{S_c}\left\{\left(\frac{Y}{X}\right)^2\frac{\partial}{\partial x}\left(\rho D\frac{\partial C}{\partial x}\right)+\frac{1}{r}\frac{\partial}{\partial r}\left(r\rho D\frac{\partial C}{\partial r}\right)\right\} \tag{7.4}$$

$$c_p\frac{\partial}{\partial x}(\rho u\theta)+\frac{XV}{XU}\frac{c_p}{r}\frac{\partial}{\partial r}(r\rho v\theta)$$
$$=\frac{XV}{YU}\frac{\nu_{r0}}{VY}\left[\frac{1}{P_r}\left\{\left(\frac{Y}{X}\right)^2\frac{\partial}{\partial x}\left(k\frac{\partial\theta}{\partial x}\right)+\frac{1}{r}\frac{\partial}{\partial r}\left(rk\frac{\partial\theta}{\partial r}\right)\right\}\right.$$
$$\left.+\frac{P_r}{S_c}\rho c_p'D\left\{\left(\frac{Y}{X}\right)^2\frac{\partial C}{\partial x}\frac{\partial\theta}{\partial x}+\frac{\partial C}{\partial r}\frac{\partial\theta}{\partial r}\right\}\right] \tag{7.5}$$

where

$$\theta=\frac{T-T_w}{T_{00}-T_w} \tag{7.6}$$

Inspections into Eq. (7.1) yields

$$\frac{X}{Y}\frac{V}{U}=1 \qquad \frac{\bar{X}}{\bar{Y}}\frac{\bar{V}}{\bar{U}}=1 \tag{7.7}$$

The condition which reduces the equations to the boundary layer type equations is

$$\left(\frac{Y}{X}\right)^2\ll 1 \qquad \left(\frac{\bar{Y}}{\bar{X}}\right)^2\ll 1 \tag{7.8}$$

From Eq. (7.3), it is seen that the condition

$$\frac{\rho_{r0}V^2}{p_{r0}}\ll 1 \qquad \frac{\bar{\rho}_{r0}\bar{V}^2}{\bar{p}_{r0}}\ll 1 \tag{7.9}$$

leads to the uniform pressure distribution across the flow passage,

$$\frac{\partial p}{\partial r}=0 \tag{7.10}$$

Under the conditions of Eqs. (7.7) to (7.9), the governing equations, Eqs (7.1) to (7.5), become

$$\frac{\partial}{\partial x}(\rho u)+\frac{1}{r}\frac{\partial}{\partial r}(r\rho v)=0 \tag{7.11}$$

$$\frac{\partial}{\partial x}(\rho uu)+\frac{1}{r}\frac{\partial}{\partial r}(r\rho vu)=-\frac{p_{r0}}{\rho_{r0}U^2}\frac{dp}{dx}+\frac{gX}{U^2}\rho+\frac{\nu_{r0}}{VY}\frac{1}{r}\frac{\partial}{\partial r}\left(r\mu\frac{\partial u}{\partial r}\right) \tag{7.12}$$

$$\frac{\partial}{\partial x}(\rho uC)+\frac{1}{r}\frac{\partial}{\partial r}(r\rho vC)=\frac{\nu_{r0}}{VY}\frac{1}{S_c}\frac{1}{r}\frac{\partial}{\partial r}\left(r\rho D\frac{\partial C}{\partial r}\right) \tag{7.13}$$

$$c_p\frac{\partial}{\partial x}(\rho u\theta)+\frac{c_p}{r}\frac{\partial}{\partial r}(r\rho v\theta)=\frac{\nu_{r0}}{VY}\frac{1}{P_r}\left\{\frac{1}{r}\frac{\partial}{\partial r}\left(rk\frac{\partial\theta}{\partial r}\right)+\frac{P_r}{S_c}\rho c_p'D\frac{\partial C}{\partial r}\frac{\partial\theta}{\partial r}\right\} \tag{7.14}$$

The boundary conditions at the liquid-vapor interface can be expressed as

$$\bar{U}\bar{u}_i=Uu_i \tag{7.15}$$

$$\bar{\theta}_i=\theta_i \tag{7.16}$$

$$\bar{\rho}_{r0}\bar{V}\left\{\bar{\rho}\left(\bar{v}-\bar{u}\frac{d\bar{R}_\delta}{d\bar{x}}\right)\right\}_i=\rho_{r0}V\left\{\rho\left(v-u\frac{dR_\delta}{dx}\right)\right\}_i=\dot{m} \tag{7.17}$$

$$\bar{\mu}_{r0}\frac{\bar{U}}{\bar{Y}}\left\{\bar{\mu}\frac{\partial\bar{u}}{\partial\bar{r}}\right\}_i=\mu_{r0}\frac{U}{Y}\left\{\mu\frac{\partial u}{\partial r}\right\}_i \tag{7.18}$$

$$\left\{\dot{m}\bar{C}-\frac{\bar{\rho}_r\bar{D}_r}{\bar{Y}}\left(\bar{\rho}\bar{D}\frac{\partial\bar{C}}{\partial\bar{r}}\right)\right\}_i=\left\{\dot{m}C-\frac{\rho_{r0}D_{r0}}{Y}\left(\rho D\frac{\partial C}{\partial r}\right)\right\}_i \tag{7.19}$$

$$\frac{\bar{k}_{r0}}{\bar{Y}}\left(-\bar{k}\frac{\partial\bar{\theta}}{\partial\bar{Y}}\right)_i-\frac{k_{r0}}{Y}\left(-k\frac{\partial\theta}{\partial r}\right)_i=\frac{\lambda_{r0}}{T_{00}-T_w}\lambda\dot{m}-\frac{\bar{\lambda}_{r0}}{\bar{Y}}\bar{\rho}_{r0}\bar{D}_{r0}\left\{\lambda_{12}\bar{\rho}\bar{D}\frac{\partial\bar{C}}{\partial\bar{r}}\right\}_i \tag{7.20}$$

As for the characteristic scale of the axial length, one can chose

$$\bar{X}=X;\quad \bar{x}=x$$

Condensate Flow

By assuming a thin thickness of the flow ($\delta\ll R$) and introducing a coordinate $\bar{y}$ defined as

$$\bar{y}=\bar{R}-\bar{r}\qquad(\bar{y}\ll 1) \tag{7.21}$$

Eqs. (7.11) to (7.14) are reduced to

$$\frac{\partial}{\partial x}(\bar{\rho}\bar{u})+\frac{\partial}{\partial\bar{y}}(\bar{\rho}\bar{v})=0 \tag{7.22}$$

$$\frac{\partial}{\partial x}(\bar{\rho}\bar{u}\bar{u})+\frac{\partial}{\partial\bar{y}}(\bar{\rho}\bar{v}\bar{u})=-\frac{p_{r0}}{\bar{\rho}_{r0}\bar{U}^2}\frac{dp}{dx}+\frac{g\bar{X}}{\bar{U}^2}\bar{\rho}+\frac{\bar{\nu}_{r0}}{\bar{V}\bar{Y}}\frac{\partial}{\partial\bar{y}}\left(\bar{\mu}\frac{\partial\bar{u}}{\partial\bar{y}}\right) \tag{7.23}$$

$$\frac{\partial}{\partial x}(\bar{\rho}\bar{u}\bar{C})+\frac{\partial}{\partial\bar{y}}(\bar{\rho}\bar{v}\bar{C})=\frac{\bar{\nu}_{r0}}{\bar{V}\bar{Y}}\frac{1}{\bar{S}_c}\frac{\partial}{\partial\bar{y}}\left(\bar{\rho}\bar{D}\frac{\partial\bar{C}}{\partial\bar{y}}\right) \tag{7.24}$$

$$\bar{c}_p\frac{\partial}{\partial x}(\bar{\rho}\bar{u}\bar{\theta})+\bar{c}_p\frac{\partial}{\partial\bar{y}}(\bar{\rho}\bar{v}\bar{\theta})=\frac{\bar{\nu}_{r0}}{\bar{V}\bar{Y}}\frac{1}{\bar{P}_r}\left\{\frac{\partial}{\partial\bar{y}}\left(\bar{k}\frac{\partial\bar{\theta}}{\partial\bar{y}}\right)+\frac{\bar{P}_r}{\bar{S}_c}\bar{\rho}\bar{c}_p'\bar{D}\frac{\partial\bar{C}}{\partial\bar{y}}\frac{\partial\bar{\theta}}{\partial\bar{y}}\right\} \tag{7.25}$$

where the positive direction of $\bar{v}$ is taken as the positive direction of the $\bar{y}$-ccordinate.

If the Reynolds number $\bar{V}\bar{Y}/\nu_{r0}$ can be assumed sufficiently small that

$$\frac{\bar{V}\bar{Y}}{\bar{\nu}_{r0}} \ll 1 \qquad S_c \frac{\bar{V}\bar{Y}}{\bar{\nu}_{r0}} \ll 1 \qquad P_r \frac{\bar{V}\bar{Y}}{\bar{\nu}_{r0}} \ll 1 \tag{7.26}$$

equations of motion, species and energy are further reduced to

$$\frac{\partial}{\partial \bar{y}}\left(\bar{\mu}\frac{\partial \bar{u}}{\partial \bar{y}}\right) = \frac{p_{r0}}{\bar{\rho}_{r0}\bar{U}^2}\frac{\bar{V}\bar{Y}}{\bar{\nu}_{r0}}\frac{dp}{dx} - \frac{g\bar{Y}^2}{\bar{U}\bar{\nu}_{r0}}\bar{\rho} \tag{7.27}$$

$$\frac{\partial}{\partial \bar{y}}\left(\bar{\rho}\bar{D}\frac{\partial \bar{C}}{\partial \bar{y}}\right) = 0 \tag{7.28}$$

$$\frac{\partial}{\partial \bar{y}}\left(\bar{k}\frac{\partial \bar{\theta}}{\partial \bar{y}}\right) = -\frac{\bar{P}_r}{\bar{S}_c}\bar{\rho}\bar{c}'_p\bar{D}\frac{\partial \bar{C}}{\partial \bar{y}}\frac{\partial \bar{\theta}}{\partial \bar{y}} \tag{7.29}$$

which are subject to the boundary conditions

$$\bar{u}=0 \qquad \frac{\partial \bar{C}}{\partial \bar{y}}=0 \qquad \bar{\theta}=0 \qquad \text{at} \quad \bar{y}=0 \tag{7.30}$$

$$\bar{u}=\bar{u}_i \qquad \bar{C}=\bar{C}_i \qquad \bar{\theta}=\bar{\theta}_i \qquad \text{at} \quad \bar{y}=\bar{\delta} \tag{7.31}$$

With the reasonable assumption of constant properties within the liquid layer, Eqs. (7.27) to (7.31) yield

$$\bar{u}=\bar{u}_i\frac{\bar{y}}{\bar{\delta}}+\frac{1}{2\bar{\mu}}\left(\frac{p_{r0}}{\bar{\rho}_{r0}\bar{U}^2}\frac{\bar{V}\bar{Y}}{\bar{\nu}_{r0}}\frac{dp}{dx}-\frac{g\bar{Y}^2}{\bar{U}\bar{\nu}_{r0}}\bar{\rho}\right)(\bar{y}^2-\bar{\delta}\bar{y}) \tag{7.32}$$

$$\bar{C}=\bar{C}_i \tag{7.33}$$

$$\bar{\theta}=\bar{\theta}_i\frac{\bar{y}}{\bar{\delta}} \tag{7.34}$$

With those solutions, the boundary conditions, Eqs. (7.18) to (7.20), are written as

$$\bar{u}_i+\frac{\bar{\delta}^2}{2\bar{\mu}}\left(\frac{p_{r0}}{\bar{\rho}_{r0}\bar{U}^2}\frac{\bar{V}\bar{Y}}{\bar{\nu}_{r0}}\frac{dp}{dx}-\frac{g\bar{Y}^2}{\bar{U}\bar{\nu}_{r0}}\bar{\rho}\right) = -\frac{\mu_{r0}}{\bar{\mu}_{r0}}\frac{U}{\bar{U}}\frac{Y}{\bar{Y}}\bar{\delta}\left(\mu\frac{\partial u}{\partial r}\right)_i \tag{7.35}$$

$$\dot{m}=\frac{1}{C_i-\bar{C}_i}\frac{\rho_{r0}D_{r0}}{Y}\left(\rho D\frac{\partial C}{\partial r}\right)_i \tag{7.36}$$

$$\frac{\bar{k}_{r0}}{\bar{Y}}\left(\bar{k}\frac{\bar{\theta}_i}{\bar{\delta}}\right)-\frac{k_{r0}}{Y}\left(-k\frac{\partial \theta}{\partial r}\right)_i = \frac{\lambda_{r0}}{T_{00}-T_w}\dot{m}\lambda \tag{7.37}$$

Integration of Eq. (7.22) with respect to $\bar{y}$ yields

$$\frac{\partial}{\partial x}\left[\frac{1}{2}\bar{\rho}\bar{\delta}\left\{\bar{u}_i-\frac{\bar{\delta}^2}{6\bar{\mu}}\left(\frac{p_{r0}}{\bar{\rho}_{r0}\bar{U}^2}\frac{\bar{V}\bar{Y}}{\bar{\nu}_{r0}}\frac{dp}{dx}-\frac{g\bar{Y}^2}{\bar{U}\bar{\nu}_{r0}}\bar{\rho}\right)\right\}\right] = \bar{\rho}\left(\bar{v}-\bar{u}\frac{d\bar{R}_\delta}{dx}\right)_i \tag{7.38}$$

In Eq. (7.35), the gravity term is most predominant. In order that u_i should be of the order of unity,

$$\bar{U}=\frac{g}{\bar{\nu}_{r0}}\bar{Y}^2 \tag{7.39}$$

Combining Eq. (7.39) with Eq. (7.7) gives

$$\bar{V}=\frac{g}{\bar{\nu}_{r0}}\frac{\bar{Y}^3}{\bar{X}} \tag{7.40}$$

Vapor Flow

For vapor flows, the condition of small Reynolds number such as Eq. (7.26) is too restrictive to treat the general features of condensation flows. Usually, it is required to solve strictly the set of governing equaions. Taking the reference condition as

$$\frac{VY}{\nu_{r0}}=1 \tag{7.41}$$

Eqs. (7.11) to (7.14) are rewritten as

$$\frac{\partial}{\partial x}(\rho u)+\frac{1}{r}\frac{\partial}{\partial r}(r\rho v)=0 \tag{7.42}$$

$$\frac{\partial}{\partial x}(\rho uu)+\frac{1}{r}\frac{\partial}{\partial r}(r\rho vu)=-\frac{p_{r0}}{\rho_{r0}U^2}\frac{dp}{dx}+\frac{gX}{U^2}\rho+\frac{1}{r}\frac{\partial}{\partial r}\left(r\mu\frac{\partial u}{\partial r}\right) \tag{7.43}$$

$$\frac{\partial}{\partial x}(\rho uC)+\frac{1}{r}\frac{\partial}{\partial r}(r\rho vC)=\frac{1}{S_c}\frac{1}{r}\frac{\partial}{\partial r}\left(r\rho D\frac{\partial C}{\partial r}\right) \tag{7.44}$$

$$c_p\frac{\partial}{\partial x}(\rho u\theta)+\frac{c_p}{r}\frac{\partial}{\partial r}(r\rho v\theta)=\frac{1}{P_r}\frac{1}{r}\frac{\partial}{\partial r}\left(rk\frac{\partial\theta}{\partial r}\right)+\frac{P_r}{S_c}\rho c_p' D\frac{\partial C}{\partial r}\frac{\partial\theta}{\partial r} \tag{7.45}$$

The boundary conditions of these equations are given by Eqs. (7.35) to (7.37) with Eq. (7.39) as follows;
at $r=R-\delta$,

$$u_i=\frac{\bar{\delta}^2}{2\bar{\mu}}\left(\frac{\bar{U}}{U}\rho-\frac{\bar{U}}{U}\frac{p_{r0}}{\bar{\rho}_{r0}\bar{U}^2}\frac{\bar{V}\bar{Y}}{\bar{\nu}_{r0}}\frac{dp}{dx}\right)-\frac{\mu_{r0}}{\bar{\mu}_{r0}}\frac{\bar{Y}}{Y}\bar{\delta}\left(\mu\frac{\partial u}{\partial r}\right)_i \tag{7.46}$$

$$v_i=u_i\frac{dR_\delta}{dx}+\frac{1}{\rho_{r0}V}\frac{\dot{m}}{\rho} \tag{7.47}$$

$$C_i=C_e(T_i) \tag{7.48}$$

$$\theta_i=\frac{\lambda_{r0}}{T_{00}-T_w}\frac{\bar{Y}}{\bar{k}_{r0}}\frac{\bar{\delta}}{\bar{k}}\lambda\dot{m}-\frac{k_{r0}}{\bar{k}_{r0}}\frac{\bar{Y}}{Y}\frac{\bar{\delta}}{k}\left(k\frac{\partial\theta}{\partial r}\right)_i \tag{7.49}$$

and at $r=0$

$$\frac{\partial u}{\partial r}=0 \qquad \frac{\partial C}{\partial r}=0 \qquad \frac{\partial \theta}{\partial r}=0 \tag{7.50}$$

The film thickness is given by Eq. (7.38) with Eqs. (7.17) and (7.35) as

$$\frac{\partial}{\partial x}\left[\frac{1}{2}\bar{\rho}\bar{\delta}\left\{\frac{2}{3}\frac{\bar{\delta}^2}{\bar{\mu}}\left(\bar{\rho}-\frac{p_{r0}}{\bar{\rho}_{r0}\bar{U}^2}\frac{\bar{V}\bar{Y}}{\bar{\nu}_{r0}}\frac{dp}{dx}\right)-\frac{\mu_{r0}}{\bar{\mu}_{r0}}\frac{U}{\bar{U}}\frac{\bar{Y}}{Y}\bar{\delta}\left(\mu\frac{\partial u}{\partial r}\right)_i\right\}\right]=\frac{\dot{m}}{\bar{\rho}_{r0}\bar{V}} \tag{7.51}$$

Since the axial change in the interfacial temperature is not substantial due to the large heat conductivity of the liquid, the interfacial mass fractions in phase equilibrium can be expanded around those at the wall temperature as

$$\begin{aligned} C_i&=C_e(T_w)+\left(\frac{\partial C_e}{\partial T}\right)_w(T-T_w)+\cdots \\ \bar{C}_i&=\bar{C}_e(T_w)+\left(\frac{\partial \bar{C}_e}{\partial T}\right)_w(T-T_w+)\cdots \end{aligned} \tag{7.52}$$

where $C_e(T)$ and $\bar{C}_e(T)$ are the equilibrium mass fractions of the vapor and the liquid at T, respectively. With these expansions, the condensation rate can be expressed as

$$\begin{aligned} \frac{\dot{m}}{\bar{\rho}_{r0}\bar{V}}=&\frac{C_{00}-C_e(T_w)}{C_e(T_w)-\bar{C}_e(T_w)}\frac{\rho_{r0}}{\bar{\rho}_{r0}}\frac{D_{r0}}{\bar{V}Y}\left(\rho D\frac{\partial C}{\partial r}\right)_i \\ &\cdot\left[1+\left\{\left(\frac{\partial C_e}{\partial T}\right)_w-\left(\frac{\partial \bar{C}_e}{\partial T}\right)_w\right\}\frac{T_{00}-T_w}{C_e(T_w)-\bar{C}_e(T_w)}\theta+\cdots\right]^{-1} \end{aligned} \tag{7.53}$$

Thus, in order to obtain the film thickness $\bar{\delta}\sim 0(1)$ from Eqs. (7.51) and (7.53), it is required that

$$\frac{C_{00}-C_e(T_w)}{C_e(T_{00})-\bar{C}_e(T_w)}\frac{\rho_{r0}}{\bar{\rho}_{r0}}\frac{D_{r0}}{\bar{V}Y}=1 \tag{7.54}$$

With Eqs. (7.37) and (7.40), Eq. (7.54) gives

$$\bar{Y}^3=\Delta_w\frac{\rho_{r0}}{\bar{\rho}_{r0}}\frac{D_{r0}}{\nu_{r0}}\frac{\nu_{r0}}{\bar{\nu}_{r0}}\frac{\bar{\nu}_{r0}^2}{g}\frac{X}{Y} \tag{7.55}$$

$$\bar{U}=\left(\Delta_w\frac{\rho_{r0}}{\bar{\rho}_{r0}}\frac{D_{r0}}{\nu_{r0}}\frac{\nu_{r0}}{\bar{\nu}_{r0}}\frac{X}{Y}\right)^{2/3}(g\bar{\nu}_{r0})^{1/3} \tag{7.56}$$

$$\bar{V}=\Delta_w\frac{\rho_{r0}}{\bar{\rho}_{r0}}\frac{D_{r0}}{\nu_{r0}}\frac{\nu_{r0}}{\bar{\nu}_{r0}}\frac{\bar{\nu}_{r0}}{Y} \tag{7.57}$$

where

$$\Delta_w=\frac{C_{00}-C_e(T_w)}{C_e(T_w)-\bar{C}_e(T_w)} \tag{7.58}$$

Setting the inlet radius and the inlet vapor velocity as Y and U, respectively

$$Y=R_0 \qquad U=U_{00} \tag{7.59}$$

and using Eqs. (7.7) and (7.41) yield

$$X=\bar{X}=R_0R_e \tag{7.60}$$

$$V=U_{00}R_e^{-1} \tag{7.61}$$

where $R_e=U_{00}R_0/\nu_{r0}$. These relations give

$$\frac{\bar{V}\bar{Y}}{\bar{\nu}_{r0}}=\left(\Delta_w\frac{\rho_{r0}}{\bar{\rho}_{r0}}\frac{D_{r0}}{\nu_{r0}}\frac{\nu_{r0}}{\bar{\nu}_{r0}}\right)^{4/3}\left(\frac{R_e}{\bar{G}_r}\right)^{1/3} \tag{7.62}$$

where $\bar{G}_r=gR_0^2/\bar{\nu}_{r0}^2$. Since the right hand side of Eq. (7.62) is of the order of $10^{-2}(R_e/\bar{G}_r)^{1/3}$, it is required to satisfy Eq. (7.26) that

$$\frac{R_e}{\bar{G}_r}<10^{1\sim2} \tag{7.63}$$

Inspection into Eqs. (7.42) to (7.49) yields that the flow variables will be a function of following parameters.

$$S_c,\quad P_r,\quad \frac{gX}{U^2},\quad \frac{\rho_{r0}U^2}{p_{r0}},\quad \frac{\lambda_{r0}}{T_{00}-T_w}\frac{\bar{Y}}{\bar{k}_{r0}}\bar{\rho}_{r0}\bar{V},\quad \frac{\mu_{r0}}{\bar{\mu}_{r0}}\frac{\bar{Y}}{Y},\quad \frac{k_{r0}}{\bar{k}_{r0}}\frac{\bar{Y}}{Y},\quad \frac{\bar{U}}{U}$$

$$\frac{\bar{\rho}_{r0}\bar{V}}{\rho_{r0}V},\quad \frac{p_{r0}}{\rho_{r0}\bar{U}^2}\frac{\bar{V}\bar{Y}}{\bar{\nu}_{r0}},\quad \left(\frac{\partial C_e}{\partial T}\right)_w\frac{T_{00}-T_w}{C_{ew}-\bar{C}_{ew}},\quad \left(\frac{\partial\bar{C}_e}{\partial T}\right)_w\frac{T_{00}-T_w}{C_{ew}-\bar{C}_{ew}}$$

These parameters can be expressed by Eqs. (7.55) to (7.62) as

$$\frac{gX}{U^2}=\frac{G_r}{R_e^2} \tag{7.64}$$

$$\frac{\lambda_{r0}}{T_{00}-T_w}\frac{\bar{Y}}{\bar{k}_{r0}}\bar{\rho}_{r0}\bar{V}=\frac{\lambda_{r0}}{\bar{c}_{pr0}(T_{00}-T_w)}\bar{P}_r\left(\Delta_w\frac{\rho_{r0}}{\bar{\rho}_{r0}}\frac{D_{r0}}{\nu_{r0}}\frac{\nu_{r0}}{\bar{\nu}_{r0}}\right)^{4/3}\left(\frac{R_e}{\bar{G}_r}\right)^{1/3} \tag{7.65}$$

$$\frac{\bar{Y}}{Y}=\left(\Delta_w\frac{\rho_{r0}}{\bar{\rho}_{r0}}\frac{D_{r0}}{\nu_{r0}}\frac{\nu_{r0}}{\bar{\nu}_{r0}}\right)^{1/3}\left(\frac{R_e}{\bar{G}_r}\right)^{1/3} \tag{7.66}$$

$$\frac{\bar{U}}{U}=\frac{\bar{\nu}_{r0}}{\nu_{r0}}\left(\Delta_w\frac{\rho_{r0}}{\bar{\rho}_{r0}}\frac{D_{r0}}{\nu_{r0}}\frac{\nu_{r0}}{\bar{\nu}_{r0}}\right)^{2/3}\left(\frac{\bar{G}_r}{R_e}\right)^{1/3}\qquad \frac{\bar{\rho}_{r0}\bar{V}}{\rho_{r0}V}=\Delta_w\frac{D_{r0}}{\nu_{r0}} \tag{7.67}$$

$$\frac{p_{r0}}{\bar{\rho}_{r0}\bar{U}^2}\frac{\bar{V}\bar{Y}}{\bar{\nu}_{r0}}=\frac{p_{r0}}{\rho_{r0}U_{r0}^2}\frac{\rho_{r0}}{\bar{\rho}_{r0}}\left(\frac{\nu_{r0}}{\bar{\nu}_{r0}}\right)^2\frac{R_e}{\bar{G}_r} \tag{7.68}$$

which mean contributions of the gravity, the heat conductivity, the liquid film thickness, the interfacial velocity and the axial change in pressure, respectively, to the behavior of vapor flow. It is seen from Eqs. (7.66) and (7.67) that the film thickness and the interfacial axial velocity are of the order of, respectively,

$$\left(\Delta_w\frac{\rho_{r0}}{\bar{\rho}_{r0}}\frac{D_{r0}}{\nu_{r0}}\frac{\nu_{r0}}{\bar{\nu}_{r0}}\right)^{1/3}\left(\frac{R_e}{\bar{G}_r}\right)^{1/3}R_0,\qquad \frac{\bar{\nu}_{r0}}{\nu_{r0}}\left(\Delta_w\frac{\rho_{r0}}{\bar{\rho}_{r0}}\frac{D_{r0}}{\nu_{r0}}\frac{\nu_{r0}}{\bar{\nu}_{r0}}\right)^{2/3}\left(\frac{\bar{G}_r}{R_e}\right)^{1/3}U_{00}$$

The factor G_r/R_e^2 characterizes the natural convection induced by the density variation of vapor mixture. The density can be expanded as

$$\rho=\rho_w+\left(\frac{\partial\rho}{\partial T}\right)_w(T_{00}-T_w)\theta+\left(\frac{\partial\rho}{\partial C}\right)_w(C-C_w)+\cdots \tag{7.69}$$

Thus natural convection can be characterized by

$$\frac{G_r}{R_e^2}\frac{1}{\rho_w}\left(\frac{\partial\rho}{\partial T}\right)_w(T_{00}-T_w), \qquad \frac{G_r}{R_e^2}\frac{1}{\rho_w}\left(\frac{\partial\rho}{\partial C}\right)_w(C_{00}-C_w) \tag{7.70}$$

Since the coefficients of G_r/R_e^2 are less than unity, these parameters have little contribution to the vapor flow field as long as $G_r/R_e^2\lesssim 1$.

In Eqs. (7.64) to (7.68), the most predominant parameters are

$$\frac{\Delta_w}{S_c}, \qquad \frac{\bar{P}_r}{H_e}\left(\frac{\Delta_w}{S_c}\frac{\mu_{r0}}{\bar{\mu}_{r0}}\right)^{4/3}\left(\frac{R_e}{\bar{G}_r}\right)^{1/3}$$

where $H_e=\bar{c}_{pr0}(T_{00}-T_w)/\lambda_{r0}$. The flow variables are then expressed in the form of

$$\phi=\phi\left(\frac{\Delta_w}{S_c},\ K_t,\ K_e,\ \bar{K},\ S_c,\ P_r\right) \tag{7.71}$$

where

$$K_t=\frac{\bar{P}_r}{H_e}\left(\frac{\Delta_w}{S_c}\frac{\mu_{r0}}{\bar{\mu}_{r0}}\right)^{4/3}\left(\frac{R_e}{\bar{G}_r}\right)^{1/3} \tag{7.72}$$

$$K_e=\left(\frac{\partial C_e}{\partial T}\right)_w\frac{T_{00}-T_w}{C_e(T_w)-\bar{C}_e(T_w)} \qquad \bar{K}_e=\left(\frac{\partial\bar{C}_e}{\partial T}\right)_w\frac{T_{00}-T_w}{C_e(T_w)-\bar{C}_e(T_w)} \tag{7.73}$$

The rate of condensation and the heat flux to the wall are expressed as

$$\frac{\dot{m}/\rho_{r0}U_{00}}{(\Delta_w/S_c)(1/R_e)}=\frac{\dot{m}^*}{\Delta_w}=f_m\left(\frac{\Delta_w}{S_c},\ K_t,\ K_e,\ \bar{K}_e,\ S_c,\ P_r\right) \tag{7.74}$$

$$\frac{q}{((\Delta_w/S_c)(\mu_{r0}/\bar{\mu}_{r0})(R_e/\bar{G}_r))^{-1/3}}=f_q\left(\frac{\Delta_w}{S_c},\ K_t,\ K_e,\ \bar{K}_e,\ S_c,\ P_r\right) \tag{7.75}$$

The correlation of Eq. (7.74) is shown in Fig. 23 for the numerical results obtained in Chapter 4 of which the nondeimensional parameters are shown in Table 4.

The conditions of the boundary layer type flow, Eq. (7.8) are given by

$$R_e^2\gg 1 \qquad R_e^2\gg\left(\frac{\Delta_w}{S_c}\frac{\mu_{r0}}{\bar{\mu}_{r0}}\frac{R_e}{\bar{G}_r}\right)^{2/3} \tag{7.76}$$

and the condition of the Nusselt approximation, Eq. (7.26), is given by Eq. (7.63) as

$$1\gg\left(\frac{\Delta_w}{S_c}\frac{\mu_{r0}}{\bar{\mu}_{r0}}\right)^{4/3}\left(\frac{R_e}{\bar{G}_r}\right)^{1/3} \tag{7.77}$$

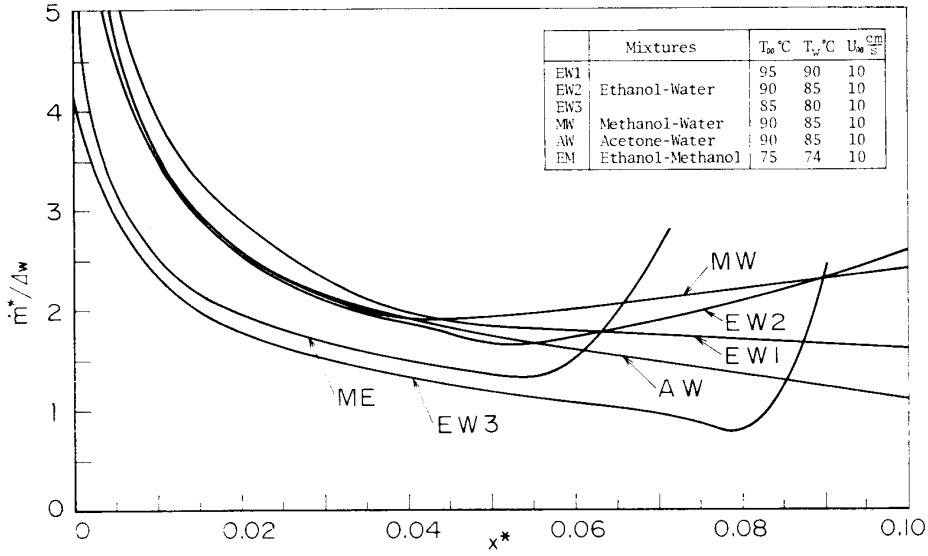

FIG. 23. Similarity correlation.

Thus, the necessary condition for the similarity correlation of Eq. (7.71) is

$$\left(\frac{\Delta_w}{S_c}\frac{\mu_{r0}}{\bar{\mu}_{r0}}\right)^{-8}\bar{G}_r^2 \gg R_e^2 \gg 1 \tag{7.78}$$

When the forced vapor-flow velocity is sufficiently small, the vapor flow will be induced mainly by the shearing stress at the liquid-vapor interface and by the natural convection, the above similarity being deteriorated. In the former case, the characteristic velocity can be related with the relation of shearing stresses at the interface, Eq. (7.18), as

$$\mu_{r0}\frac{U}{Y} = \bar{\mu}_{r0}\frac{\bar{U}}{\bar{Y}} \tag{7.79}$$

Using Eqs. (7.7) and (7.41) with Eqs. (7.55) to (7.57) gives

$$X = \bar{X} = \left(\frac{\bar{\mu}_{r0}}{\mu_{r0}}\frac{\bar{\nu}_{r0}}{\nu_{r0}}\right)^{3/2}\left(\frac{\Delta_w}{S_c}\frac{\mu_{r0}}{\bar{\mu}_{r0}}\right)^{1/2}\bar{G}_r R_0$$

$$\bar{Y} = \left(\frac{\bar{\mu}_{r0}}{\mu_{r0}}\frac{\bar{\nu}_{r0}}{\nu_{r0}}\right)^{1/2}\left(\frac{\Delta_w}{S_c}\frac{\mu_{r0}}{\bar{\mu}_{r0}}\right)^{1/2}R_0 \qquad Y = R_0$$

$$\bar{V} = \frac{\Delta_w}{S_c}\frac{\rho_{r0}}{\bar{\rho}_{r0}}\frac{\nu_{r0}}{R_0}$$

$$\bar{U} = \frac{\bar{\mu}_{r0}}{\mu_{r0}}\frac{\bar{\nu}_{r0}}{\nu_{r0}}\left(\frac{\Delta_w}{S_c}\frac{\mu_{r0}}{\bar{\mu}_{r0}}\right)\bar{G}_r\frac{\bar{\nu}_{r0}}{R_0}$$

$$V = \frac{\nu_{r0}}{R_0}$$

$$U = \left(\frac{\bar{\mu}_{r0}}{\mu_{r0}}\frac{\bar{\nu}_{r0}}{\nu_{r0}}\right)^{1/2}\left(\frac{\Delta_w}{S_c}\frac{\mu_{r0}}{\bar{\mu}_{r0}}\right)^{1/2}\bar{G}_r\frac{\nu_{r0}}{R_0}$$

The similarity correlation is then

$$\phi=\phi\left(\frac{\Delta_w}{S_c},\ K_t',\ K_e,\ \bar{K}_e,\ S_c,\ P_r\right) \tag{7.80}$$

where

$$K_t'=\frac{\bar{P}_r}{H_e}\left(\frac{\Delta_w}{S_c}\frac{\mu_{r0}}{\bar{\mu}_{r0}}\right)^{3/2}\left(\frac{\bar{\mu}_{r0}}{\mu_{r0}}\frac{\bar{\nu}_{r0}}{\nu_{r0}}\right)^{1/2}$$

The rate of condensation and the heat flux are

$$\begin{aligned}\frac{\dot{m}(R_e/\rho_{r0}\nu_{r0})S_c}{\Delta_w}&=f_m\left(\frac{\Delta_w}{S_c},\ K_t',\ K_e,\ \bar{K}_e,\ S_c,\ P_r\right)\\ \frac{q}{((\Delta_w/S_c)(\bar{\nu}_{r0}/\nu_{r0}))^{1/2}}&=f_q\left(\frac{\Delta_w}{S_c},\ K_t',\ K_e,\ \bar{K}_e,\ S_c,\ P_r\right)\end{aligned} \tag{7.81}$$

When the vapor flow is induced by the natural convection, the characteristic scales can be related by the parameter, gX/U^2, as

$$\frac{gX}{U^2}\beta=1 \tag{7.82}$$

where β is $(\partial\rho/\partial T)_w(T_{00}-T_w)/\rho_w$ or $(\partial\rho/\partial C)_w(c_{00}-c_w)/\rho_w$. Using Eqs. (7.7), (7.41) and (7.55) to (7.57) yields

$$\begin{aligned}X&=\bar{X}=\frac{\beta g R_0^3}{\nu_{r0}^2}R_0\\ \bar{Y}&=\left(\frac{\Delta_w}{S_c}\frac{\mu_{r0}}{\bar{\mu}_{r0}}\right)^{1/3}\left(\beta\frac{\bar{\nu}_{r0}^2}{\nu_{r0}^2}\right)^{1/3}R_0 \qquad Y=R_0\\ \bar{V}&=\frac{\Delta_w}{S_c}\frac{\rho_{r0}}{\bar{\rho}_{r0}}\frac{\nu_{r0}}{R_0}\\ \bar{U}&=\left(\frac{\Delta_w}{S_c}\frac{\mu_{r0}}{\bar{\mu}_{r0}}\right)^{2/3}\left(\beta\frac{\bar{\nu}_{r0}^2}{\nu_{r0}^2}\right)^{2/3}\frac{gR_0^2}{\bar{\nu}_{r0}}\\ V&=\frac{\nu_{r0}}{R_0}\\ U&=\left(\frac{\beta g R_0^3}{\nu_{r0}^2}\right)\frac{\nu_{r0}}{R_0}\end{aligned}$$

The similarity is then

$$\phi=\phi\left(\frac{\Delta_w}{S_c},\ K_t'',\ K_e,\ \bar{K}_e,\ S_c,\ P_r\right) \tag{7.83}$$

where

$$K_t''=\frac{\bar{P}_r}{H_e}\left(\frac{\Delta_w}{S_c}\frac{\mu_{r0}}{\bar{\mu}_{r0}}\right)^{4/3}\left(\beta\frac{\bar{\nu}_{r0}^2}{\nu_{r0}^2}\right)^{1/3}$$

The rate of condensation and the heat flux are

$$\frac{\dot{m}(R_0/\rho_{r0}\nu_{r0})S_c}{\Delta_w}=f_m\left(\frac{\Delta_w}{S_c},\ K_t'',\ K_e,\ \bar{K}_e,\ S_c,\ P_r\right)$$
$$\frac{q}{((\Delta_w/S_c)(\mu_{r0}/\bar{\mu}_{r0}))^{1/3}(\beta(\bar{\nu}_{r0}^2/\nu_{r0}^2))^{1/3}}=f_q\left(\frac{\Delta_w}{S_c},\ K_t'',\ K_e,\ \bar{K}_e,\ S_c,\ P_r\right) \tag{7.84}$$

8. Conclusion

Film condensation of binary-mixture flows in a vertical channel of variable cross-section is studied by using the integral method for vapor flow and the Nusselt model for the condensate flow. The two flow fields coupled with the interfacial conditions are solved numerically to predict the effects of the channel geometry, the vapor flow speed and direction, the inlet and wall temperatures and the type of binary mixtures on the behavior of film condensation. At the boundary between the vapor and the condensate, an infinitesmally thin layer of mixtures is assumed to be in liquid-vapor equilibrium. A saturated vapor mixture is introduced downward or upward into a vertical channel of variable circular cross-section with a wall cooled isothermally.

The film condensation is appreciably affected by the liquid-vapor equilibrium characteristics and the mass transfer processes in the vapor mixture. The condensation rate takes very large values close to the starting point of condensation. It then decreases rapidly due to the growth of concentration layer in the developing region. After taking a minimum, it tends to increase again in the developed region owing to the behavior of mass transfer. This is remarkably different from that of film condensation of external flows. It is caused by the fact that high rates of condensation in the developing region lead to intensive consumption of the volatile species in the bulk vapor mixture which promotes the mass transfer from the interface. In the case of external flows, they have infinite sources of the species to compensate the consumption.

The heat flux to the wall has the same features as the condensation rate. The interfacial temperature also decreases rapidly from large values close to the flow inlet in the developing region and then increases again in the developed region. Due to small difference of temperatures at the interface and the wall, the change in the interfacial mass fractions in the flow direction is not appreciable. The film thickness varies in the direction of the condensate flow with the exponent power of 0.15 to 0.3 depending on the channel geometry, the flow direction, the temperature difference and the type of mixture.

The nozzle-type flow always yields larger values of the condensation rate, heat flux, film thickness, and interfacial temperature and velocity compared with those of the diffuser-type flow. Due to compensating effect of axial changes in the condensation rate and the interfacial area, the overall condensation rate and the heat flux are not considerably affected by the channel geometry. The developing process of concentration and temperature layers of the vapor mixture is not appreciably influenced by the flow direction. After developed, especially close to the vapor-flow outlet, the flow

direction has a considerable effect on condensation. The effect of vapor-flow velocity on the condensation rate can be correlated with the Reynolds number based on the distance from the vapor-flow inlet. Concerning the type of mixture and the system temperatures, the features of condensation can be characterized by the factor, Δ_w, the ratio of the difference of mass fractions at the inlet and the wall state to that of equilibrium mass fractions of the vapor and the liquid at the wall state;

$$\Delta_w = \frac{C_e(T_w) - C_e(T_w)}{C_e(T_w) - \bar{C}_e(T_w)}.$$

As a comparison with the developing flow field, concentration and temperature fields of a quasi-developed profile are considered with emprical transfer coefficients for laminar and turbulent flows. Due to lower rates of condensation in the starting region, they show different features of condensation process compared with those of developing flows, although they also are much characterized by the equilibrium feature Δ_w and the mass transfer at the interface. The rate of condensation and the heat flux are monotonously decreasing in the direction of the condensate flow. The interfacial temperature is increasing monotonously or after a maximum gradually decreasing. The vapor-flow direction has little influence. These imply that flow behavior in the starting region of condensation has an appreciable effect on the film condensation of binary mixtures in a vertical channel.

Based on the knowledge of numerical results, similarity behavior is considered of the film condessation by examining strictly the governing equations and their boundary conditions. For usual cases, the condensation process can be characterized by the following parameters.

$$\phi = \phi\left(x^*;\ \frac{\Delta_w}{S_c},\ K_e,\ K_e,\ \bar{K}_e,\ S_c,\ P_r\right)$$

where Δ_w/S_c, K_e, K_e and $\bar{K}_e$ mean the characteristic factors of mass transfer, heat transfer and phase equilibrium of the vapor and the liquid, respectively. The conditions of the boundary-layer type flow for the vapor mixture and the Nusselt approximation for the condensate are expressed in terms of R_e, $\bar{G}_r$ and Δ_w/S_c.

Acknowledgements

The author wishes to express his much appreciation to Professor Klaus Oswatitsch and Dr. Gustav A. M. Wondrak at Institut für Strömungslehre, Technische Universität Wien who provided the opportunity of the present work and gave helpful advice and discussions throughout the work.

References

[1] A. P. Colburn and T. B. Drew, The condensation of mixed vapors, Trans. AIChE **33**, 157 (1937).

[2] E. M. Sparrow and E. Marschall, Binary, gravity-flow film condensation, Trans. ASME, J. Heat Transfer **91**, 205 (1969).
[3] V. E. Denny and V. J. Jusionis, Effects of forced flow and variable properties on binary film condensation, Int. J. Heat Mass Transfer **15**, 2143 (1972).
[4] V. E. Denny and V. South III, Effects of forced flow, noncondensibles, and variable properties on film condensation of pure and binary vapors at the forward stagnation point of a horizontal cylinder, Int. J. Heat Mass Transfer, **5**, 2133 (1972).
[5] A. Tamir, Condensation of binary mixture of miscible vapors, Int. J. Heat Mass Transfer **16**, 683 (1973).
[6] Y. Taitel and A. Tamir, Film condensation of multicomponent mixtures, Int. J. Multiphase Flow **1**, 679 (1974).
[7] J. Bandrowski and A. Bryczkowski, Experimental study of heat transfer at the total condensation of mixed vapors of miscible liquids, Int. J. Heat Mass Transfer **8**, 503 (1975).
[8] E. Marschall and J. A. Hall, Binary, gravity flow film condensation, Trans. ASME, J. Heat Transfer **97**, 492 (1975).
[9] J. P. Van Es and P. M. Heertjes, The condensation of a vapor of a binary mixture, Brit. Chem. Engng. **8**, 580 (1962).
[10] E. Kirschbaum and E. Tröster, Untersuchungen zum Stoffübergang bei der Teilkondensation von Gemischdämpfen, Chem. Ing. Technik **37**, 395 (1960).
[11] E. Tröster, Berechnung der Trennwirkung von Teilkondensation (Dephlegmatoren), Chem. Ing. Technik **32**, 525 (1960).
[12] G. A. M. Wondrak, Zur Strofftrennung durch Dephlegmation bei hohen Dampfgeschwindigkeiten, Universität Wien, Dissertation 1968.
[13] E. Hala et al., Vapour liquid equilibrium data at normal pressures, Pergamon Press, Oxford (1968).
[14] S. Bretsznajder, Prediction of transport and other physical properties of fluids, Pergamon Press, Oxford (1971).
[15] VDI Wärmeatlas, Deutscher Ingenieur-Verlag, Düsseldorf (1953).
[16] W. M. Kays, Convective heat and mass transfer, McGraw-Hill, B. C. (1966).
[17] K. Feind. Strömungsuntersuchungen bei Gegenstrom von Reisenfilmen und Gas in lotrechten Rohren, VDI-Forschungsheft 481 B26 (1966).
[18] J. R. Sellars, M. Tribus and J. S. Klein, Heat transfer to laminar flow in a round tube or flat conduit—The Graetz problem extended, Trans. ASME **78**, 441 (1956).
[19] S. Kotake, Film condensation of binary mixture flow in a vertical channel, Int. J. Heat Mass Transfer **21**, 875 (1978).

Appendix A Conservation Equations for Mixtures

Considering a chemical Species α having the velocity $v_i^\alpha(x_j, t)$ and the density $\rho_\alpha(x_j, t)$ at a point (x_j, t), the continuity of the mass of species α without any chemical reaction is then given by

$$\frac{\partial \rho^\alpha}{\partial t}+\frac{\partial}{\partial x_i}(\rho^\alpha v_i^\alpha)=0 \tag{A.1}$$

When species α is acted by the stress tensor π_{ij}^α and the body force f_i^α, the conservation equation of linear momentum is written as

$$\frac{\partial}{\partial t}(\rho^\alpha v_i^\alpha)+\frac{\partial}{\partial x_j}(\rho^\alpha v_i^\alpha v_j^\alpha)=\frac{\partial}{\partial x_j}(\pi_{ij}^\alpha)+\rho^\alpha f_i^\alpha \tag{A.2}$$

The stress tensor π_{ij}^α can be expressed in terms of pressure and viscous stress tensors;

$$\pi_{ij}^{\alpha} = -p^{\alpha}\delta_{ij} + \tau_{ij}^{\alpha} \tag{A.3}$$

The conservation of energy is given by

$$\frac{\partial}{\partial t}(\rho^{\alpha}\hat{e}^{\alpha}) + \frac{\partial}{\partial x_i}(\rho_{\alpha}\hat{e}^{\alpha}v_i^{\alpha}) = \frac{\partial}{\partial x_j}(v_i^{\alpha}\pi_{ij}^{\alpha}) + \frac{\partial q_i^{\alpha}}{\partial x_i} + \rho^{\alpha}f_i^{\alpha}v_i^{\alpha} \tag{A.4}$$

where $\hat{e}^{\alpha}$ is the sum of the internal energy of species α per unit mass of species α, e^{α}, and the kinetic energy of species α, $v_k^{\alpha}v_k^{\alpha}/2$, and q_i^{α} is the heat flux vector for species α.

When the reference coordinate system for the mixture is taken to move with the mass-weighted average velocity for all molecules in the mixture, v_i, the mass-weighted average velocity for molecules in species α results in the diffusion velocity of species α, V_i^{α};

$$v_i^{\alpha} = v_i + V_i^{\alpha} \tag{A.5}$$

where

$$v_i = \sum_{\alpha} \rho^{\alpha}v_i^{\alpha}\frac{1}{\rho} \qquad \sum_{\alpha} \rho^{\alpha}V_i^{\alpha} = 0 \tag{A.6}$$

In the term of mass fraction of species α

$$C^{\alpha} = \frac{\rho^{\alpha}}{\rho} \tag{A.7}$$

Eq. (A.1) is written as

$$\frac{\partial}{\partial t}(\rho C^{\alpha}) + \frac{\partial}{\partial x_i}(\rho v_i C^{\alpha}) = -\frac{\partial}{\partial x_i}(\rho^{\alpha}V_i^{\alpha}) \tag{A.8}$$

As for summing Eqs. (A.1), (A.2) and (A.4) with respect to α to obtain the overall conservation equations of the mixture, the physical quantities as ensemble can be introduced. The total stress tensor π_{ij} and the total viscous stress tensor τ_{ij} are defined as

$$\pi_{ij} = -p\delta_{ij} + \tau_{ij} = \sum_{\alpha}(-p^{\alpha}\delta_{ij} + \tau_{ij}^{\alpha} - \rho^{\alpha}V_i^{\alpha}V_j^{\alpha}) \tag{A.9}$$

where p^{α} is the equilibrium or thermodynamic pressure of species α. Equilibrium occurs when each component is in equilibrium and when the diffusion velocity is zero. Then, the above relation yields the definition of the total pressure

$$p = \sum_{\alpha} p^{\alpha} \tag{A.10}$$

The total thermodynamic energy e and the total enthalpy of the mixture h are defined as

$$\rho e = \sum_{\alpha} \rho^{\alpha}e^{\alpha} \qquad \rho h = \sum_{\alpha} \rho^{\alpha}h^{\alpha} = \sum_{\alpha}(\rho^{\alpha}e^{\alpha} + p^{\alpha}) \tag{A.11}$$

The specific heat of species α, c_p^α, and the total specific heat of the mixture, c_p, at constant pressure are

$$c_p^\alpha=\left(\frac{\partial h^\alpha}{\partial T}\right)_p \qquad c_p=\sum_\alpha C^\alpha c_p^\alpha \tag{A.12}$$

By assuming that the diffusion process has little contribution to the kinetic energy and to the stress work and that the kinetic energy, viscous work and body force work are negligible, the summation of Eqs. (4.1), (4.2) and (4.4) with respect to α for steady state gives the overall conservation equations;

$$\frac{\partial}{\partial x_i}(\rho v_i)=0 \tag{A.13}$$

$$\frac{\partial}{\partial x_i}(\rho v_i v_j)=-\frac{\partial p}{\partial x_j}+\frac{\partial \tau_{ij}}{\partial x_i}+\sum_\alpha \rho^\alpha f_j^\alpha \tag{A.14}$$

$$\frac{\partial}{\partial x_i}(\rho v_i h)=\frac{\partial}{\partial x_i}\left\{-q_i-\sum_\alpha \rho^\alpha h^\alpha V_i^\alpha\right\} \tag{A.15}$$

$$c_p\frac{\partial}{\partial x_i}(\rho v_i T)=-\frac{\partial q_i}{\partial x_i}-\sum_p \rho^\alpha V_i^\alpha c_p^\alpha\frac{\partial T}{\partial x_i} \tag{A.15}'$$

In the cylindrical coordinates with axial symmetry, Eqs. (A.8), (A.14), (A.15) and (A.15)′ are written as,

$$\frac{\partial}{\partial x}(\rho u C^\alpha)+\frac{1}{r}\frac{\partial}{\partial r}(r\rho v C^\alpha)=-\frac{\partial}{\partial x}(\rho^\alpha V_x^\alpha)-\frac{1}{r}\frac{\partial}{\partial r}(r\rho^\alpha V_r^\alpha) \tag{A.16}$$

$$\frac{\partial}{\partial x}(\rho uu)+\frac{1}{r}\frac{\partial}{\partial r}(r\rho vu)=-\frac{\partial p}{\partial x}+\frac{\partial \tau_{xx}}{\partial x}+\frac{1}{r}\frac{\partial}{\partial r}(r\tau_{xr})+\sum_\alpha \rho^\alpha f_x^\alpha \tag{A.17}$$

$$\frac{\partial}{\partial x}(\rho uv)+\frac{1}{r}\frac{\partial}{\partial r}(r\rho vv)=-\frac{\partial p}{\partial r}+\frac{\partial \tau_{rx}}{\partial x}+\frac{1}{r}\frac{\partial}{\partial r}(r\tau_{rr})+\sum_\alpha \rho^\alpha f_r^\alpha \tag{A.18}$$

$$\begin{aligned}\frac{\partial}{\partial x}(\rho uh)+\frac{1}{r}\frac{\partial}{\partial r}(r\rho vh)=&-\frac{\partial}{\partial x}\left(q_x+\sum_\alpha \rho^\alpha h^\alpha V_x^\alpha\right)\\&-\frac{1}{r}\frac{\partial}{\partial r}\left\{r\left(q_r+\sum_\alpha \rho^\alpha h^\alpha V_r^\alpha\right)\right\}\end{aligned} \tag{A.19}$$

$$\begin{aligned}c_p\frac{\partial}{\partial x}(\rho uT)+c_p\frac{1}{r}\frac{\partial}{\partial r}(r\rho vT)=&-\frac{\partial q_x}{\partial x}-\frac{1}{r}\frac{\partial}{\partial r}(rq_r)\\&-\sum_\alpha\left(\rho^\alpha V_x^\alpha c_p^\alpha\frac{\partial T}{\partial x}+\rho^\alpha V_r^\alpha c_p^\alpha\frac{\partial T}{\partial r}\right)\end{aligned} \tag{A.19}'$$

where u and v are the velocity components in the x and r dirctions, respectively. The diffusion velocity of species α for a binary mixture ($\alpha=1, 2$) can be expressed as

$$\rho^\alpha V_i^\alpha=-\rho D^\alpha\frac{\partial C^\alpha}{\partial x_i} \tag{A.20}$$

where D^α is the binary diffusion coefficient of species α. The viscous stress and the heat flux are given by

$$\tau_{ij}=\mu\frac{\partial v_i}{\partial x_j} \qquad q_i=-k\frac{\partial T}{\partial x_i} \tag{A.21}$$

where μ and k are the dynamic viscosity and the heat conductivity of the mixture, respectively.

Appendix B Boundary Conditions at the Interface

Assume two mixture flows contacting each other at an interface of infinitesmal thickness where the change in physical phases takes place without any chemical reaction. The interface is located at $\eta(x_i, t)$. When the conservation equation of a property, ϕ, is written in the form of

$$\frac{\partial\phi}{\partial t}+\frac{\partial\phi_i}{\partial x_i}=0 \tag{B.1}$$

where ϕ_i is the flux vector of ϕ, the continuity condition of the property flux across the interface is given by

$$\left(\phi\frac{\partial\eta}{\partial t}+\phi_i\frac{\partial\eta}{\partial x_i}\right)_+=\left(\phi\frac{\partial\eta}{\partial t}+\phi_i\frac{\partial\eta}{\partial x_i}\right)_- \tag{B.2}$$

where subscripts $+$ and $-$ denote values evaluated at the point of positive and negative sides of the interface, respectively.

From Eqs. (A.1), (A.2) and (A.4), the continuity conditions of the mass, momentum and energy fluxes of species α are expressed as

$$\dot m^\alpha_+=\dot m^\alpha_- \qquad \dot m^\alpha\equiv\rho^\alpha\frac{\partial\eta}{\partial t}+\rho^\alpha v^\alpha_i\frac{\partial\eta}{\partial x_i} \tag{B.3}$$

$$\dot F^\alpha_{i+}=\dot F^\alpha_{i-} \qquad \dot F^\alpha_i\equiv\rho^\alpha v^\alpha_i\frac{\partial\eta}{\partial t}+(\rho^\alpha v^\alpha_i v^\alpha_j-\pi^\alpha_{ij})\frac{\partial\eta}{\partial x_j} \tag{B.4}$$

$$\dot E^\alpha_+=\dot E^\alpha_- \qquad \dot E^\alpha\equiv\rho^\alpha\hat e^\alpha\frac{\partial\eta}{\partial t}+(\rho_\alpha\hat e^\alpha v^\alpha_j-v^\alpha_i\pi^\alpha_{ij}+q^\alpha_j)\frac{\partial\eta}{\varrho x_j} \tag{B.5}$$

Summing Eqs. (B.3) to (B.5) with respect to species α gives

$$\dot m_+=\dot m_- \qquad \dot m=\sum_\alpha\dot m^\alpha \tag{B.6}$$

$$\dot F_{i+}=\dot F_{i-} \qquad \dot F_i=\sum_\alpha\dot F^\alpha_i \tag{B.7}$$

$$\dot E_+=\dot E_- \qquad \dot E=\sum_\alpha\dot E^\alpha \tag{B.8}$$

In terms of the diffusion velocity V^α_i, the fluxes are written as

$$\dot{m}=\rho\frac{\partial\eta}{\partial t}+\rho v_i\frac{\partial\eta}{\partial x_i} \tag{B.9}$$

$$\dot{F}_i=\dot{m}v_i-\pi_{ij}\frac{\partial\eta}{\partial x_j} \tag{B.10}$$

$$\dot{E}=\dot{m}\left(e+\frac{1}{2}v_kv_k+\sum_\alpha\frac{1}{2}C^\alpha V_k^\alpha V_k^\alpha\right)-(v_i\pi_{ij}-\hat{q}_j)\frac{\partial\eta}{\partial x_j} \tag{B.11}$$

$$\hat{q}_j=\sum_\alpha\left\{q_j^\alpha+\rho^\alpha\left(e^\alpha+\frac{1}{2}V_k^\alpha V_k^\alpha\right)V_j^\alpha-\pi_{jk}^\alpha V_k^\alpha\right\}$$

The energy flux is rewritten by using the enthalpy as

$$\dot{E}=\dot{m}\left(h+\frac{1}{2}v_kv_k+\sum_\alpha\frac{1}{2}C^\alpha V_k^\alpha V_k^\alpha\right)-(v_i\tau_{ij}-\hat{q}'_j)\frac{\partial\eta}{\partial x_j} \tag{B.12}$$

$$\hat{q}'_j\equiv\sum_\alpha\left\{q_j^\alpha+\rho^\alpha\left(h^\alpha+\frac{1}{2}V_k^\alpha V_k^\alpha\right)V_j^\alpha-\tau_{jk}^\alpha V_k^\alpha\right\}$$

Equation (B.3) with (B.9) gives the continuity of the mass flux of species

$$\dot{m}_+^\alpha=\dot{m}_-^\alpha \qquad \dot{m}^\alpha=\dot{m}C^\alpha+\rho^\alpha V_i^\alpha\frac{\partial\eta}{\partial x_i} \tag{B.13}$$

With Eq. (B.13), the energy flux, Eq. (B.12), is further rewritten as

$$\dot{E}=\sum_\alpha\left[\dot{m}^\alpha\left(h^\alpha+\frac{1}{2}v_kv_k+\sum_\alpha\frac{1}{2}C^\alpha V_k^\alpha V_k^\alpha\right)-\left\{(v_i+V_i^\alpha)\tau_{ij}^\alpha-q_j^\alpha\right\}\frac{\partial\eta}{\partial x_j}\right] \tag{B.14}$$

The latter expression for the energy flux is more convenient than Eq. (B12), from the standpoint of the definition of the latent heat of phase change.

When the flow is steady and diffusion has little contribution to the kinetic energy and the stress works, Eqs. (B.12) and (B.14) become, respectively,

$$\dot{E}=\dot{m}\left(h+\frac{1}{2}v_kv_k\right)-\left(v_i\tau_{ij}-q_j-\sum_\alpha\rho^\alpha h^\alpha V_j^\alpha\right)\frac{\partial\eta}{\partial x_j} \tag{B.15}$$

$$\dot{E}=\sum_\alpha\dot{m}^\alpha\left(h^\alpha+\frac{1}{2}v_kv_k\right)-(v_i\tau_{ij}-q_j)\frac{\partial\eta}{\partial x_j} \tag{B.16}$$

where $q_i=\sum_\alpha q_i^\alpha$. Further, if the kinetic energy and the viscous works are negligibly small in comparison with the enthalpy and the heat conduction, respectively, these fluxes are reduced to

$$\dot{E}=\dot{m}h+\left(q_i+\sum_\alpha\rho^\alpha h^\alpha V_i^\alpha\right)\frac{\partial\eta}{\partial x_i} \tag{B.17}$$

$$\dot{E}=\sum_\alpha\dot{m}^\alpha h^\alpha+q_i\frac{\partial\eta}{\partial x_i} \tag{B.18}$$

The continuity of energy flux at the interface is then expressed as

$$m\lambda^* = \left\{\left(q_i - \sum_\alpha \rho^\alpha h^\alpha V_i^\alpha\right)_- - \left(q_i - \sum_\alpha \rho^\alpha h^\alpha V_i^\alpha\right)_+\right\}\frac{\partial \eta}{\partial x_i} \tag{B.19}$$

$$\dot{m}\lambda + \sum_\alpha \lambda^\alpha (\rho^\alpha V_i^\alpha)_- \frac{\partial \eta}{\partial x_i} = \{(q_i)_- - (q_i)_+\}\frac{\partial \eta}{\partial x_i} \tag{B.20}$$

where the latent heat of phase change is defined as

$$\lambda^* = h_+ - h_- \qquad h = \sum_\alpha C^\alpha h^\alpha \tag{B.21}$$

$$\lambda = \sum_\alpha C_-^\alpha \lambda^\alpha \qquad \lambda^\alpha = h_+^\alpha - h_-^\alpha \tag{B.22}$$

When the interface is steady and two-dimensional or axisymmetric, and its location is given by

$$\eta = y - \delta(x) = 0 \tag{B.23}$$

the continuity conditions, Eqs. (B.6) to (B.8), are

$$\left(\rho v - \rho u \frac{d\delta}{dx}\right)_+ = \left(\rho v - \rho u \frac{d\delta}{dx}\right)_- = \dot{m} \tag{B.24}$$

$$\left\{\dot{m}u - (p - \tau_{xx})\frac{d\delta}{dx} - \tau_{xy}\right\}_+ = \left\{\dot{m}u - (p - \tau_{xx})\frac{d\delta}{dx} - \tau_{xy}\right\}_- \tag{B.25}$$

$$\left\{\dot{m}v + \tau_{yx}\frac{d\delta}{dx} + (p - \tau_{yy})\right\}_+ = \left\{\dot{m}v + \tau_{yx}\frac{d\delta}{dx} + (p - \tau_{yy})\right\}_- \tag{B.26}$$

$$\begin{aligned}\dot{m}\lambda^* = &\left\{\left(q_y + \sum_\alpha \rho^\alpha h^\alpha V_y^\alpha\right)_- - \left(q_y + \sum_\alpha \rho^\alpha h^\alpha V_y^\alpha\right)_+\right\} \\ &- \left\{\left(q_x + \sum_\alpha \rho^\alpha h^\alpha V_x^\alpha\right)_- - \left(q_x + \sum_\alpha \rho^\alpha h^\alpha V_x^\alpha\right)_+\right\}\frac{d\delta}{dx}\end{aligned} \tag{B.27}$$

$$\begin{aligned}&\dot{m}\lambda + \sum_\alpha \left\{(\rho^\alpha V_y^\alpha)_- - (\rho^\alpha V_x^\alpha)_- \frac{d\delta}{dx}\right\}\lambda^\alpha \\ &\qquad = (q_{y-} - q_{y+}) - (q_{x-} - q_{x+})\frac{d\delta}{dx}\end{aligned} \tag{B.28}$$

The continuity of mass flux of species α, Eq. (B.3) is

$$\left\{\dot{m}C^\alpha + \left(\rho^\alpha V_y^\alpha - \rho^\alpha V_x^\alpha \frac{d\delta}{dx}\right)\right\}_+ = \left\{\dot{m}C^\alpha + \left(\rho^\alpha V_y^\alpha - \rho^\alpha V_x^\alpha \frac{d\delta}{dx}\right)\right\}_- \tag{B.29}$$

With the boundary layer assumption ($\partial/\partial x \ll \partial/\partial y$) and $d\delta/dx \ll 1$, these equations are reduced to

$$\left(\mu \frac{\partial u}{\partial y}\right)_+ = \left(\mu \frac{\partial u}{\partial y}\right)_- \tag{B.30}$$

$$p_+ = p_- \tag{B.31}$$

$$\dot{m}\lambda^* = \left(k\frac{\partial T}{\partial y} + \rho\sum_\alpha h^\alpha D^\alpha \frac{\partial C^\alpha}{\partial y}\right)_+ - \left(k\frac{\partial T}{\partial y} + \rho\sum_\alpha h^\alpha D^\alpha \frac{\partial C^\alpha}{\partial y}\right)_- \tag{B.32}$$

$$\dot{m}\lambda - \sum_\alpha \left(\rho D^\alpha \frac{\partial C^\alpha}{\partial y}\right)_- \lambda^\alpha = \left(k\frac{\partial T}{\partial y}\right)_+ - \left(k\frac{\partial T}{\partial y}\right)_- \tag{B.33}$$

$$\left(\dot{m}C^\alpha - \rho D^\alpha \frac{\partial C^\alpha}{\partial y}\right)_+ = \left(\dot{m}C^\alpha - \rho D^\alpha \frac{\partial C^\alpha}{\partial y}\right)_- \tag{B.34}$$

where $u_+ = u_-$ is assumed.

Appendix C Numerical Procedure

The numerical procedure employed to solve the governing equations are as follows:

1. Functions generating mixture properties are defined;

Dynamic viscosity

$$\mu = \left(1 + \frac{X_1}{X_2}\phi_{12}\right)^{-1}\mu_1 + \left(1 + \frac{X_1}{X_2}\phi_{21}\right)^{-1}\mu_2 \qquad \mu_i = \mu_{i0}\frac{T_{i0} + C_{si}}{T + C_{si}}\left(\frac{T}{T_{i0}}\right)^{1.5}$$

$$\bar{\mu} = \exp\left(\bar{X}_1 \ln \mu_1 + \bar{X}_2 \ln \mu_2\right) \qquad \bar{\mu}_i = \exp\left(\frac{\alpha_i}{\bar{T}^2} + \frac{\beta}{\bar{T}} + \gamma_i\right), \quad \frac{\gamma_i}{\alpha_i \bar{T}^2 + \beta_i \bar{T} + 1}$$

Heat conductivity

$$k = X_1 k_1 + X_2 k_2 \qquad k_i = k_{i0}\frac{\mu_i}{\mu_{i0}}$$

$$\bar{k} = \bar{C}_1 k_1 + \bar{C}_2 k_2 - 0.72\bar{C}_1\bar{C}_2(k_2 - k_1) \qquad \bar{k}_i = \bar{k}_{i0}\left(\frac{\bar{\rho}_i}{\bar{\rho}_{i0}}\right)^{4/3}$$

Diffusion coefficient

$$D = \frac{0.00837T^{2.5}}{p(V_{b1}^{1/3} + V_{b2}^{1/3})(T + F\sqrt{C_{s1}C_{s2}})}\left(\frac{1}{M_1} + \frac{1}{M_2}\right)^{0.5}$$

Density

$$\rho = p\left(\frac{C_1}{M_1} + \frac{C_2}{M_2}\right)^{-1}(\mathscr{R}T)^{-1}$$

$$\bar{\rho} = \left(\frac{\bar{C}_1}{\rho_1} + \frac{\bar{C}_2}{\rho_2}\right)^{-1} \qquad \bar{\rho}_i = \bar{a}_\rho \bar{T}^2 + \bar{b}_\rho \bar{T} + \bar{c}_\rho$$

Specific heat

$$c_p = C_1 c_{p1} + C_2 c_{p2} \qquad c_{pi} = a_{ci}T^2 + b_{ci}T + c_{ci}$$
$$\bar{c}_p = \bar{C}_1 \bar{c}_{p1} + \bar{C}_2 \bar{c}_{p2} \qquad \bar{c}_{pi} = \bar{a}_{ci}\bar{T}^2 + \bar{b}_{ci}\bar{T} + \bar{c}_{ci}$$

Latent heat

$$\lambda=\bar{C}_1\lambda_1+\bar{C}_2\lambda_2+\Delta h_s \qquad \lambda_i=\frac{\mathscr{R}B_i}{(1+C_i/T)^2} \qquad \Delta h_s=-\mathscr{R}T(\bar{X}_1\ln\bar{\gamma}_1+\bar{X}_2\ln\bar{\gamma}_2)$$

Equilibrium concentration

$$\bar{X}_1=\frac{p-\bar{\gamma}_2 p_{s2}}{\bar{\gamma}_1 p_{s1}-\bar{\gamma}_2 p_{s2}} \qquad X_1=\left(1+\frac{\bar{\gamma}_2 p_{s2}\bar{X}_2}{\bar{\gamma}_1 p_{s1}\bar{X}_1}\right)$$

2. The type of binary mixture is specified.
3. The inlet flow condition and the channel geometry are given;

$$U_{00},\ T_{00},\ T_w,\ P,\ R_0,\ R(x).$$

4. Dimensionless parameters are calculated;

$$R_e,\ \bar{R}_e,\ P_r,\ \bar{P}_r,\ S_c,\ G_r,\ \bar{G}_r,\ H_e,\ M_c,\ \rho_r,\ \mu_r,\ k_r,\ c_{pr}.$$

5. For counter-current flows, the film thickness at the flow inlet is assumed;

$$\delta(L)=\delta_L \qquad (U_{00}<0).$$

6. The axial step is advanced;

$$x=x+\Delta x\ (U_{00}>0), \qquad x=x-\Delta x\ (U_{00}<0).$$

7. Thermophysical properties are evaluated at the reference state.
8. The vapor flow variables are calculated in the manner

$$F\{\phi(x)\}=F\{\phi(x_0)\}+\int_{x_0}^{x}E\{\phi(\xi)\}d\xi$$

$$\phi(x):\quad R_c,\ R_t,\ C_0,\ \theta_0,\ u_0,\ p.$$

9. The film thickness and the interfacial velocity are calculated: δ, u_i.
10. The interfacial temperature is calculated; θ_i.
11. The interfacial concentrations are computed by the equilibrium condition; C_i, $\bar{C}_i$.
12. Steps 10 and 12 are repeated until a sufficient convergence is established.
13. Local and overall values of the condensation rate and the heat flow are calculated; $\dot{m},\ q,\ \int_0^x \dot{m}dx,\ \int_0^x qdx.$
14. Steps 6 to 13 are repeated until the axial step comes to the end, $x=L$, for co-current flows.For counter-current flows, if the film thickness is larger than $10^{-6}R_0$ at $x=0$, δ_L is reassumed, going back to step 5, and steps 5 to 13 are repeated.

Appendix D Approximate Solution for Entry Flows

When the radial flow caused by distributed sinks on the interface due to condensation has little contribution to the convective transport of mass and energy, and further

the liquid film flow hardly affects the flow field of vapor mixture, the situation of the vapor flow is that the solutions of the temperature and concentration are those for a tube flow with axial variation of the surface temperature and concentration at the wall. Equations of concentration and temperature, Eqs. (2.3) and (2.4) with Eq. (2.1) are written in the x^* coordinate as

$$u\frac{\partial C}{\partial x^*}+v^*\frac{\partial C}{\partial r}=\frac{1}{\rho}\frac{1}{r}\frac{\partial}{\partial r}\left(r\rho D\frac{\partial C}{\partial r}\right) \tag{D.1}$$

$$u\frac{\partial \theta}{\partial x^*}+v^*\frac{\partial \theta}{\partial r}=\frac{1}{\rho c_p}\frac{S_c}{P_r}\frac{1}{r}\frac{\partial}{\partial r}\left(rk\frac{\partial \theta}{\partial r}\right)+c_p'D\frac{\partial C}{\partial r}\frac{\partial \theta}{\partial r} \tag{D.2}$$

where $x^*=x/(R_eS_c)$ and $v^*=R_eS_cv$. The convective transport of energy due to diffusion velocity is not substantial for usual cases, and can be neglected. The fluid properties may be evaluated at an appropriate state so as to be regarded as constant. Then Eqs. (D.1) and (D.2) are rewritten as

$$u\frac{\partial C}{\partial x^*}+v^*\frac{\partial C}{\partial r}=\frac{\partial^2 C}{\partial r^2}+\frac{1}{r}\frac{\partial C}{\partial r} \tag{D.3}$$

$$u\frac{\partial \theta}{\partial x^*}+v^*\frac{\partial \theta}{\partial r}=\frac{S_c}{P_r}\left(\frac{\partial^2 \theta}{\partial r^2}+\frac{1}{r}\frac{\partial \theta}{\partial r}\right) \tag{D.4}$$

The v-component velocity at the interface is estimated by Eq. (3.39)

$$v_R^*\simeq\frac{2}{R_\delta-R_c}\frac{C_i-C_0}{C_i-\bar{C}_i}$$

When $(T_{00}-T_w)/T_{00}\ll 1$, $v^*\ll 1$ can be expected except for very close to $x=0$ where $R_c\simeq R_\delta$. In the case of $v^*\ll 1$, Eqs. (D.3) and (D.4) are further reduced to

$$u\frac{\partial C}{\partial x^*}=\frac{\partial^2 C}{\partial r^2}+\frac{1}{r}\frac{\partial C}{\partial r} \tag{D.5}$$

$$\frac{P_r}{S_c}u\frac{\partial \theta}{\partial x^*}=\frac{\partial^2 \theta}{\partial r^2}+\frac{1}{r}\frac{\partial \theta}{\partial r} \tag{D.6}$$

The radial profile of u-velocity may be assumed of a fully-developed flow,

$$u=u_0(x^*)(1-r^2) \tag{D.7}$$

where u can be obtained by the continuity equation, Eq. (3.12);

$$u_0=1-\int_0^{x^*}4\dot{m}dx^*. \tag{D.8}$$

With this u-velocity profile, Eqs. (D.5) and (D.6) become

$$u_0(1-r^2)\frac{\partial C}{\partial x}=\frac{\partial^2 C}{\partial r^2}+\frac{1}{r}\frac{\partial C}{\partial r} \tag{D.9}$$

$$\frac{P_r}{S_c}u_0(1-r^2)\frac{\partial\theta}{\partial x}=\frac{\partial^2\theta}{\partial r^2}+\frac{1}{r}\frac{\partial\theta}{\partial r} \tag{D.10}$$

where the superscript $*$ is abbreviated.

At the liquid vapor interface which is regarded to be located at $r=1$, the boundary conditions are given by

$$C=C_i(x) \qquad \theta=\theta_i(x) \qquad \text{at } r=1 \tag{D.11}$$

$C_i(x)$ and $\theta(x)$ are to be determined by the condition of flux continuity at the interface. At the center,

$$\frac{\partial C}{\partial r}=0 \qquad \frac{\partial\theta}{\partial r}=0 \qquad \text{at } r=0 \tag{D.12}$$

At the starting point of condensation,

$$C=C_{00} \qquad \theta=1 \qquad \text{at } x=0 \tag{D.13}$$

The solutions of Eqs. (D.9) and (D.10) for variable concentration and temperature at the "wall" can be easily found by superposing solutions for constant wall conditions. Equations (D.9) and (D.10) for constant concentration and temperature at the wall are solved with the variable separate method;

$$C(x,r)=X_c(x)\cdot R_c(r)$$
$$\theta(x,r)=X_t(x)\cdot R_t(r)$$

These separate variables reduce Eqs. (D.9) and (D.10) to a set of equations in the form of

$$u_0\frac{dX}{dx}+\alpha^2X=0$$
$$\frac{dR^2}{dr^2}+\frac{1}{r}\frac{dR}{dr}+\alpha^2(1-r)=0$$

which give a solution of

$$R^{(n)}(r)\exp\left(-\alpha_n^2\int_0^x\frac{d\xi}{u_0}\right)$$

where α_n is the eigen value and $R^{(n)}$ is the corresponding eigen function. Thus, the solution for the constant wall condition can be expressed as

$$C(x,r)=\sum_{n=0}^{\infty}a_nR^{(n)}(r)\exp\left(-\alpha_n^2\int_0^x u_0^{-1}d\xi\right) \tag{D.14}$$

$$\theta(x,r)=\sum_{n=0}^{\infty}b_nR^{(n)}(r)\exp\left(-\alpha_n^2\frac{S_c}{P_r}\int_0^x u_0^{-1}d\xi\right) \tag{D.15}$$

and the gradient at the interface as

$$-\left(\frac{\partial C}{\partial r}\right)_{r=1}=\sum_{n=0}^{\infty}\beta_n \exp\left(-\alpha_n^2\int_0^x u_0^{-1}d\xi\right) \tag{D.16}$$

$$-\left(\frac{\partial \theta}{\partial r}\right)_{r=1}=\sum_{n=0}^{\infty}\beta_n \exp\left(-\alpha_n^2\frac{S_c}{P_r}\int_0^x u_0^{-1}d\xi\right) \tag{D.17}$$

Values of α_n and β_n are numerically calculated by Sellars et al. [18] and listed as follows.

n	α_n^2	$\beta_n/2$
0	7.312	0.749
1	44.62	0.544
2	113.8	0.463
3	215.2	0.414
4	348.5	0.382
$\geqslant 5$	$(4n+8/3)^2$	$1.0126\,\alpha_n^{-1/3}$

When the concentration and temperature at the wall vary in the axial direction, the solution can be obtained by Duahmel's superposition theory;

$$\left(\frac{\partial C}{\partial r}\right)_1=-\int_0^x\left\{\frac{\partial C(x-\xi,r)}{\partial r}\right\}_1\frac{dC_i}{d\xi}d\xi-\left\{\frac{\partial C(x,r)}{\partial r}\right\}_1(C_i-C_0)_0 \tag{D.18}$$

$$\left(\frac{\partial \theta}{\partial r}\right)_1=-\int_0^x\left\{\frac{\partial \theta(x-\xi,r)}{\partial r}\right\}_1\frac{d\theta_i}{d\xi}d\xi-\left\{\frac{\partial \theta(x,r)}{\partial r}\right\}_1(\theta_i-\theta_0)_0 \tag{D.19}$$

where subscripts 1 and 0 means values at $r=1$ and $x=0$, respectively. Substituting Eqs. (D.16) and (D.17) into Eqs. (D.18) and (D.19) yields

$$\left(\frac{\partial C}{\partial r}\right)_1=\int_0^x\sum_{n=0}^{\infty}\beta_n \exp\left(-\alpha_n^2\int_\xi^x u_0^{-1}d\eta\right)\frac{dC_i}{d\xi}d\xi + \sum_{n=0}^{\infty}\beta_n \exp\left(-\alpha_n^2\int_0^x u_0^{-1}d\eta\right)(C_i-C_0)_0 \tag{D.20}$$

$$\left(\frac{\partial \theta}{\partial r}\right)_1=\int_0^x\sum_{n=0}^{\infty}\beta_n \exp\left(-\alpha_n^2\frac{S_c}{P_r}\int_\xi^x u_0^{-1}d\eta\right)\frac{d\theta_i}{d\xi}d\xi + \sum_{n=0}^{\infty}\beta_n \exp\left(-\alpha_n^2\frac{S_c}{P_r}\int_0^x u_0^{-1}d\eta\right)(\theta_i-\theta_0)_0 \tag{D.21}$$

From Eqs. (3.19) and (3.20),

$$k_r\left(\frac{\partial \theta}{\partial r}\right)_1+\frac{\theta_i}{\delta}=\frac{\rho_r \bar{P}_r \bar{R}_e}{H_e R_e S_c}\frac{1}{C_i-\bar{C}_i}\left(\frac{\partial C}{\partial r}\right)_1 \tag{D.22}$$

With Eqs. (D.20) and (D.21), Eq. (D.22) gives

$$\theta_i+2k_r\delta\left\{\int_0^x\sum_{n=0}^{\infty}\beta_n \exp\left(-\alpha_n^2\frac{S_c}{P_r}\int_\xi^x u_0^{-1}d\eta\right)\frac{d\theta_i}{d\xi}d\xi$$

$$+\sum_{n=0}^{\infty}\beta_n \exp\left(-\alpha_n^2\frac{S_c}{P_r}\int_0^x u_0^{-1}d\eta\right)(\theta_i-\theta_0)_0\Bigg\}$$

$$=\frac{\rho_r\bar{P}_r\bar{R}_e}{H_eR_eS_c}\frac{\delta}{C_i-\bar{C}_i}\left\{\int_0^x\sum_{n=0}^{\infty}\beta_n \exp\left(-\alpha_n^2\int_\xi^x u_0^{-1}d\eta\right)\frac{d\theta_i}{d\xi}d\xi\right.$$

$$\left.+\sum_{n=0}^{\infty}\beta_n \exp\left(-\alpha_n^2\int_0^x u_0^{-1}d\eta\right)(C_i-C_0)_0\right\} \tag{D.23}$$

Coupling Eq. (D.23) with the phase equilibrium gives θ_i, C_i and $\bar{C}_i$.

The mass flux of the condensate at the interface can be expressed by Eqs. (3.38), (3.39) and (3.40) as

$$\dot{m}^*=\frac{1}{\rho_r}\frac{d}{dx}\left\{\left(\frac{\bar{G}_r}{\bar{R}_e}-\frac{\bar{R}_e}{\bar{M}_c^2R_eS_c}\frac{dp}{dx}\right)\delta^3+\mu_r\mu_0\delta^2\right\} \tag{D.24}$$

$$\dot{m}^*=\frac{1}{C_i-\bar{C}_i}\left\{\int_0^x\sum_{n=0}^{\infty}\beta_n \exp\left(-\alpha_n^2\int_\xi^x u_0^{-1}d\eta\right)\frac{dC_i}{d\xi}d\xi\right.$$

$$\left.+\sum_{n=0}^{\infty}\beta_n \exp\left(-\alpha_n^2\int_0^x u_0^{-1}d\eta\right)(C_i-C_0)_0\right\} \tag{D.25}$$

$$\dot{m}^*=\frac{H_eR_eS_c}{\rho_r\bar{P}_r\bar{R}_e}\left[\frac{\theta_i}{\delta}+k_r\left\{\int_0^x\sum_{n=0}^{\infty}\beta_n \exp\left(-\alpha_n^2\frac{S_c}{P_r}\int_\xi^x u_0^{-1}d\eta\right)\frac{d\theta_i}{d\xi}d\xi\right.\right.$$

$$\left.\left.+\sum_{n=0}^{\infty}\beta_n \exp\left(-\alpha_n^2\frac{S_c}{P_r}\int_0^x u_0^{-1}d\eta\right)(\theta_i-\theta_0)_0\right\}\right] \tag{D.26}$$

Combining Eqs. (D.24) and (D.26) gives the film thickness δ;

$$\delta\frac{d}{dx}\left\{\left(\frac{\bar{G}_r}{\bar{R}_e}-\frac{\bar{R}_e}{\bar{M}_c^2R_eS_c}\frac{dp}{dx}\right)\delta^3+\mu_r\mu_0\delta^2\right\}$$

$$=\frac{H_eR_eS_c}{\rho_r\bar{P}_r\bar{R}_e}\left[\theta_i+k_r\delta\left\{\int_0^x\sum_{n=0}^{\infty}\beta_n \exp\left(-\alpha_n^2\frac{S_c}{P_r}\int_\xi^x u_0^{-1}d\eta\right)\frac{d\theta_i}{d\xi}d\xi\right.\right.$$

$$\left.\left.+\sum_{n=0}^{\infty}\beta_n \exp\left(-\alpha_n^2\frac{S_c}{P_r}\int_0^x u_0^{-1}d\eta\right)(\theta_i-\theta_0)_0\right\}\right] \tag{D.27}$$

The interfacial velocity u_i, and the pressure can be obtained by the same equations in Chapter 3, although these effects on the vapor flow are negligibly small.

The integro-differential equations, Eqs. (D. 23) and (D. 26), can be solved numerically. They require an initial condition at $x=0$, which hardly affects the result except for in the vicinity of the origin. For this condition, $\delta=0$ and $\theta_i=1$ may be taken. A numerical example obtained by this procedure is shown in Fig. 24 for the case of ethanol-water mixture with $T_{00}=90°C$, $T_w=89°C$, and $U_{00}=1$ cm/s. The dashed lines means the result by the integral method. Difference is remarkable of the rate of condensation and the heat flux, although the film thickness shows nearly same values. In Eqs. (D.9) and (D.10), the contribution of the radial convective transport of mass and energy is neglected. Close to the interface, the result shows that $v_i^*\simeq 0.1$ and $u_i\simeq 0.03$. Thus, the neglected contribution is substantial, not being

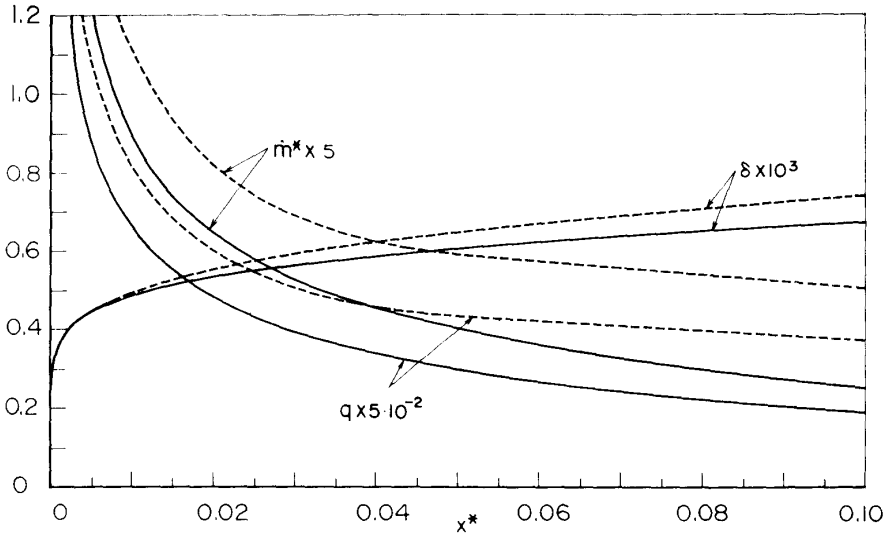

FIG. 24. Approximate solution of entry flow; ethanol-water, C, $T_{00}=90°C$, $T_w=89°C$, $U_{00}=1$ cm/s (---, integral method).

ignored. However, for cases of further smaller difference of T_{00} and T_w, this approximate solution may provde more useful results.

Department of Propulsion
Institute of Space and Aeronautical Science
Unicersity of Tokyo
October, 16, 1980